FATE AND EFFECTS OF POLYETHYLENE TEREPHTHALATE (PET) MICROPLASTICS DURING ANAEROBIC DIGESTION OF DISINTEGRATED SLUDGE

A THESIS SUBMITTED TO
THE GRADUATE SCHOOL OF NATURAL AND APPLIED SCIENCES
OF
MIDDLE EAST TECHNICAL UNIVERSITY

BY

MAKBULE DİLARA HATİNOĞLU

IN PARTIAL FULFILLMENT OF THE REQUIREMENTS
FOR
THE DEGREE OF MASTER OF SCIENCE
IN
ENVIRONMENTAL ENGINEERING

DECEMBER 2021

Approval of the thesis:

FATE AND EFFECTS OF POLYETHYLENE TEREPHTHALATE (PET) MICROPLASTICS DURING ANAEROBIC DIGESTION OF DISINTEGRATED SLUDGE

submitted by **MAKBULE DİLARA HATİNOĞLU** in partial fulfillment of the requirements for the degree of **Master of Science** i**n Environmental Engineering, Middle East Technical University** by,

Prof. Dr. Halil Kalıpçılar
Dean, Graduate School of **Natural and Applied Sciences** _____

Prof. Dr. Bülent İçgen
Head of the Department, **Environmental Engineering** _____

Prof. Dr. F. Dilek Sanin
Supervisor, **Environmental Engineering, METU** _____

Examining Committee Members:

Prof. Dr. İpek İmamoğlu
Environmental Engineering, METU _____

Prof. Dr. F. Dilek Sanin
Environmental Engineering, METU _____

Prof. Dr. Gülay Ertaş
Chemistry, METU _____

Assoc. Prof. Dr. Tuba Hande Bayramoğlu
Environmental Engineering, METU _____

Assist. Prof. Dr. Onur Güven Apul
Civil and Environmental Engineering, University of Maine _____

Date: 24.12.2021

I hereby declare that all information in this document has been obtained and presented in accordance with academic rules and ethical conduct. I also declare that, as required by these rules and conduct, I have fully cited and referenced all material and results that are not original to this work.

Name Last name : Makbule Dilara Hatinoğlu

Signature :

ABSTRACT

FATE AND EFFECTS OF POLYETHYLENE TEREPHTHALATE (PET) MICROPLASTICS DURING ANAEROBIC DIGESTION OF DISINTEGRATED SLUDGE

Hatinoğlu, Makbule Dilara
Master of Science, Environmental Engineering
Supervisor: Prof. Dr. F. Dilek Sanin

December 2021, 184 pages

Modern wastewater treatment plants effectively remove microplastics (MPs) from wastewater but unfortunately concentrate them in sludge. Anaerobic digesters were recently reported to be affected by MPs. Despite their resilience to natural degradation, polyethylene terephthalate (PET) plastics have inherent weaknesses to alkali and thermal conditions and become more susceptible to biodegradation if exposed to them. Sludge disintegration practices aiming to increase the biogas production by disrupting sludge's floc structure show great similarity with the stress factors mentioned. Thus, this study aimed to integrate disintegration with anaerobic digesters and investigate the fate and effects of PET MPs during these processes. With this purpose, waste activated sludge samples spiked with different doses of PET (0,1,3,6 mg/g TS) in sizes of 250-500 μm were disintegrated by 0.5 M alkali for two days and thermally hydrolyzed at 127°C for 120 min. 60 days of biochemical methane potential reactor operation concluded that MPs dose significantly affected the methane yield positively in non-disintegrated reactors. Integrating disintegration prior to digestion, on the other hand, increased the yield by 22.0% and made the

impact of MPs on digester efficiency no longer observable. PET also experienced changes in their physical (surface morphology/mass) and chemical (crystallinity/carbonyl index) properties depending on whether they were exposed to disintegration before digestion. Moreover, for the first time in literature, a method was developed for the analysis of MPs in sludge based on chemical oxygen demand removal as the indicator of organic matter removal. The method provides over 80% MPs recovery efficiency, meeting the recommendations in the literature.

Keywords: Microplastics, Sewage Sludge, Anaerobic Digestion, Sludge Disintegration, Biofragmentation

ÖZ

POLİETİLEN TEREFTALAT (PET) MİKROPLASTİKLERİN DEZENTEGRASYON UYGULANMIŞ ARITMA ÇAMURLARININ ANAEROBİK ÇÜRÜTME SÜREÇLERİNDEKİ ETKİLERİ VE BU SÜREÇLERDEKİ AKIBETİ

Hatinoğlu, Makbule Dilara
Yüksek Lisans, Çevre Mühendisliği
Tez Yöneticisi: Prof. Dr. F. Dilek Sanin

Aralık 2021, 184 sayfa

Modern atıksu arıtma tesisleri atıksudaki mikroplastikleri (MP'ler) etkin şekilde uzaklaştırırken ne yazık ki bunları arıtma çamurunda biriktirmektedir. Anaerobik çürütücülerin son zamanlarda MP'lerden etkilendiği rapor edilmiştir. Doğal yollar ile bozunmaya karşı dirençlerine rağmen, PET plastikler alkali ve termal koşullara karşı zayıf olup; bunlara maruziyetleri durumunda biyolojik bozunmaya karşı hassasiyetleri artmaktadır. Arıtma çamurunun yumak yapısını bozarak biyogaz üretim verimini artırmayı hedefleyen dezentegrasyon yöntemleri bahsi geçen stres faktörleri ile büyük benzerlik göstermektedir. Bu nedenle çalışma dezentegrasyon yöntemlerini anaerobik çürütücülere entegre ederek PET MP'lerin bu süreçlerdeki akıbeti ve etkilerini incelemeyi hedeflemektedir. Bu amaçla 250-500 µm boyutlarına sahip PET MP'lerin farklı dozlarda (0, 1, 3, 6 mg/g TS) eklendiği atık aktif çamur numuneleri iki gün boyunca 0,5 M alkali dezentegrasyon ve 127°C'de 120 dk boyunca termal hidroliz işlemlerine tabii tutulmuştur. 60 günlük biyokimyasal metan potansiyeli reaktör işletimi ile MP dozunun dezentegrasyona uğramamış

reaktörlerde metan verimini önemli ölçüde olumlu etkilediği sonucuna varılmıştır. Öte yandan, dezentegrasyon işlemlerini çürütme işlemi öncesine entegre etmek verimi %22,0 oranında artırmış ve MP'lerin çürütücü verimi üzerindeki etkisini gözlemlenemez kılmıştır. Ayrıca, PET, çürütmeden önce dezentegrasyona maruz bırakılma durumuna bağlı olarak fiziksel (yüzey morfolojisi/kütle) ve kimyasal (kristallik/karbonil indeksi) özelliklerinde değişiklikler yaşamıştır. Ayrıca, literatürde ilk kez, organik madde gideriminin göstergesi olarak kimyasal oksijen ihtiyacı giderimine dayalı çamurdaki MP'lerin analizi için bir yöntem geliştirilmiştir. Yöntem, literatürdeki tavsiyeleri karşılayarak %80'in üzerinde MP geri kazanım verimliliği sağlamaktadır.

Anahtar Kelimeler: Mikroplastikler, Arıtma Çamuru, Anaerobik Çürütme, Çamur Dezentegrasyonu, Biyofragmentasyon

To my family

ACKNOWLEDGMENTS

First of all, I would like to express my deepest appreciation to my supervisor Prof. Dr. F. Dilek Sanin for her precious advice, guidance and endless support throughout my graduate studies. It was a unique opportunity to work with such a great scientist inspiring me with her motivation to do research.

I would also like to thank the thesis committee members Prof. Dr. İpek İmamoğlu, Prof. Dr. Gülay Ertaş, Assoc. Prof. Dr. Tuba Hande Bayramoğlu and Assist. Prof. Dr. Onur Güven Apul for their valuable contributions.

I am grateful to the Scientific and Technological Research Council of Turkey (TUBITAK) for awarding me a full graduate scholarship (BIDEB 2210/A) and providing financial support to the project (Project No: 121Y156) which partly covers this thesis.

My special thanks are to the brilliant members of D.Sanin Research Group, İrem Şimşek, Ozan Karakurt, Nermin Cemalgil, Gülçin Gülletutan, Işıl Doğan, Göksu Yurtseven, Oğuzhan Altuntaş, Elif Güzel, Eda Sakınmaz, Gizem Soyer and Buse Berfin Kart. I can extend the list to my friends Hazal Başköy, Selin Gökçe, Ebru Selen Güven, Ece Kutlar, Berivan Tunca, Gökçe Çiftçi, Amin Ghaderi Kia and Yasin Odabaş for their endless support in every way possible during this period of my life.

I am dedicating this thesis with wholehearted appreciation to my mother Seyhan Hatinoğlu, my father Ahmet Fazıl Hatinoğlu and my brothers Uğur Hatinoğlu and Adil Mert Hatinoğlu. Finally, I would like to express my deepest gratitude to my biggest supporters, my grandparents, Pakize Sevinç and Cevat Sevinç. Having this wonderful family is the golden ticket of my life that gives me strength and motivation in everything I do.

TABLE OF CONTENTS

LIST OF TABLES

TABLES

LIST OF FIGURES

FIGURES

LIST OF ABBREVIATIONS

AD : Anaerobic digestion

ADS : Anaerobically digested sludge

BMP : Biochemical methane potential

CPL : Caprolactam

DSC : Differential Scanning Calorimetry

EPS : Extracellular polymeric substances

FTIR : Fourier Transform Infrared Spectroscopy

GPC : Gel Permeation Chromatography

HRT : Hydraulic retention time

KHP : Potassium Hydrogen Phthalate

MPs : Microplastics

NPs : Nanoplastics

PCTE : Polycarbonate Track Etched membrane filter

PET : Polyethylene terephthalate

PFOS : Perfluorooctane sulfonate

ROS : Reactive oxygen species

SBR : Styrene butadiene rubber

sCOD : Soluble chemical oxygen demand

SEM : Scanning Electron Microscopy

SR : Synthetic rubber

SRT : Solids retention time

tCOD : Total chemical oxygen demand

THP : Thermal hydrolysis process

TS : Total solids

TSS : Total suspended solids

VS : Volatile solids

VSS : Volatile suspended solids

WAS : Waste activated sludge

WWTP: Wastewater treatment plant

CHAPTER 1

INTRODUCTION

Due to their lightweight, low production cost and durability, plastics hold a significant place in daily life with extensive use in industrial and medical applications. They provide many societal benefits for health, safety, material conservation and energy saving. For example, plastics are used in (i) supply and storage of clean drinking water, (ii) food packaging, allowing safe and sterile storage; (iii) transportation vehicles and packaging, providing savings in materials and fossil fuel energy (Andrady and Neal, 2009). Therefore, plastics are considered to be the most versatile materials of the modern age, resulting in a substantial increase in global plastic production to meet the steadily growing demand of society (Crawford and Quinn, 2016). However, increasing plastic pollution with rapid growth in global plastic production and consumption has started to create scientific and social concerns (Rolsky et al., 2020; B. Zhang et al., 2020). The rate of global plastic production in 1950 increased from 1.5 million tonnes to 368 million tonnes in 2019 (PlasticsEurope, 2020). Despite the growing waste management activities, most of the plastic waste continues to be released into the environment (Bläsing and Amelung, 2018). According to the United Nations Environment Programme's report, keeping the current production patterns and waste management activities will result in 12 billion tonnes of plastic waste to be in landfills and the natural environment by 2050 (UNEP, 2018). Moreover, nearly 10% of all land-based plastics are suggested to end up in the marine environment (Jahan et al., 2019; Thompson, 2006). This situation creates concerns not only with aesthetical issues and environmental pollution but also due to negative impacts on the ecosystem and human health. Furthermore, plastic pollution is a significant problem that causes economic losses exceeding hundreds of millions of dollars annually (Hardesty et al., 2015).

Once in the environment, plastic wastes degrade at a very slow rate into smaller particles via natural weathering mechanisms either physically or biologically (Zhang et al., 2021). Plastic debris formed smaller than 5 mm in size, called microplastics (MPs), have become a global issue of emerging concern for the last 10 years. MPs pollution in the environment is primarily contributed by domestic, industrial and coastal activities in the form of secondary MPs. The other entry route for MPs is through direct release of primary MPs (intentionally produced MPs) from industrial feedstocks and personal care products (Sharma and Chatterjee, 2017). Due to their small sizes and high specific surface area, MPs hold potential to block digestive system of living organisms and to be the vector for the transfer of hazardous pollutants into biota (Lv et al., 2019; Yang et al., 2021a).

WWTPs receive a high amount of MPs via domestic and industrial wastewaters, storm water, and landfill leachate inputs (Ou and Zeng, 2018). WWTPs have been reported to have MP removal efficiency of up to 99.9%, however they still release a daily average of 10^5-10^8 MPs with the effluent, due to highly loaded influent wastewater (Sun et al., 2019). Besides, MPs removed from the wastewater are transferred into sludge, rather than being eliminated during treatment processes (Okoffo et al., 2019). Therefore, WWTPs have been identified as both sources and sinks of MPs pollution in the environment (Mintenig et al., 2017).

Sewage sludge is the main by-product of WWTPs, the disposal of which accounts for up to 50% of the operating costs of a plant (Li et al., 2012). Realizing the continuous generation of vast amounts of sludge and the beneficial constituents in it, nations have been considering sludge as a resource rather than a waste. As a prerequisite for further handling, high amount of water needs to be removed by thickening/dewatering/drying, so that sludge can be managed more cost effectively. Due to high organic and nutrient content, land application as a soil conditioner or fertilizer has been the major recycling route. In North America and Europe sewage sludge generated is beneficially used up to 50% by recycling on land (Nizzetto et al., 2016). On the other hand, land application of improperly treated sewage sludge creates increasing concern due to the presence of pathogens and more importantly

accumulation of some trace pollutants, including toxic organics and MPs in the ecosystem (Z. Chen et al., 2020). Due to the fact that over 90% of MPs in wastewater are accumulated in sludge that has potential for beneficial use and some to be disposed of, it is clear that WWTPs lead to an additional pathway for MP pollution in the environment (L. Zhang et al., 2020). An annual average of 10^6-10^{14} MPs have been shown to be released into the environment through incineration, landfilling, and land application of sludge from a WWTP. Strikingly, the annual amount of MPs entering the soil through land application of sludge is greater than that enters the oceans (B. Zhang et al., 2020). Thus, agricultural use of sludge is pointed out as one of the largest source of MPs entering the environment (Hurley and Nizzetto, 2018). L. Zhang et al. (2020) has observed 87.6 to 545.9 MPs/kg of soil after annual amendment with sludge-based composts, which also led to MP uptake in earthworms. Similarly, Corradini et al. (2019) reported as high as 3500 MPs/kg of dry agricultural soils which was exposed to 10 years of continuous sludge disposal.

Anaerobic digestion is a widely used sludge management option aiming to minimize the costs related to disposal. It converts organic material into biogas, stabilizes the sludge, and reduces the amount of sludge to be disposed of (Appels et al., 2008). Due to the complex floc structure and hard cell wall of sludge, hydrolysis of particulate organic matter to soluble substances is the rate-limiting step during anaerobic digestion. To improve the rate of sludge hydrolysis and hence the efficiency of the anaerobic digestion process, various sludge disintegration methods have been developed, such as thermal, chemical, ultrasonic, and biological (Chen et al., 2007). They can be applied individually or in combination to maximize WAS solubilization. These methods are all based on the principle of lysing the sludge cells, releasing the intracellular substances, and making them more amenable to further microbial action.

Limited recent studies have investigated the effects of MPs on sludge stabilization processes and found that depending on their physical and chemical properties, MPs may pose different impacts on anaerobic digestion of sludge. The corresponding effects of stabilization on MPs have yet superficially addressed, which only hints on

possible deterioration of MPs during these processes. Despite their complex nature that makes them hard to be degraded by microorganisms, exposing plastics to abiotic factors such as heat, light, gases, water and mechanical impacts may initiate structural changes and may induce some degree of biodeterioration (Iram et al., 2019). For example, polyethylene terephthalate (PET), which is a semicrystalline thermoplastic polyester, can hydrolyze to a certain degree in the presence of alkaline solutions. In addition, they can hydrolyze in wet conditions at high temperatures (>73–78°C) (Crawford and Quinn, 2016). In real life, these abiotic factors are unintentionally applied to MPs during sludge treatment processes including disintegration practices to increase solubilization of sludge before anaerobic digestion.

In consideration of all these results, first time in literature this study aims to investigate whether the disintegration processes applied for sludge minimization and biogas enhancement can act similarly to the abiotic factors mentioned, leading to the deterioration of PET MPs and easing up biodegradation during anaerobic digestion, while examining the effects of MPs on anaerobic digestion of disintegrated sludge.

To better represent the magnitude of the MPs pollution in the environment, this study also aims to develop a reliable and repeatable analysis method for MPs in sludge. Despite the rising concerns about MPs pollution, there is no globally accepted and applied standard method for detecting MPs in sludge, making it nearly impossible to make a comparison between concentration of MPs reported in different studies. The quantities of MPs reported in sludges indicate that the numbers are generally high but also widely varied (510 to 495,000 MPs per kg dry weight of sludge) from one plant to the other around the world. To ensure an overall understanding of the data from different studies, creating a uniformity of terminologies in the identification and classification of MPs is another motivation of this study.

Specific objectives of this study are listed below:

- To logically sequence the steps given in the literature for the analysis of MPs and optimize each step for sludge samples, including removal of organics in

the sample, extraction of MPs and subsequent identification and quantification.

- To quantify MPs in sludge from Ankara Central WWTP with this optimized method and reveal the extent of MPs pollution in the samples.
- To scrutinize the efficacy of alkaline, thermal and combined disintegration techniques in solubilizing waste activated sludge (WAS).
- To investigate whether sludge disintegration techniques can deteriorate PET-MPs to some extent.
- To set-up and operate BMP reactors with disintegrated and non-disintegrated sludges, spiked with different doses of PET MPs (i.e., 0, 1, 3, 6 mg PET-MPs/g TS of sludge); thereby, investigate the fate and effects of PET MPs in anaerobic digesters as well as whether there are additional effects from the disintegration process.

CHAPTER 2

LITERATURE REVIEW

2.1 Plastics in the Daily Life

Plastics are synthetic organic polymers formed by the reaction of small organic molecules mostly derived from fossil fuels resulting in long polymer chains. As they are cheap, lightweight and resilient against degradation, synthetic plastics have become essential in various sectors including transport, construction, electronics, packaging, textile and agriculture. Moreover, plastics take an important place in daily life, including plastic bags, packaging, toys, throwaway plastic products, microbeads, fishing and aquaculture equipment, etc. (Filho et al., 2021).

There are two main types of plastics based on their physical characteristics: thermoplastics and thermoset plastics. Thermoplastics, the recyclable group of plastics, can be molten when heated and harden upon cooling repeatedly. The largest market shares belong to thermoplastics, examples of which are polyethylene (PE), polypropylene (PP), polyethylene terephthalate (PET), poly(vinyl chloride) (PVC), polystyrene (PS), polycarbonate (PC), and polyamide (PA) (Chamas et al., 2020). Thermosets, on the other hand, become irreversibly rigid upon heating due to the formation of permanent chemical bonds between polymer chains. The examples of thermosets include some polyesters, polyurethane (PUR), epoxy resin, and acrylic resin (WHO, 2019).

Today, plastics are the most versatile materials of the modern age with ever increasing demand for their production (Crawford and Quinn, 2016). The global plastic production rate in 1950 increased from 1.5 million tonnes to 368 million tonnes in 2019, corresponding to a cumulative production of 9.1 billion tonnes in total as shown in Figure 2.1 (a). By 2019, the top three plastic producers were China,

rest of Asia and NAFTA countries at 31%, 20% and 16%, respectively (Figure 2.1 (b)). Moreover, Germany (24.2%), Italy (13.8%), France (9.5%), Spain (7.1%), the United Kingdom (7%) and Poland (7%) were the top-six plastic demanding European countries with more than 3 million tonnes in a year (PlasticsEurope, 2020).

Most plastics have been designed for single use only, causing packaging materials and more specifically PE and PP to account for half of the world's plastic waste. Although China, with the largest population, takes the largest share in world's plastic production, high-income countries such as the US, European countries and Japan dominates in production when per capita production is considered. However, the sophisticated waste management systems of the developed countries generally compensate their production rate. Thus, middle and low-income countries with mismanaged wastes become the main contributors of global plastic waste (Ncube et al., 2021).

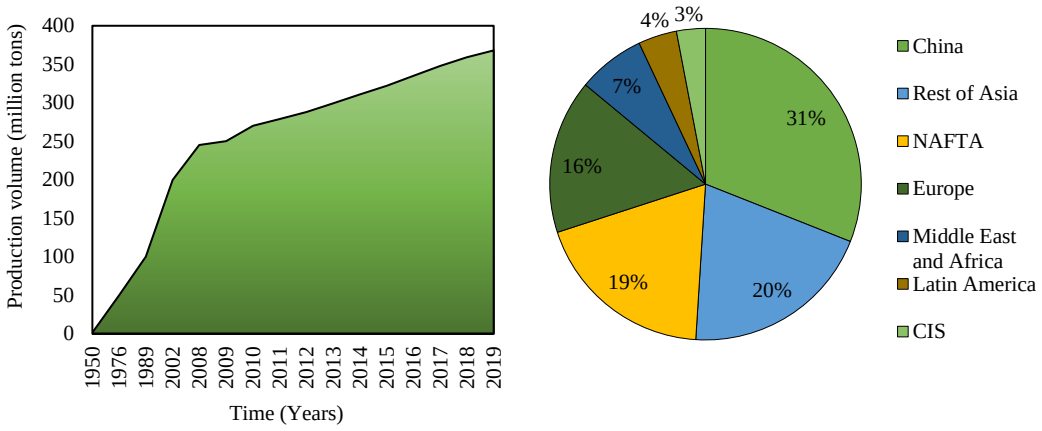

(a) **(b)**

Figure 2.1. Annual production of plastics worldwide from 1950 to 2019 (a) Adapted from Statistica (2021); distribution of global plastic production (b) Adapted from (PlasticsEurope, 2020).

2.2 Plastic Waste

Since 1950, approximately 6.9 billion tonnes of the total plastic production ended up being waste and 4.5 billion tonnes of them either dumped into landfills or released into the environment (Ali et al., 2021b). The intensive production, extensive use and mismanagement of plastics have led them to enter the environment for decades. Current projections demonstrate that maintaining the existing production trends and waste management activities would lead to 12 billion tons of plastic waste to be distributed across the natural environment by 2050 (UNEP, 2018). More specifically, almost 10% of all land-based plastics would accumulate in the marine environment (Jahan et al., 2019). This pollution results in many deteriorative effects on the ecosystem health through biological disruption, leaching of toxic chemicals and sorption and transfer of hazardous substances into biota (Reimonn et al., 2019).

Currently, plastic waste is handled by three different routes: landfilling, incineration, and recycling (Webb et al., 2013). In global scale, only a small portion of plastic wastes generated are recycled (18%) and incinerated (24%). The rest (58%), unfortunately, end up in landfills or reach to the natural environment and accumulate there (Chamas et al., 2020). Figure 2.2 demonstrates the historical trend in plastic waste handling and projections from 2015 to 2050. Projections assuming a consistent trend in plastic waste generation and disposal show that by 2050 the amount of plastic waste to be landfilled, incinerated, and recycled will be 12,000, 12,000 and 9000 Mt, respectively (Geyer et al., 2017).

Landfilling is the least attractive route as plastic waste can persist for more than 20 years in landfills where a limited amount of oxygen is present, and it occupies huge space. Besides, plastics may release toxic chemicals both as gases and contained in leachate. Incineration overcomes the space requirements of landfills; however, it may cause the release of polymer-based harmful gases to the atmosphere. The undeniable drawbacks of landfilling and incineration promote the development of plastic recycling processes. Recycling is generally carried out by chemical and mechanical techniques after sorting and intensive plastics cleaning to remove

contaminants (Ncube et al., 2021). While chemical methods aim to depolymerize plastics into monomers to produce new products, the latter option is the reuse of plastics after mechanical handling. Hard to remove additives and impurities are the challenges of recycling that result in expensive operation and low-quality products.

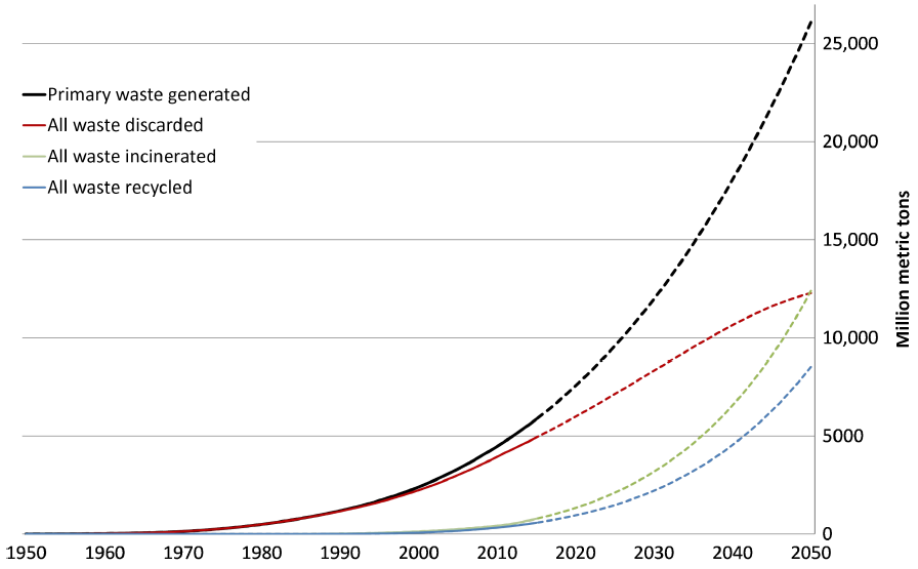

Figure 2.2. Cumulative plastic waste generation and disposal (in million metric tons) (Geyer et al., 2017)

As an environmentally friendly approach, biodegradation could be an attractive option for plastic waste handling, but no protocol has been developed yet on a large scale. Most studies up to now have focused on abiotic mechanisms affecting plastics in nature, giving only a hint that biodegradation can occur through depolymerization (e.g., breakage of ester bonds for PET) (Webb, 2012).

2.3 Natural Degradation of Plastics

Degradation is defined as the process causing decline of polymer properties by polymer engineers. Environmental chemists, on the other hand, focus on governing

chemical reactions that cause breakdown of polymers and the danger linked to chemicals released by degradation of plastics (Gewert et al., 2015).

Mismanagement and disposal of plastic waste causes them to reach and accumulate in the environment, where their degradation by natural weathering mechanisms occurs at a very slow rate. Nevertheless, these mechanisms cause changes in polymer properties to some extent (Zhang et al., 2021). Degradation pathways of plastic polymers in the environment can be categorized as biotic and abiotic mechanisms including photo, thermal, mechanical and biological degradation. By these mechanisms, polymers are transformed into smaller molecular units first (e.g., monomers) and then potentially mineralized as shown in Figure 2.3 (Klein et al., 2018).

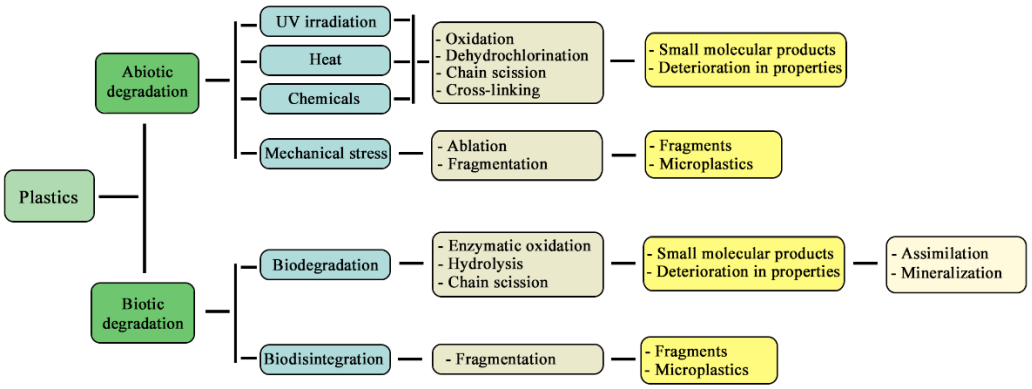

Figure 2.3. Natural degradation mechanisms of plastics. Adapted from Zhang et al. (2021)

Natural degradation often starts with photodegradation causing plastic debris to become brittle and get into smaller pieces (i.e., MPs). However, it is hard to degrade plastics biotically in nature due to 1) their high molecular weight and large polymer structure restricting their penetration into microbial cell; 2) lack of genetical information in microorganisms required to degrade synthetic chemicals such as plastic additives; and 3) insoluble and highly hydrophobic nature of polymers

(Eubeler et al., 2009). Theoretically, plastics can biodegrade both under aerobic and anaerobic conditions into CO_2, H_2O, CH_4, salts, minerals and even to biomass fully or partially if appropriate conditions are provided. Along with the availability of microorganisms in a suitable environment, biodegradation process also requires that the morphology of plastic particles should provide a surface on which microorganisms can attach to form a biofilm. Furthermore, the chemistry of the plastics (degree of polymerization, branching, chemical bonds, hydrophobicity, and crystallinity) must not prevent microbial actions (Klein et al., 2018). Iram et al. (2019) claims that exposure of plastics to abiotic factors such as heat, light, gases, water and mechanical impacts contributes to some degree of polymer's biodeterioration after initiating mechanical, physical, and chemical changes in plastics.

2.3.1 Abiotic Degradation

The main abiotic mechanisms that contribute to degradation of plastics in the environment are photodegradation, thermal degradation and mechanical degradation.

2.3.1.1 Photodegradation

Photodegradation is considered as the most significant mechanism initiating degradation of plastics in the environment (Zhang et al., 2021). The vulnerability of plastics to photodegradation originate from their tendency to absorb the harmful portion of tropospheric solar irradiation such as UV-B, UV-A, visible part of sunlight and infrared radiation, that further causes degradation through direct photodegradation, heating, and thermal oxidation. During photodegradation, high-energy radiation in the UV spectrum activates plastics' electrons to higher reactivity, which leads free radical mediated reactions to occur such as oxidation, cleavage, and other degradation pathways (Shah et al., 2008).

2.3.1.2 Thermal Degradation

Thermal degradation is the decomposition of plastics by applying elevated temperatures. When plastics absorb adequate amount of heat to overcome the energy barrier, their long polymer chains can be broken, and radicals are formed. In an aerobic environment, these radicals interact with oxygen and produce hydroperoxide that cleave to form hydroxyl free radicals, which is called thermo-oxidative reaction. In an anaerobic environment, on the other hand, hydrolysis process mediated by heating is favored (Alimi et al., 2022).

The specific temperature required for each polymer type is related to their glass transition temperature (T_g) and melting point (T_m), as well as oxygen availability. Consequently, thermal degradation may either reduce or enlarge plastics as a result of chain scission and cross-linking. This process often alters the molecular weight of plastics which further causes cracking, color changes and reduction in ductility (Shah et al., 2008).

In the environment, plastics can undergo thermal oxidation at a slow rate jointly with photodegradation, especially in places exposed to direct sunlight such as beaches and pavements. The rate of reactions increases with the temperature. Moreover, humidity decreases the activation energy required for thermal degradation of plastics (Zhang et al., 2021).

2.3.1.3 Mechanical Degradation

External forces are acting during mechanical degradation of plastics. Two examples for these forces in the environment are collision of plastics with rocks by wind and waves and freezing and thawing in aquatic environment (Zhang et al., 2021). The resistance of plastics against external forces are determined by their mechanical properties, such as elongation at break. Having a low elongation at break value causes plastics to fragment in response to an external force.

2.3.2 Biotic Degradation

Biodegradation is the deterioration of plastics that may occur when they are exposed to organisms. This process can take place either physically by chewing and digestive fragmentation or biologically by biochemical processes. It is basically hydrolysis of polymers into monomers and even mineralization by enzymatic activity (Alimi et al., 2022). Several different group of organisms (e.g., bacteria and fungi) are involved in this process (i) to break down polymers into monomers, (ii) to consume monomers and excrete wasted substances, (iii) to use these substances.

Biodegradation of plastics takes place in five main steps that are colonization, biodeterioration, biofragmentation, assimilation and mineralization. Microorganisms first colonize on plastic surface by the formation of proteins and polysaccharides, which then penetrate inside and change the polymer's pore size. The biofilm formed causes further microbial activity on plastic surface which results with changes in physicochemical properties of plastics, called biodeterioration. Then, the complex polymers that are too large to pass though cellular membranes are broken down into short chain ones (e.g., oligomers, dimers, and monomers). This process, "depolymerization/biofragmentation", occurs when enzymes secreted from microorganisms bind to polymers and catalyze the hydrolytic cleavage (Ali et al., 2021a, 2021b). Hence polymers become more likely to be absorbed and degraded within bacterial cells (Shah et al., 2008). During assimilation, microorganisms consume small intermediates, produced from biofragmentation stage, as carbon and energy source for their growth. Molecules that cannot be assimilated are biotransformed via enzyme-catalyzed transformation. Once they are in microbial cells, molecules undergo catalytic activity (i.e., mineralization) to produce adenosine triphosphate (ATP) and new biomass, via aerobic respiration, anaerobic respiration or fermentation (Ali et al., 2021a, 2021b).

2.4 Microplastics from Macroplastics

Although the mechanism behind the fragmentation of plastics has not yet been fully explored, it is a widely held belief that plastic debris accumulating in the environment gradually degrade through environmental mechanisms mentioned in the previous part and form highly persistent MPs (Chamas et al., 2020; Chatterjee and Sharma, 2019). MPs are plastic particles smaller than 5 mm in size that are easily transported in environmental systems. There are two categories of MPs based on their sources (Gatidou et al., 2019; Mintenig et al., 2017). Primary MPs are intentionally produced in micrometer sizes to be used in cosmetic and personal care products, whereas secondary MPs, which constitute the largest portion of MPs in water, result from the degradation of larger plastic products by exposure to environmental stressors (e.g., water, wind, and sunlight) (Lv et al., 2019; Ngo et al., 2019). Hence, both primary and secondary MPs enter the terrestrial and aquatic environments via effluents from domestic, industrial and agricultural activities, transportation, and wastewater treatment plants (WWTPs) (Gao et al., 2020; Waldschläger et al., 2020). In addition, MPs accumulating in landfills are resuspended by wind and become air-borne, which can spread further in the environment through atmospheric transport (Rillig, 2012; Rocha-Santos and Duarte, 2015).

Therefore, MP pollution is encountered in all kinds of environmental systems, including water, soil, air, and sediment. In addition to being ubiquitous in the environment, MPs also raise concern with their potential to block the digestive system of animals and to be the vector for the transfer of hazardous pollutants into biota (Yang et al., 2021a). Because of their hydrophobicity and high specific surface area, MPs can adsorb organic pollutants and heavy metals on their surfaces and transfer them to the food chain. In addition, providing available hydrophobic surfaces for biofilm formation causes MPs to carry microbes to organisms (Zettler et al., 2013). These factors bring numerous negative impacts on living organisms, such as toxicity, enzyme inhibition and immobilization (Rehse et al., 2016). By the

realization of their danger, MPs have started to hold a significant place in environmental research for the last 10 years (predominantly in the last 5 years).

2.4.1 Ecological Effects of Microplastics

MPs pose danger in the environment primarily due to their small sizes (i.e., high specific surface area) which is in the optimal prey range for most animals in the marine environment (Galloway et al., 2017). Ecological and ecotoxicological concerns with MPs can be categorized as (i) biological disruption, (ii) additive leaching, and (iii) exterior sorption.

Once MPs are ingested by organisms, physical damage occurs in their body to as low as cellular level. Besides, the shift of small organisms' (e.g., zooplanktons) diet to MPs decreases the trophic energy which affects the whole population involved in the food web. Furthermore, MPs alter the quantity and quality of sediment in marine environment by acting like an additional sediment input.

Fragmentation of polymers into monomers as well as leaching of plastic additives such as plasticizers (e.g., bisphenol A (BPA), phthalates) and fillers hold potential for a significant toxicological effect. Finally, the exterior mechanism, ecocorona formation, enables MPs to become vector of hazardous pollutants and home for bacteria in the aqueous environment. Thus, the pollutants are transferred to organisms feeding with MPs, which causes disruption in cell division, secretion of hormones and immunity (Reimonn et al., 2019). Due to the lack of evidence for impact of MPs on human health, World Health Organization (WHO) has not yet listed MPs as hazardous substances in drinking water. However, the organization calls for more research providing quality-assured toxicological data to assess the potential health risk associated with MPs in drinking water (WHO, 2019).

2.4.2 Microplastics Reaching Wastewater Treatment Plants

Water is considered as the main vector for transport of MPs in the environment (Sol et al., 2020). WWTPs receive a high amount of MPs via domestic and industrial wastewaters, storm water, and landfill leachate inputs as shown in Figure 2.4. WWTPs have been reported to have MP removal efficiency of up to 99.9%, mainly due to the high hydrophobicity of MPs which facilitates their adsorption onto organic surfaces of sewage sludge. Most of the MPs reaching WWTPs are removed in primary and secondary treatment units (Gies et al., 2018; Ou and Zeng, 2018). While pre-treatment and primary treatment units remove up to 98% of MPs, adding a successive secondary treatment unit provides an extra 7% to 20% removal (Murphy et al., 2016). Efficiency of a tertiary treatment technology in removal of MPs varies depending on the technology used. Literature shows that membrane bioreactor (MBR) (99.1-99.9%) (Lares et al., 2018; Lv et al., 2019) dissolved air flotation (95%) (Talvitie et al., 2017), granular sand filtration (72.7%) (Michielssen et al., 2016), and disk filter (40-98.5) (Talvitie et al., 2017) technologies make a significant contribution to reduce the amount of MPs emissions from a WWTP.

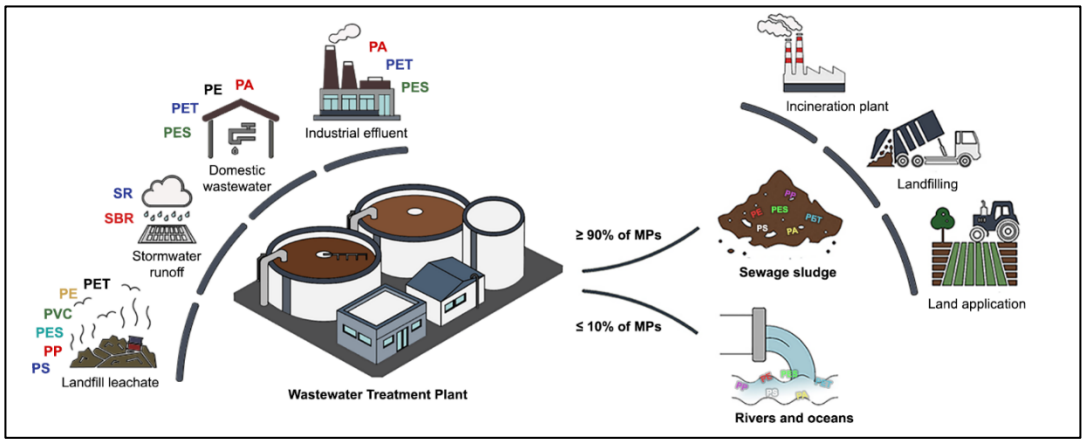

Figure 2.4. Sources and pathways of MPs in WWTPs

Despite the high removal efficiency, WWTPs still release a daily average of 10^5-10^8 MPs with the effluent, due to highly loaded influent wastewater (Sun et al., 2019; Ziajahromi et al., 2016). Besides, the MPs removed from the wastewater are transferred into sludge, rather than being eliminated during treatment processes (Okoffo et al., 2019). Therefore, WWTPs have been identified as both sources and sinks of MPs pollution in the environment (Mintenig et al., 2017; J. Zhang et al., 2019).

2.4.3 Accumulation of Microplastics in Sewage Sludge

Sewage sludge is a semi-solid residual produced during wastewater treatment processes (Sanin et al., 2011). Depending on the level of treatment and the unit operations involved, quality and quantity of sludge produced largely vary across WWTPs. Daily sludge production ranges from 60-90 g dry solids (DS) per population equivalent (Appels et al., 2008). Ever-increasing production of sludge necessitates the development of suitable management approaches.

At a WWTP, sludge is settled out in primary and secondary clarifiers along with the suspended solids present in wastewater including MPs. Thus, over 90% of MPs removed from wastewater by the adsorption mechanism accumulate in sewage sludge (J. Zhang et al., 2019). As the wastewater is cleared from sludge by separation during primary/secondary clarification, sludge that already accumulated almost all the MPs continue its own route of treatment. In many modern WWTPs, sludge is further treated in digesters, thickened, dewatered, and dried. With all the valuable constituents in it, it is a logical outcome that the treated sludge can hold many beneficial uses, including land application for agricultural purposes. Studies show that today, the annual amount of MPs passing into the terrestrial environment through land-use of sludge is much higher than MPs entering into the oceans and freshwater sediments from a variety of sources (Gong and Xie, 2020; Nizzetto et al., 2016). This is the point where the concern escalates!

2.4.3.1 Abundance of MPs in Sewage Sludge

Table 2.1 lists the data obtained from WWTPs in different countries, to summarize the abundance of MPs in sewage sludge samples globally and the annual amount of MP discharge through these sludges. Table demonstrates that WWTPs are among the key elements in the release of MPs into the environment, somewhere between 10^6-10^{14} MPs annually, regardless of the differences between the plants. Studies listed in Table 2.1 reveal two striking findings. First one is that MP concentrations in the sludge vary largely, from 510 to 495,000 particle/kg dry weight (dw) of sludge independent of the country or the region. The large variation between the results can be associated with a number of factors including diversity in urbanization, population density, plastic consumption, seasonality, and treatment processes at the studied WWTP, as well as the inconsistencies in sampling and analysis methods. So, it becomes of critical importance to assess the MP concentration in wastewater and sludge on an annual basis by considering seasonal variations, and to relate the results to the WWTP processes. In other words, the fate of MPs throughout the WWTP should be evaluated holistically, including sludge. The second striking fact is the reported amounts of MP discharge via sludge. We can see that up to thousands of billions of MP particles are released into the environment annually by means of sludge. Considering the resistance of these polymers for degradation, one can easily develop an idea about fast accumulation of MPs in environmental compartments. Table 2.1 also demonstrates the wide-spread nature of the problem on the global scale.

Table 2.1. Reported MPs concentrations in sewage sludge and annual MPs discharges via sludge in different countries

Location of WWTP	Population served or PE	Sludge type	Concentration (# of MPs/kg dw of sludge)	MP size range	Discharge by sludge (# of MPs/year)	Reference
Australia	1.90×10^5	- WAS	7.91 ± 0.44[a]	1.5 µm – 1.0 mm and >1.0 mm	$(4.19 – 4.69) \times 10^9$	Raju et al. (2020)
Australia	NR	- Biosolid	$(2.80 - 6.60) \times 10^3$[b]	NR	NR	Okoffo et al. (2020)
Australia	2.34×10^5 – 7.00×10^5	- Primary sludge - Secondary sludge - Digested sludge - Chemically stabilized sludge	$(15.90 – 45.70) \times 10^3$ $(37.80 – 46.10) \times 10^3$ $(48.50 – 56.50) \times 10^3$ 51.20×10^3	>25 µm	NR NR $(3.15 – 3.72) \times 10^{11}$ 3.47×10^{11}	Ziajahromi et al. (2021)
Canada	1.30×10^6	- Primary sludge - Secondary sludge	$(14.90 \pm 6.30) \times 10^3$[c] $(4.40 \pm 2.80) \times 10^3$[c]	>1.0 µm	$(1.28 \pm 0.54) \times 10^{12}$ $(0.36 \pm 0.22) \times 10^{12}$	Gies et al. (2018)
China	5.19×10^4 – 1.37×10^6	- Dewatered sludge	$(1.60 – 56.40) \times 10^3$	37 µm – 5.0 mm	1.56×10^{14}[d]	Li et al. (2018)
China	NR	- Dewatered sludge	$(240.30 \pm 31.40) \times 10^3$	60 µm – 4.2 mm	NR	Liu et al. (2019)
China	NR	- Dewatered sludge	$(4.04 \pm 1.36) \times 10^3$	NR	NR	Xu et al. (2020)
China	3.10×10^6	- RAS - Sludge filter cake	$(36.30 \pm 5.70) \times 10^3$ $(46.30 \pm 6.20) \times 10^3$	0.02 mm – 5.0 mm	7.74×10^{12}	Jiang et al. (2020)
China	1.00×10^5	- Dewatered sludge	2.92×10^3	0.08 mm – 1.70 mm	1.14×10^{11}	Ren et al. (2020)
Finland	NR	- Activated sludge - Digested sludge - MBR sludge	$(23.00 \pm 4.20) \times 10^3$ $(170.90 \pm 28.70) \times 10^3$ $(27.30 \pm 4.70) \times 10^3$	<250 µm and 250 µm – 5 mm <250 µm, 250 µm – 5 mm and >5.0 mm <250 µm and 250 µm – 5 mm	NR	Lares et al. (2018)
Germany	5.00×10^4	- RAS	495.00×10^3	20 µm – 500 µm	8.00×10^8[f]	Sujathan et al. (2017)
Germany	1.10×10^4 – 2.10×10^5	- Dewatered sludge	$(1.00 – 24.00) \times 10^3$	<500 µm	$(1.24– 5.67) \times 10^9$	Mintenig et al. (2017)
Ireland	6.50×10^3 – 2.36×10^6	- Anaerobically digested sludge - Thermally dried sludge - Lime-stabilized sludge	$(4.20 – 15.39) \times 10^3$	45 µm - 212 µm and >212 µm <45 µm, 45 µm - 212 µm and >212 µm	NR	Mahon et al. (2017)

Table 2.1. Continued

Location of WWTP	Population served or PE	Sludge type	Concentration (# of MPs/kg dw of sludge)	MP size range	Discharge by sludge (# of MPs/year)	Reference
Italy	1.20×10^6	- RAS	$(113.00 \pm 57.00) \times 10^3$	10 µm – 5.0 mm	1.24×10^{12}	Magni et al. (2019)
Italy	8.00×10^4	- Primary sludge - WAS - Dewatered sludge	$1.67 \times 10^{3, g}$ $5.30 \times 10^{3, g}$ $4.74 \times 10^{3, g}$	300 µm – 5.0 mm	NR	Pittura et al. (2021)
Korea	6.77×10^4 2.36×10^5 2.45×10^5	- Sludge cake	14.90×10^3 9.66×10^3 13.20×10^3	106 µm - 300 µm and >300 µm	1.09×10^{11} 2.14×10^{11} 2.67×10^{11}	Lee and Kim (2018
Netherlands	NR	- Sewage sludge[h]	510.00 – 760.00[d]	10 µm – 5 mm	NR	Leslie et al. (2017)
Norway	1.82×10^4 – 6.15×10^5	- Dewatered sludge	$(1.70 – 19.84) \times 10^3$	54 µm – 4.99 mm	$5.00 \times 10^{11, d}$	Lusher et al. (2017)
Scotland	6.50×10^5	- Sludge cake	$1.20 \times 10^{3, i}$	1.2 mm – 2 mm	NR	Murphy et al. (2016)
Spain	3.00×10^5	- Anaerobically digested sludge - Heat-dried sludge	$(133.00 \pm 59.00) \times 10^3$ $(101.00 \pm 19.00) \times 10^3$	36 µm – 4.72 mm 29 µm – 2.22 mm	8.00×10^{11}	Edo et al. (2020)
Sweden	1.40×10^4	- Slightly dewatered sludge	$(16.70 \pm 1.96) \times 10^3$	≥ 300 µm	NR	Magnusson and Norén (2014)
Thailand	5.20×10^5	- RAS+WAS	103.40[a]	NR	NR	Hongprasith et al. (2020)
Turkey	1.63×10^6	- WAS	$(5.70 – 11.10) \times 10^{2, a}$	NR	NR	Bilgin et al. (2020)
USA	NR	- Sewage sludge[h]	1×10^3	45 µm – 400 µm	3.98×10^{11}	Carr et al. (2016)

[a] This value represents the number of MPs per liter of sludge. [b] The unit is "mg/kg dry weight of sludge". [c] This value indicates the number of MPs per kg wet weight of sludge. [d] This value reflects the average number of sludge-based MPs determined based on annual total sludge production within that country. [f] This value represents the annual number of MPs per hectare. [g] The unit is "number of MPs/kg TS". [h] Sludge sampling point could not be understood from this article. [i] This value was given as Sun et al. (2019) have reported.

PE: Population equivalent; NR: Not reported; dw: Dry weight; RAS: Return activated sludge; WAS: Waste activated sludge

2.4.3.2 Characteristics of Microplastics in Sewage Sludge

It is not a straightforward task to bring together and summarize the polymer type, shape, and color of MPs in sludge from different studies due to limitations about exact quantification. The first limitation is that the studies typically tend to analyze only a subset of MPs in samples, which brings a question of representativeness. The second limitation is about the varying size ranges targeted from one study to the other, that limits the comparability. In the hint of these limitations, the summary provided below examined 26 different studies that have reported on polymer type, shape, and color of MPs in sewage sludge.

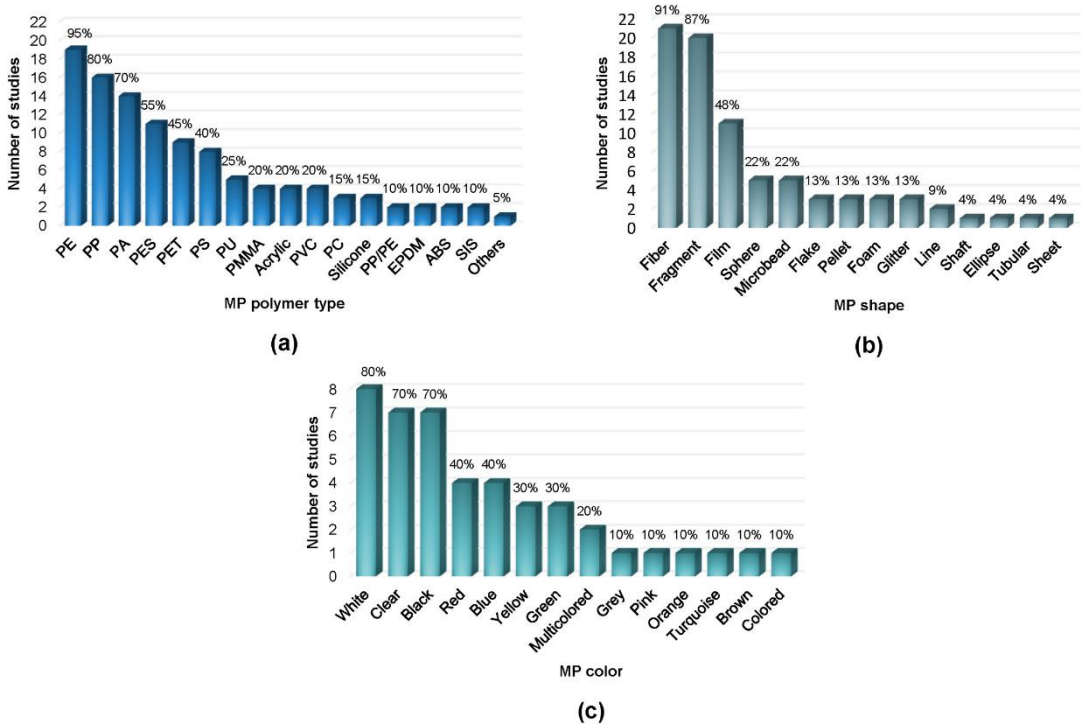

Figure 2.5. Relative reporting frequencies of MPs' (a) polymer types (in a total of 20 studies); (b) shapes (in a total of 23 studies) and (c) colors (in a total of 10 studies) in sludge samples by the results obtained from 26 total articles analyzing sewage sludge samples.

Rather than evaluating the relative abundances of a particular characteristic (i.e., type, shape, and color) per study, their relative reporting frequencies across different studies are combined and summarized in Figure 2.5.

In 20 out of 26 studies, polymer types of MPs have been identified using advanced analytical techniques (Figure 2.5 (a)). Results show that MP composition of sludge reflects our daily habits of plastic consumption and mainly comprises of PE, PP, PA, polyester (PES), PET, and PS. MPs found in sludge and the everyday products containing them have been itemized as PE that is used in personal care products, shampoo bottles, pipes, etc.; PP used in food packaging, snack wrappers, auto parts, etc.; PA used in synthetic clothes, etc.; PES used in synthetic clothes, etc.; PET used for water and other beverage bottles and PS used in foam food containers, eyeglasses, building insulation, etc. One should keep in mind the methodology followed in this part, that brings together data from different studies when assessing the reported existence of polymers. On the other hand, in any individual study, the relative abundance of polymer types in a sample reflects the origin of wastewater (Sol et al., 2020). For example, Xu et al. (2020) have revealed that the detected microfibers (i.e., rayon and PET) and the content of poly(propylene:ethylene) (PP/PE), acrylonitrile butadiene styrene (ABS), and ethylene acrylic elastomer (Vamac) indicated domestic applications and vehicle products as the major MP sources in sludge, respectively.

Majority of examined studies (23 out of 26) have classified MPs into various categories depending on shape, namely, fiber, fragment, film, sphere, microbeads, flake, pellet, foam, glitter, line, shaft, ellipse, tubular, and sheet (Figure 2.5 (b)). According to the studies, classification with respect to shape gives an idea about MP sources. Fibers are the most frequently reported MPs due to high production of synthetic fibers and they generally originate from washing of synthetic clothes and textile handling activities (Li et al., 2018). The second-ranked fragments are mostly secondary MPs, which usually result from industrial production and eroded everyday products. The third-ranked films may originate from erosion of plastic bags and packaging materials (e.g., wrappers). The remaining ones have relatively much less abundances. Literature shows that the lifestyle of people in a country or a region may

be an important factor determining the dominant MPs shape. For instance, high production of textiles such as carpets and curtains in Iran causes fibers to dominate in sludge (Alavian Petroody et al., 2020). Another example is that microbeads are highly abundant in Xu et al. (2020)'s dewatered sludge while not even observed in L. Zhang et al. (2020)'s sludge which clearly reflects the society's habits of consuming daily personal care products.

Only a limited number of studies (10 out of 26) have classified MPs in sludge by their color. Among the reported colors, white, clear/transparent, black, red, blue, yellow, and green are accounted for the highest proportion as shown in Figure 2.5 (c). The distribution is in the same line with results of a survey conducted in China which states that black, red, white, gray, and blue have a greater usage and are the preferred colors (Ren et al., 2020).

Most of the studies have shown that the size of MPs retained in sludge is generally larger than those in wastewater. This can be attributed to the fact that larger MPs hold potential for sinking to the bottom of the tank, while smaller MPs continue to move along the WWTP (Murphy et al., 2016). A study examining both wastewater and sludge treatment lines of a WWTP revealed that 54% of MPs in sludge were between 100-500 µm, 24% were between 10-100 µm, 12% were between 500-1000 µm, and the rest were between 1-5 mm (Magni et al., 2019). Similarly, Raju et al. (2020) revealed that MPs in WAS predominated in larger size classes compared to those in wastewater samples. The MPs in WAS was assorted as follows: >1 mm (9.04%), 250 µm-1 mm (12.65%), 125 µm-250 µm (39.76%), 38 µm-125 µm (21.08%) and 1.5 µm -38 µm (9.68%). Contrarily, some other studies have observed a higher fraction of smaller sized MPs compared to those of larger MPs in sludge (Liu et al., 2019; Mason et al., 2016). Talvitie et al. (2017) attributed this result to the fact that smaller MPs are removed at a higher rate via adsorption on sludge during the sedimentation process.

2.5 Fate of Microplastics During Sludge Treatment Processes

In sludge treatment line of a WWTP, MPs are brought into contact with a wide variety of microorganisms as well as abiotic stress factors including chemicals, heat and pressure (Alimi et al., 2022). Therefore, sludge treatment processes (thickening, dewatering, drying, stabilization, etc.) have a potential to alter the characteristics and the number of MPs, which may increase surface area available for adsorption and desorption of pollutants. Besides, existence of MPs has been claimed to effect sludges starting from the floc formation in biological treatment. Some recent studies have shown that MPs in sludge affect anaerobic digestion efficiency through different impact mechanisms such as excessive reactive oxygen species (ROS) formation and leaching of toxic chemicals.

2.5.1 Effects of Sludge Treatment Processes on Microplastics

2.5.1.1 Thickening/Dewatering/Drying

Thickening is a physical process that concentrate suspended solids through removal of water fraction of sludge. Gravity thickening, dissolved air floatation, centrifugation, gravity belt thickener, and rotary drum thickener are the examples of sludge thickening techniques where physical forces such as gravity settling, floatation and centrifugation are involved. Conditioning is a chemical, physical or thermal process applied on sludge to promote the efficiency of thickening or dewatering by altering the sludge properties. Thus, dewatering capability of sludge is enhanced. Dewatering is the process where significant reduction in water content of sludge is achieved using non-mechanical (e.g., drying beds, lagoons) and mechanical (e.g., filter press, belt press, centrifuges) techniques (Gurjar and Tyagi, 2017; Sanin et al., 2011). Both thickening and dewatering are highly unexplored for MPs' fate and effects. In one recent study it was shown that 6% of the MPs reaching the thickener tank was separated from the sludge solids fraction and returned to the

head of the aeration tank via supernatant (Alavian Petroody et al., 2021). Further in this study, dewatered sludge was found to contain 54% fewer MPs than preceding aerobically digested sludge which was again attributed to the recirculation of MPs via reject water. In another study examining the effects of sludge dewatering techniques with different operating principles on MP concentrations, Li et al. (2018) revealed that the concentration of MPs taken from different sludge dewatering units, in descending order, are belt filter, filter press, centrifuge, and plate-frame filtration. The centrifuge, which provides dewatering based on the density difference between liquid and solids, caused low-density MPs to remain in water phase and, hence yielded the concentration of MPs to be underestimated. Similarly, plate-frame technique caused underestimation of MP concentration, because inorganic conditioners (i.e., lime) added to reduce moisture content of sludge complicated the analysis of MPs (Li et al., 2018).

The treated sludge is intended to be more like a solid rather than a liquid before its disposal, but current dewatering techniques are limited to increasing the solids content up to 35%. To make the sludge drier and even to produce biosolids with high volatile solids content, sludge drying processes are applied with the addition of thermal energy. Direct sludge driers (e.g., belt dryer and flash dryer) and indirect sludge driers (e.g., paddle dryer, hollow-flight dryer and disc dryer) are the common techniques used for this purpose. Drying too has rarely been investigated in the literature; one study encountered showed that MP concentration in the heat-dried sludge did not significantly differ from preceding anaerobically digested sludge (Edo et al., 2020). From this finding, it is inferred that sludge processing at around 300°C may not significantly affect MP particles. In contrast, through visual analysis of MPs in thermally dried sludge, Mahon et al. (2017) have observed that MPs showed characteristics of melting and blistering. With these conflicting findings it is obvious that there is still work to be done to investigate MPs' fate during drying. Sunlight is known to be one of the parameters to induce ageing in plastics and solar dryers are used in drying sludge in medium sized WWTPs in areas of suitable climate. Both

thermal and solar dryers have to be investigated for their effects on MPs as the points of release of sludge from WWTPs.

2.5.1.2 Stabilization

Stabilization process basically aims to reduce the organic matter content in sludge, remove pathogenic organisms and toxicity, reduce odor and promote biogas production potential of sludge through a serious of biological or chemical processes. The most commonly used biological stabilization methods are aerobic and anaerobic digestion, alkali stabilization and composting. By means of these techniques, 35-50% of VS reduction in sludge is generally achieved, making sludge more stable and less attractive to vectors (Sanin et al., 2011).

Limited number of studies have shown that the amount and characteristics of MPs may change depending on the stabilization technique applied on sludge. In order to assess these effects, Mahon et al. (2017) have analyzed the MPs in sludges taken from full-scale anaerobic digestion, thermal drying, and lime stabilization processes. The majority of MPs from lime stabilization was in smaller size classes, which was attributed to shredding and flaking of MPs resulting from the combination of elevated pH, temperature and mechanical mixing. In contrast, MPs from anaerobically digested sludge had the lowest number, which reflected the potential effect of digestion on MPs, but not sufficient evidence of degradation was reached. This study demonstrates that there may be an effect of treatment processes on MPs which in-turn may increase the surface area available for adsorption and desorption of organic pollutants. In another study, the concentrations of MPs have been found in similar levels in sewage sludge samples from full-scale lime stabilization and anaerobic digestion processes (Lusher et al., 2017). Moreover, there was no difference in MP concentrations between full-scale thermophilic and mesophilic anaerobic digesters (Lusher et al., 2017). Similarly, Alavian Petroody et al. (2021) did not experience much difference in the number of MPs when thickened sludge was aerobically digested in laboratory. On the other hand, Chen et al. (2020) have

observed that a full-scale hyperthermophilic composting process biologically degraded 43.7% of PS MPs in sludge within 45 days. In the light of this evidence, two laboratory-scale composting reactors were operated at hyperthermophilic (70°C) and conventional thermophilic (40°C) conditions for 56 days. This study demonstrated that hyperthermophilic bacteria were 6.6 times more effective than the conventional thermophilic bacteria and degraded 7.3% of PS MPs. L. Zhang et al. (2020) have reported that the predominant MPs (>90%) in sewage sludge compost samples was in flake form, which can be attributed to degradation and fragmentation of cellulose-based plastics through aerobic composting at high temperatures (~70°C). They also noted that following fragmentation, it became difficult to detect small sized MPs and the concentration of MPs in finished compost was found lower than that of the raw compost despite compost was reduced to its half in mass during the process (L. Zhang et al., 2020). This finding also critically highlights the need for a reliable analysis method for MPs in sludge samples. In order to examine whether MPs degrade at conventional conditions, El Hayany et al. (2020) monitored their behavior during a semi-industrial scale aerated windrow composting process. While the number of MPs was not affected, particle sizes were reduced during the process. These findings suggested that conventional co-composting performed at lower temperatures cannot biodegrade MPs in contrast to the hyperthermophilic composting technology (El Hayany et al., 2020).

2.5.1.3 Sludge Disintegration

Application of anaerobic digestion, the energy positive stabilization process of WWTPs, is often limited by long retention time (20–50 days) and low digestability (20–50%) due to slow hydrolysis rate of sewage sludge, consisting of microorganisms, extracellular polymeric substances (EPS) and inorganic salts (Gurjar and Tyagi, 2017; Yan et al., 2021). EPS is a high-molecular weight mixture of polymers excreted from microorganisms, composed of proteins, polysaccharides, humic substances and nucleic acids (Zeng et al., 2016). The low biodegradability of

EPS (30-50%) and microbial cell wall made of peptidoglycans are responsible for extending the hydrolysis step of anaerobic digestion (Yan et al., 2021).

To improve the rate of sludge hydrolysis and hence the efficiency of the anaerobic digestion process, various sludge disintegration methods have been developed, such as thermal, chemical, ultrasonic, and biological as shown in Table 2.2 (Chen et al., 2007). They can be applied individually or in combination to maximize WAS solubilization. These methods are all based on the principle of lysing the sludge cells, releasing the intracellular substances, and making them more amenable to further microbial action. So, (i) hydrolysis rate is increased; (ii) hydraulic retention time is decreased resulting in enhancement in amount of sludge to be treated in the same volume; (iii) biogas production is promoted; and (iv) dewatering properties of sludge are enhanced.

Although it is very likely to observe changes in physical and chemical properties of MPs during sludge disintegration due to the harsh conditions applied (e.g., chemicals, heat, microorganisms), there is no study investigating this mechanism in the literature yet.

Table 2.2. Disintegration methods applied for improving the efficiency of anaerobic digestion (Khanh Nguyen et al., 2021; Shrestha et al., 2020; Y. Xu et al., 2020; Zhen et al., 2017)

Disintegration method	Type of method	Mechanisms involved	Effect on anaerobic digestion
Mechanical	Ultrasonication	Cavitation formation at low frequencies Chemical reactions at high frequencies	40-58% increase in biogas production
	Microwave	Internal heat mechanism with frequencies from 0.3 to 300 GHz	20-53% increase in biogas production
	High Pressure Homogenizer	Strong depressurization	43-90% increase in biogas production
Chemical	Acidic	Hydrolysis of hemicellulose using HCl, H_2SO_4, H_3PO_4 or HNO_3 Breakage of sludge flocs	14-24% increase in biogas production
	Alkaline	Solvation and saponification using NaOH, KOH, $Mg(OH)_2$ or $Ca(OH)_2$	38-80% increase in biogas production
	Ozonation	Kinetic reaction between dissolved ozone and sludge liquor	9% increase in VS removal 8-200% increase in biogas production
	Fenton Oxidation	Formation of destructive hydroxyl radicals	31-72% increase in VS removal 19-30% increase in CH_4 production
Thermal	Low Temperature	Heating at T<100ºC	20-150% decrease in VS content 10-100% increase in CH_4 production
	High Temperature	Heating at T>100 ºC	10-160% decrease in VS content 10-150% increase in CH_4 production
Biological	Thermal phased AD (TPAD)	Thermophilic temperature promotes hydrolysis of sludge prior to mesophilic AD	10-70% decrease in VS content 20-50% increase in CH4 yield
	Enzymatic	External addition of enzymes to break organic constituents in sludge	16-55% decrease in VS content 12-40% increase in CH_4 yield

2.5.1.4 Final Disposal

Final disposal option adopted for treated sludge largely varies in different countries according to their related regulations. Due to its high organic and nutrient content, land application of sludge as a soil conditioner or fertilizer has been the major recycling route. In North America and Europe sewage sludge generated is beneficially used up to 50% by recycling on land. Landfilling is an unsustainable but still in use sludge disposal option in some countries. While the U.S. continue to use, Europe has started to restrict applying this method. Incineration, a common approach in Europe, convert volatile solids in sludge into CO_2, H_2O and inert residue, thus recovers the energy content of sludge for beneficial use. Besides, sufficiently dried sludge can be incinerated in cement kilns to provide additional energy source. Residual ash from incineration can also be used as a raw material.

Both land application and landfilling methods have the potential to spread MPs accumulated in sludge to the environmental systems. Mohajerani and Karabatak (2020) have estimated that the biosolids applications in the EU, USA, China, Canada, and Australia annually add 26,042, 21,249, 13,660, 1,518 and 1,241 tonnes of MPs to farmlands, respectively. As covered above, there are very limited studies in literature on the fate of MPs in sludge treatment and those demonstrate that existing sludge treatment processes cannot remove MPs effectively. For that reason, studies suggest that land application of sludge can be a significant source of MP pollution in the environment (Z. Chen et al., 2020). An additional concern is that MPs with large specific surface area, act as vectors for micropollutants, and may further enhance the detrimental effects on organisms (X. Li et al., 2019). Wastewater treatment processes have been found to cause changes in MPs' physicochemical properties through mechanical abrasion and microbial interaction, which may enhance their capacity to adsorb pollutants (Mohajerani and Karabatak, 2020). Additional findings such as the one by Li et al. (2019) reveals that the adsorption potential of sludge-based MPs for

Cadmium (Cd) was an order of magnitude higher than that of virgin MPs, strengthens the concerns related to land application.

2.5.2 Effects of Microplastics on Sludge Treatment Processes

Apart from the studies summarizing the fate of MPs during sludge treatment processes, the existence of MPs has also been reported to affect the operation of some sludge treatment processes starting from the floc formation stage.

2.5.2.1 Floc Formation

Recent studies are showing that MPs can affect sludge floc formation and hence affect sludge characteristics which ultimately impact dewatering and thickening properties of sludge. Biological sludge with high activity, strong floc structure and good sedimentation performance are critical in sustaining effluent quality (H. Li et al., 2020). Considering treatment and disposal of WAS holds a significant share in total operational costs of WWTPs, it is important to understand the potential effects of MPs on sludge formation and characteristics such as settleability, floc size and EPS composition, which further impact the thickening and dewaterability behavior of sludge. With this intention, Xu et al. (2021) have inspected the effects of chronic exposure of activated sludge for different MP types and sizes on sludge characteristics by analyzing floc structure, EPS composition, sludge activity and microbial community structure. They have reported that MPs in millimeter sizes significantly (29.6 – 47.7%) reduced the dewaterability of sludge mainly due to their physical crushing effect on sludge flocs. Nano-sized MPs also caused loss in dewaterability, but via different and indirect mechanism: inhibiting the sludge activity and thus reducing the abundance of microorganisms and further changing the composition of EPS. Qian et al. (2021), on the other hand, investigated the acute effects of PS NPs with different surface functional groups (i.e., PS, PS-COOH, PS-NH_2) on EPS composition of activated sludge and experienced varying levels of

cytotoxicity attributed to the difference in surface potentials and hence the binding affinity to the cells. Reasonably but different from Xu et al. (2021), all three types of PS NPs were found to promote the dewatering capacity of activated sludge. Similarly, Li et al. (2020) inspected the effect of short-term exposure to PS NPs on the activity and sedimentation performance of activated sludge and revealed that 1) increasing plastic concentration inhibited the endogenous respiration and negatively affected the mass transfer in sludge; 2) PS NPs adsorbed on the floc surfaces increased the zeta potential which resulted in low sludge aggregation; 3) increasing PS NPs concentration gradually decreased the protein/polysaccharide ratio in EPS, which affected the sludge aggregation and sedimentation. These findings show that in addition to the observations of direct effects of MPs in thickening and dewatering, MPs in wastewater may induce an indirect effect on these processes starting from the sludge floc formation stage affecting EPS formation and possibly the dominating microbial consortia.

2.5.2.2 Anaerobic Digestion

Anaerobic digestion is a biochemical process by which complex organic matter is decomposed by a diverse microbial consortium under anaerobic environment, resulting in the formation of methane and carbon dioxide. It is a well-established and largely implemented sludge stabilization process providing pathogen removal, reduction of sludge volume, and thereby production of biogas (Khanh Nguyen et al., 2021). The degradation reaction is shown in Equation 2.1.

$$\text{Organic matter} + H_2O \rightarrow CH_4 + CO_2 + \text{new cells} \qquad \text{(Equation 2.1)}$$

Either primary or secondary sludge, and in most of the cases mixture of them, can be fed into anaerobic digesters as an organic matter. Methane production makes this process the energy-positive unit of WWTPs. Due to its high energy content (35,800

kS/m^3), methane can be used for electricity generation and meets the heating requirements of a WWTP. New cells, on the other hand, are produced in minor quantities (4-10% of COD) (Sanin et al., 2011).

During AD, typical VS reductions are 40-70% for primary sludge, 20-50% for WAS, and 40-60% for mixture of these sludges. COD reductions are also in the same line with those of VS. The volume of biogas produced is related to the amount of organic matter destroyed during digestion. In theory, for each gram of COD destroyed, 0.35 m^3/kg of methane is produced, regardless of the organic matter used. In terms of VS content, specific gas production is in the range of 0.75-1.12 m^3/kg VS destroyed or 0.5-0.75 m^3/kg VS loaded (Appels et al., 2008; Metcalf and Eddy, 2003). Moreover, typical methane content of biogas produced from anaerobic digestion of municipal sludges are 60-75% (Parkin and Owen, 1986).

Anaerobic digestion is a multi-stage process that includes hydrolysis, acidogenesis, acetogenesis and methanogenesis as shown in Figure 2.6. In the hydrolysis step, both insoluble organic material and higher molecular compounds such as lipids, polysaccharides, proteins and nucleic acids are degraded into soluble organic materials. The acidogenesis step further breaks these smaller substances into volatile fatty acids (VFA), carbon dioxide, hydrogen sulfide, ammonia, and other byproducts. The next step includes conversion of VFAs into acetate, hydrogen and carbon dioxide by acetogens. In the final step of methanogenesis, two different groups of methanogenic bacteria take part in methane production. While the first group of organisms (acetoclastics) split acetate into methane and carbon dioxide; the second group (hydrogenotrophics) utilizes hydrogen (electron donor) and carbon dioxide (electron acceptor) to produce methane (Appels et al., 2008; Fang et al., 2014). In theory, as 70% of methane is produced from acetate; 30% is generated from carbon dioxide and hydrogen (Elalami et al., 2019).

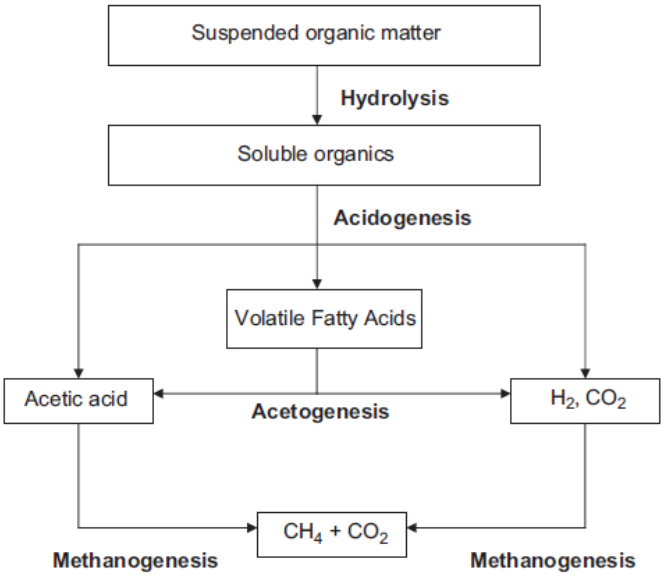

Figure 2.6. Steps in anaerobic digestion process (Appels et al., 2008)

The main factors affecting the digestion efficiency are pH, temperature, C/N ratio, organic loading rate, mixing, retention time, as well as presence of inhibitory substances. 1) Various groups of microorganisms are involved in anaerobic digestion, and they have different vulnerabilities to pH alterations. It is critical to adjust an optimal pH value for each microorganism group to make them work in a healthy coordination. The pH range of 6.5-7.5 is generally recommended to promote the growth of methanogens, the most sensitive group. 2) Temperature affects the reaction rate as it has a direct impact on microbial growth. Anaerobic digestion process can be conducted at three different temperature ranges: psychrophilic (10-15°C), mesophilic (25-48°C), and thermophilic (>60°C). Although thermophilic conditions yield the best biogas production rate, its high energy requirement for temperature maintenance makes it costly to implement. Mesophilic AD is the most commonly applied option with low energy requirements, the production of stable solids, and pleasant biogas production (Shrestha et al., 2020). 3) C/N ratio defines the amount of carbon and nitrogen present in substrate consumed by microorganisms to grow and build cell structure. The ratio should be 20-25 to conduct anaerobic

digestion optimally. 4) The organic loading rate is the amount of substrate fed per day and per unit volume of the digester. When a digester with a limited hydrolysis rate is overloaded, an unhydrolyzed portion of sludge remains that entails low methane yield. If the methanogenesis step is having difficulty and the digester is highly loaded, VFA accumulation and thus low methane production occur. 5) Adequate mixing should be provided to enhance the contact between substrate and microorganisms, as well as to maintain the homogeneity of critical parameters throughout the digester (Elalami et al., 2019; Sanin et al., 2011). 6) Time is very critical in achieving adequate contact and hence VS reduction in a digester. The relevant operational parameters to be optimized are hydraulic retention time (HRT) and solids retention time (SRT), the average time water molecules and solids reside in a digester, respectively. Having a sufficient SRT is also important when microorganisms need to adapt to toxic conditions. 7) The most common inhibitory substances reported for the anaerobic digestion process are alkali and alkaline-earth metals, heavy metals, ammonia-nitrogen, sulfide, and various organic compounds. Even a necessary nutrient can cause toxicity if added in excessive amounts (e.g., nitrogen and phosphorus). In some cases, detoxification can be accomplished by precipitation or complex formation, stripping, adsorption, and the addition of antagonistic chemicals. Along with these methods, providing long SRT has extreme importance in allowing microorganisms to get a chance to acclimatize toxic substances (Parkin and Owen, 1986).

Existence of MPs in sludge has been lately shown to affect the efficiency of anaerobic digestion both positively and negatively. Their impact on methane and hydrogen production through anaerobic digestion of sludge were investigated based on the type, size and amount of MPs, and the summary of these studies are given in Table 2.3. These effects can be associated with four different toxicity mechanisms as given in Figure 2.7.

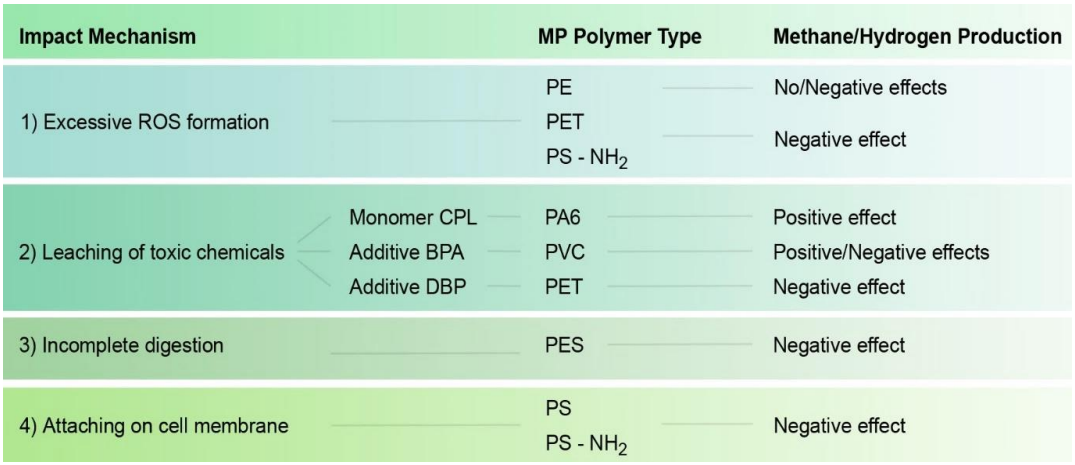

Figure 2.7. Summary of effects of different MPs on anaerobic digester performance

First, the existence of large amount of MPs in digesting sludge can induce cytotoxicity by generating reactive oxygen species (ROS) which further causes loss in cell viability. ROS formation is a natural process, and they are by-products of normal cell activity. However, their overproduction causes oxidative stress and even oxidative damage. MPs with large specific surface area are shown to be responsible for additional ROS production (Wei et al., 2019a, 2019c). For instance, Wei et al. (2019a) showed that while low dose (10-60 particles/g TS) of PE MPs in sludge did not have a significant effect, their high dose (100-200 particles/g TS) led to a decrease in methane production. They attributed this pattern to rising ROS levels in response to increasing MP number, which negatively affected the hydrolysis, acidification, and methanogenesis processes during anaerobic digestion of WAS.

Second, toxic chemicals leaching from MPs can affect the digestion efficiency differently depending on their concentration in sludge as reported by Wei et al. (2019b) When BPA leached from small amount of PVC MPs (10 particles/g TS), a positive contribution to methane production has been observed due to the enhanced sludge solubilization. The reason behind that is, leaching BPA intensifies the breakdown of microbial cell walls and EPS in WAS to form more soluble substances. Despite the improved solubilization at higher doses (>20 particles/g TS), inhibitory effect of BPA on sludge hydrolysis and acidification processes overweighed, resulting in decreased digestion efficiency in parallel with the reported enzyme

activities (Wei et al., 2019b). Besides, H. Chen et al. (2020) has shown that leaching of monomer Caprolactam (CPL) from PA6 MPs was the primary mechanism responsible for the increase in methane production at all doses (5-50 particles/g TS). Unlike BPA, the leaching CPL resulted in binding onto enzyme molecules and improved their affinity with substrates and catalytical activity. However, at higher doses of PA6 MPs (20-50 particles/g TS), this promoting effect weakened because higher concentrations of CPL might occupy active sites of the enzymes (H. Chen et al., 2020). In another study, Wei et al. (2019c) observed the combined impact of the leaching additive (i.e., Di-n-butyl phthalate (DBP)) and ROS production from PET MPs during alkaline anaerobic fermentation of WAS. They have reported a declined hydrogen yield at all doses of PET MPs (10-60 particles/g TS) due to the loss of cell viability and the change in the shift of microbial community toward the direction against hydrolysis and acidification processes.

The third mechanism, where MPs' existence causes incomplete digestion, was reported by L. Li et al. (2020). They have shown that PES MPs at the abundance of 1-200 particles/g TS caused high amounts of organic matters and nutrients to accumulate during the process, which further led to a decrease in methane production without any linear correlation with the number of MPs.

Lastly, nanoplastics (NPs) with small sizes can attach onto cell membranes in sludge, change cell permeability and may further enter the cell. Fu et al. (2018) showed PS NPs to adhere to the cell membrane of microorganisms during anaerobic digestion, which adversely affected their activities (i.e., growth and mechanism) and hence methane production. Similarly, PS-NH_2 (amino polystyrene) NPs increased cell permeability and induced ROS generation during the anaerobic hydrogen fermentation of sludge, resulting in a significant reduction in hydrogen yield (W. Chen et al., 2020). Interestingly, the addition of perfluorooctane sulfonate (PFOS) into the reactors considerably alleviated the NPs' toxic impact on thermophilic hydrogen producing bacteria because the interaction of PFOS with EPS might disable NPs to enter the bacterial cells (W. Chen et al., 2020).

Table 2.3. Reported effects of MPs and NPs on methane and hydrogen production from sludge

MP type	Process details	Time (days)	Operational conditions	Size	Amount (# of MPs/g TS)	Effect of plastics	Reference
PS	Lab-scale batch AD of sewage sludge	37	Mesophilic	54.8 nm	0.05[a] 0.1[a] 0.2[a]	↓ CH_4 by 4.7% ↓ CH_4 by 6.6% ↓ CH_4 by 14.4%	Fu et al. (2018)
PE	Lab-scale AD of WAS (BMP test)	44	Mesophilic	40 µm	10.0 30.0 60.0 100.0 200.0	No effect No effect No effect ↓ CH_4 by 12.4% ↓ CH_4 by 27.5%	Wei et al. (2019a)
PVC	Lab-scale AD of WAS (BMP test)	45	Mesophilic	1.0 mm	10.0 20.0 40.0 60.0	↑ CH_4 by 5.9% ↓ CH_4 by 9.4% ↓ CH_4 by 19.5% ↓ CH_4 by 24.2%	Wei et al. (2019b)
PES	Lab-scale AD of WAS (BMP test)	59	Mesophilic	200 µm	1.0 3.0 6.0 10.0 30.0 60.0 100.0 200.0	↓ CH_4 by 11.5% ↓ CH_4 by 9.1% ↓ CH_4 by 10.1% ↓ CH_4 by 4.9% ↓ CH_4 by 9.7% ↓ CH_4 by 6.8% ↓ CH_4 by 7.1% ↓ CH_4 by 7.3%	L. Li et al. (2020)
PA6	Lab-scale AD of WAS (BMP test)	45	Mesophilic	425-850 µm	5.0 10.0 20.0 50.0	↑ CH_4 by 4.84% ↑ CH_4 by 39.5% ↑ CH_4 by 16.1% ↑ CH_4 by 12.9%	H. Chen et al. (2020)
PET	Lab-scale alkaline anaerobic fermentation of WAS	21	Mesophilic	25 ± 2 µm	10.0 30.0 60.0	↓ H_2 by 11.6% ↓ H_2 by 18.4% ↓ H_2 by 29.3%	Wei et al. (2019c)
PS-NH_2	Lab-scale fermentative hydrogen production from sludge	7	Thermophilic	70 nm	0.2 x 10^{-3}[a]	↓ H_2 by 53.9%	W. Chen et al. (2020).

AD: Anaerobic digestion; WAS: Waste activated sludge; BMP: Biomethane production; NR: Not reported.
[a] The unit of this value is "g NPs/L sludge".

In summary, depending on the type, size, and concentration, MPs and NPs can exert dissimilar effects on different steps of the anaerobic process. In fact, an efficiently working anaerobic digestion process is critical to ensure sustainable sludge

management. Concordantly, exploring the scenarios where different MP and NP polymers, operational conditions (e.g., temperature, pH, time, etc.), and microbial communities are involved is of great importance.

Much limited studies are focusing on aerobic digestion process compared to anaerobic digestion. One study reviewed comparatively evaluated the effects of MPs on aerobic digestion of WAS via two different entry routes of MPs into the WWTP (Wei et al., 2021). In addition to the common approach of direct addition to a digester, authors also spiked PET MPs into the biological wastewater treatment system to better reflect real life and observed differences in toxicity mechanisms and the level of inhibition on digestion efficiency. When MPs were spiked into wastewater, hydrolysis decreased but WAS solubilization increased due to the change in characteristics of WAS in the existence of MPs. Direct addition into the digester, on the other hand, caused fewer impact on solubilization and severe inhibition on hydrolysis, thus posed a lot more serious inhibition on digestion occurred (Wei et al., 2021).

2.6 Degradation Potential of Polyethylene Terephthalate

PET is a semi-crystalline thermoplastic polyester that is strong and durable in various environmental conditions, intrinsic properties of which are given in Table 2.4. It is one of the most commonly used polymer types in the packaging and textile industries and accounts for 8% of global plastic demand based on 2019 data (PlasticsEurope, 2020).

The chemical structure of PET is composed of repeating units. Its monomer consists of an aliphatic chain coupled with an aromatic ring, as shown in Figure 2.8 (Fotopoulou and Karapanagioti, 2015). Polymers with “hetero” or C-O backbones (e.g., PET, PU) are particularly more susceptible to degradation than those with “pure” or C-C backbones (e.g., PVC, PS, PE, PP). Another determinant of polymer degradability is related to the functional groups involved. Having an aromatic group makes it difficult to degrade polymer structure. Therefore, PET having easily

hydrolysable ester bonds is non-degradable under natural conditions due to its aromatic group (Webb et al., 2013).

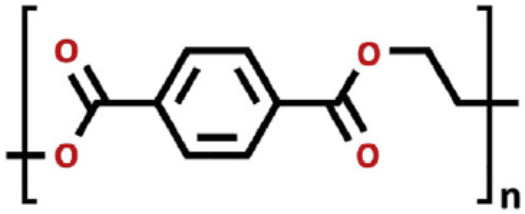

Figure 2.8. Chemical structure of PET (Crawford and Quinn, 2016)

PET polymers are produced with different crystallinities according to their usage area. While PET used for bottle and textile have high crystallinity of 30-40%; those used for packaging have a low crystallinity of 8% (Kawai et al., 2019). The increased degree of crystallization limits the movement of polymer chains and decreases the availability of the chains for any degradative agents such as enzymes (Webb et al., 2013).

Table 2.4. Intrinsic properties of PET polymers (Webb et al., 2013)

Parameter	Value
Average molecular weight	30,000 – 80,000 g/mol
Density	1.41 g/cm^3
Melting temperature	255 – 265°C
Glass transition temperature	69 – 115°C
Young's modulus	1700 MPa
Water absorption (24 h)	0.5%

Despite their non-biodegradable nature, PET type plastics may experience chemical and physical changes in their structure under environmental conditions. When released into the environment, PET plastics are exposed to natural weathering conditions, which causes them to break down to micron sizes (i.e., MPs) (Sang et al., 2020). Up to now, several lab-scale studies trying to mimic natural weathering mechanisms and field studies investigating the effects were conducted. In a field

study, Ioakeimidis et al. (2016) collected PET bottles from the bottom of Saronikos Gulf (from 150-350 m deep) and classified them according to their expiration dates, that are 90's bottles (1997, 1998, 1999) and millennium bottles (2001, 2008, 2011, 2014). In order to determine any changes occurred in functional groups and surface morphology, all the collected bottles were analyzed using the attenuated total reflectance - Fourier transform infrared spectroscopy (ATR-FTIR) and scanning electron microscope (SEM), respectively. Compared to the virgin PET bottles of 2015, a decrease in intensity at 1715 cm^{-1}, 1245 cm^{-1} and 1100 cm^{-1}; and even disappearance at 870 cm^{-1} and 730 cm^{-1} were observed in eroded plastics, which correspond to ketones (C=O), ether aromatic (C-O), ether aliphatic (C-O), aromatic (C-H) and aromatic (C-H) bonds, respectively. Besides, outer and inside PET surfaces showed similar spectra, attributed to that degradation occurred on both sides. In line with the results of ATR-FTIR, SEM showed that older PET bottles had more cracked and uneven surfaces. According to the authors, the estimated degradation mechanism starts with the photolysis of PET and continue with hydrolysis after sinking of weathered bottle to the sea floor (Ioakeimidis et al., 2016).

PET is susceptible to hydrolytic degradation in water via cleavage of ester linkages, especially above its glass transition temperature (Allen et al., 1991). This process results in formation of carboxylic acid and alcohol functional groups and its rate is promoted under acidic and alkaline conditions, as shown in Figure 2.9. Hence, once carboxylic end groups are formed, hydrolysis of PET is autocatalyzed (Gewert et al., 2015). In a lab-scale study aiming to understand hydrolysis mechanism of PET under different conditions, PET films in size of 100 nm were submersed in (1) deionized water at 90°C for 8 days and (2) 1% KOH solution at 90°C for 4 h. Using FTIR-RAIRS (reflection absorption infrared spectroscopy), they observed that hydrolytic degradation occurs much faster in alkaline environment. Both applications caused significant changes in carbonyl bonds, which was attributed the formation of seven-membered rings and acid dimers in water and alkaline solution, respectively. Authors concluded that hydrolysis in water occurred at terminal ester linkages while it happened randomly in alkaline solution (Sammon et al., 2000).

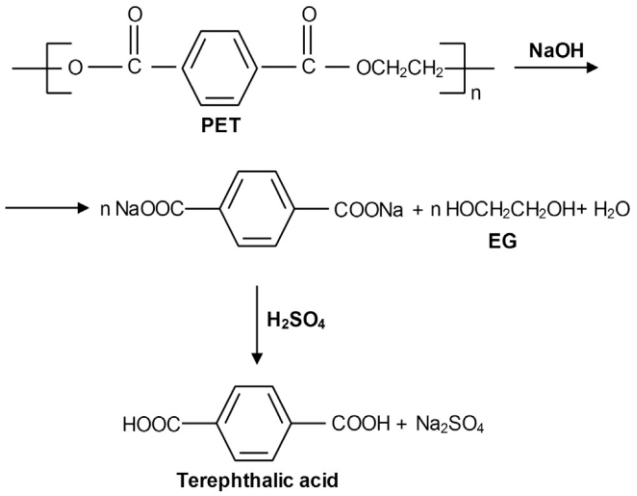

Figure 2.9. Alkaline hydrolysis of PET using NaOH (EG stands for ethylene glycol) (Al-Sabagh et al., 2016)

In order to understand the hydrolytic degradation mechanism resulting in the formation of secondary MPs, Arhant et al. (2019) immersed 200 µm sized films of PET into pure water at 80-110°C for up to 150 days. Based on differential scanning calorimetry (DSC) results, they observed an increase in crystallinity from 33% (unaged) to 50% in 14 days of heat application. This was attributed to the chemi-crystallization process since the heat applied was above T_g that causes chain scission in the amorphous phase of PET MPs. Moreover, size exclusion chromatography (SEC) measurements showed a linear decrease in molar mass as the ageing time progressed. These changes altered polymer's tensile properties. Once molar mass of PET reached 17 kg/mol, its behavior switched from ductile to brittle, which further would stimulate the formation of microplastics.

The compact structure of PET makes it strong against microbial or enzymatic attack. Yet, Zhang et al. (2004) found evidence of PET fiber degradation by the applications of both lipase and different microbes. After analyzing it using SEM and high-performance liquid chromatography (HPLC) techniques, they found small cracks and voids on plastic surface and the formation of terephthalate acid (TA), a degradation product of PET. Other than PET fiber, they tried to biodegrade its subunit diethylene glycol terephthalate (DTP) and achieved more than 90% DTP

degradation by microbes in 24 days and 40% by lipase in 24 h. This demonstrate the fact that polymeric state is the reason for stability of PET plastics.

2.6.1 Effect of Sludge Disintegration

As mentioned in the previous chapters, when plastics are exposed to abiotic factors, the changes observed in their mechanical, physical, and chemical structure make them more vulnerable to biodeterioration. In real life, a number of external stress conditions are unintentionally applied to MPs in sludge during sludge treatment processes including disintegration practices to increase the level of solubilization before anaerobic digestion.

Although no study has yet considered the impact of sludge disintegration processes on deterioration of MPs, an idea can be derived from the results of Hurley et al. (2018) and X. Li et al. (2020) investigating the impacts of methods which are used to remove organic materials in samples during MPs analysis on MPs' characteristics.

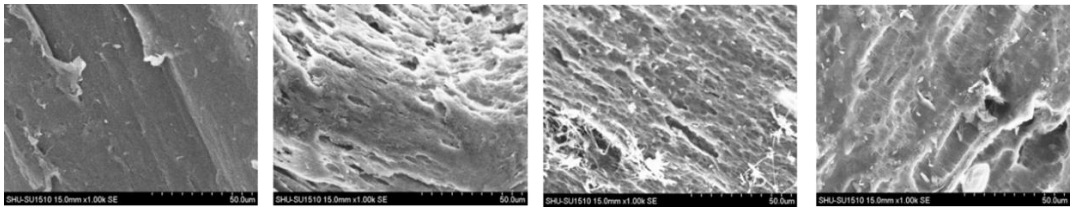

(a) **(b)** **(c)** **(d)**

Figure 2.10. Change in morphology of PET MPs after exposed to alkaline pretreatment. SEM images of virgin PET (a); and PET after 1 M NaOH (b); 5 M NaOH (c); 10 M NaOH (d). Adapted from X. Li et al. (2020)

Hurley et al. (2018) found that treatment of sludge with NaOH (1 and 10 M) caused up to 59.9% and 27.8% decrease in mass and size of PET type of MPs, respectively. Similarly, X. Li et al. (2020) revealed that application of NaOH (1, 5 and 10 M) causes 53.5% and 16.7% decrease in mass and size of PET MPs, respectively, as shown in Figure 2.10.

Consideration of all these results bring the question whether the disintegration processes applied for sludge minimization and biogas maximization can act similarly to the abiotic factors mentioned leading to the deterioration of plastics and easing up possible biodegradation during stabilization.

2.6.2 Disintegration Methods Prevailing in Degradation of PET MPs

As mentioned earlier, PET is prone to hydrolysis in their ester groups in an alkaline environment as well as in the presence of heat. These are the conventional conditions applied to WAS with disintegration techniques prior to anaerobic digestion in WWTPs. Thus, PET MPs in sludges subjected to alkaline and/or thermal disintegration may deteriorate to some extent, initiating biodegradation in subsequent anaerobic digesters.

2.6.2.1 Alkaline Disintegration

Alkaline disintegration is a widely used technique based on solvation and saponification mechanisms to make refractory putrescibles accessible to extracellular enzyme (Chen et al., 2007). Ability to depolymerize and cleave lignin-carbohydrate linkages makes alkaline disintegration more suitable for lignin breakdown compared to acidic pretreatment. It also saponifies intermolecular ester bonds -to a lesser degree than acidic pretreatment- and hence solubilizes xylan hemicellulose. Moreover, adding alkalies into sludge provides additional alkalinity, which enhances the buffer capacity of anaerobic digester and process stability (Zhen et al., 2017). Alkaline disintegration was also proven to increase the sludge loading rates per reactor volume as it efficiently solubilized sludges both with low and high TS content (up to 25 g TS/L) (de Sousa et al., 2021).

The solubilization efficiency achieved depends on the chemical type and dose used. Studies in literature applied pH ranges from 8 to 12 for 30 min to 8 days (Elalami et al., 2019). The relative effectiveness of alkalies can be listed in descending order:

$NaOH > KOH > Mg(OH)_2 > Ca(OH)_2$. The reasons have been attributed in literature to divalent agents' (i) partial dissolution behavior; (ii) potential to re-flocculate the sludge; and (iii) potential to precipitate carbonate and phosphate, which reduces the methanogenic activity during anaerobic digestion and buffer capacity of sludge (Jin et al., 2016; Kim et al., 2003). However, too high sodium and potassium concentrations may also cause inhibitory impact on anaerobic digestion (Carrère et al., 2010). Besides, neutralization of the disintegrated sludge, which is a necessity before adding into digester, increases mineral content of digested sludge (Zhen et al., 2017). In a study investigating relative efficiencies of different NaOH concentrations, disintegration with 0.5 M NaOH caused strong inhibition on anaerobic digestion due to the formation of high salinity environment. It was also found that 0.1 M NaOH is the optimal dose providing 38.3% of organic degradation, 0.65 L/g VSS of biogas yield and improved settling ability of digested sludge (Li et al., 2012). Doğan and Sanin (2009) compared the effects of applying pH 10 and pH 12 on batch anaerobic digestion. Even though pH 12 provided more than 2 times higher COD solubilization compared to pH 10, each technique provided almost the same amount of enhancement (by 5.8% over the control) in methane production. Similarly, de Sousa et al. (2021) compared the disintegration efficiencies of applying pH 10, 11 and 12 by considering solubilized compounds, treatment time and TS content of WAS. WAS solubilization was achieved the highest at pH 12 and it increased over time. Yet, highest increase in solubilization occurred in the first 0.25 h. Thus, BMP test carried out at these conditions showed an increase in methane yield by 3.6-fold over the control sludge.

2.6.2.2 Thermal Hydrolysis Process (THP)

THP is a largely implemented disintegration technique during which heat is applied to break the gel structure in sludge and release of linked water at around 60 to 180°C. It provides sludge dewatering, pathogen destruction, odor removal, and sludge volume reduction along with enhancement of biogas (Chen et al., 2007). Sludge

solubilization efficiency of this method theoretically relies on treatment time and applied temperature. However, duration of treatment is shown to have relatively less importance (Carrère et al., 2010). There are different temperature configurations applied up to now: low-temperature (<100°C), high-temperature (>100°C), and freeze/thaw disintegration (Khanh Nguyen et al., 2021). THP has been mostly used in combination with other techniques.

In literature, laboratory scale low temperature applications have yielded 20-150% decrease in VS content of sludge and 10-100% increase in methane production compared to a control. High temperature applications, on the other hand, have ensured 10-160% decrease and 10-150% increase, respectively (Khanh Nguyen et al., 2021).

Low temperature hydrolysis is generally applied at temperatures around 70-95°C, and the duration of treatment dominates in determining the solubilization efficiency. Low temperature THP applications have been reported to require longer time to obtain a similar level of biogas enhancement compared to those with high temperatures. Xu et al. (2014) thermally disintegrated WAS at 70°C for 9 h and obtained almost 72-fold increase in sCOD, which yields 32.07% improvement in biogas production over the control sludge.

High temperature applications have been reported to be more effective at 160-180°C with less time requirements (> 1 hour) for higher COD solubilization along with a pleaser increase in dewaterability and reduction in VS (Shrestha et al., 2020). However, increased solubilization achieved after disintegration may not always result in an improved digestion efficiency. Applying harsh disintegration conditions have been shown to cause release of inhibitory substances to liquid portion of sludge. At higher temperatures (>200°C), refractory products can be formed as a result of caramelization. Therefore, the efficacy of disintegration methods should be linked to the digestion efficiency obtained rather than the WAS solubilization (Mostafa et al., 2020).

Moreover, full-scale applications of THP are very popular and there are several patented systems efficiently operated. Blue Plains WWTP, located in Washington DC, is the first full-scale example of the Cambi thermal hydrolysis process in the US and is currently the largest Cambi system facility in the world (Cambi Group AS., 2019). The process treats sludge at 150-165°C for 20-30 min at 8-9 bar pressure (Zhen et al., 2017). Pilot-scale studies prior to the installation of the full-scale Cambi system showed that THP applications produce 24 to 59% more biogas compared to the conventional digestion system (Wilson et al., 2011).

2.6.2.3 Combined Disintegration

Several disintegration techniques have been integrated up to now with the intent of obtaining synergetic impacts on AD of sludge (Elalami et al., 2019). These combined techniques generally prevail with less energy and capital cost requirements, as well as easy operation, which strongly effect the choice of the techniques to be integrated (Shrestha et al., 2020). Some examples of this method can be listed as thermal& alkaline, thermal& ultrasound, and microwave& acidic.

The sequence of methods has an important effect on dissolution rate. In a study integrating alkaline and thermal disintegration in different orders, Zou et al. (2020) found that alkali-thermal disintegration surpass in COD solubilization rate to simultaneous thermal and alkali, and thermal-alkali disintegration techniques. The findings of Mostafa et al. (2020) promote this claim that higher solubilization of WAS is achieved when alkaline addition is applied prior to thermal disintegration. They attributed this to the better dissolution of the lipid content of WAS, which has low solubility by thermal treatment, by saponification with strong OH- attack (Mostafa et al., 2020). Similarly, Toutian et al. (2021) believe that alkali dosing before thermal hydrolysis is a more cost-effective option as organic acids are released from the microbial biomass during thermal hydrolysis leading to self-neutralization of sludge. If heating is applied first, organic acids released from the disintegrated biomass reduces pH of sludge, which causes two problems: (1) more

alkali would be required to obtain the same degree of dissolution; (2) sludge would leave with less organic acid release potential, resulting in the need to add extra acid to neutralize the sludge prior to anaerobic digestion.

2.6.2.3.1 Thermo-Chemical Disintegration

The integration of chemical and thermal techniques mainly aims to reduce the chemical consumption. Moreover, the use of high temperatures in combination with chemicals generally increases the solubilization efficiency. Hence, 22 to 97% increase in biomethane yield is achieved by thermo-chemical disintegration depending on the initial biodegradability of sludge (Toutian et al., 2021). Alkaline-thermal disintegration is the most popular version of this method, examples of which are given in Table 2.5.

Xu et al. (2014) disintegrated WAS samples with thermal, alkaline and thermo-alkaline disintegration techniques and observed a synergetic effect of the combined application in cumulative methane production. However, this integration did not ensure additional COD solubilization. In a similar study where relative disintegration efficiency of different techniques (thermal, alkaline and thermo-alkaline) are examined, Kim et al. (2003) stated thermo-chemical disintegration as the prominent method in terms of organic removal efficiency including sCOD and VS removal. The integrated method (121°C for 30 min and 7 g NaOH/L) provided 34.3% increase in methane production and 67.8% increase in sCOD removal compared to the control.

Toutian et al. (2021) has shown that low temperature thermo-alkaline disintegration (80 mg NaOH/g TS, 70°C, 2 h) and high temperature thermal hydrolysis (170°C, 30 min) provided similar level of increase in biomethane yield (by 25% and 26%, respectively). This indicates that combined application decreases the need for high energy consumption. Moreover, this integration has been shown to reduce the treatment time required for THP. Similarly, Y. Zhang et al. (2019) proved that

thermo-alkaline disintegration (80°C with NaOH for 1.3 h) increases biomethane yield more than that of THP alone (80°C for 12 h), by 56% and 40%, respectively.

Table 2.5. Review of studies disintegrating WAS with combined alkaline-thermal technique

Substrate	Disintegration conditions	AD conditions	Results	Reference
WAS, domestic	0.3 g NaOH/g VSS heated at 130°C for 5 min	Batch, 37°C for 8 days	1.27 times increase in CH_4 production	Tanaka et al. (1997)
WAS, industrial+ domestic	0.3 g NaOH/g VSS heated at 130°C for 5 min	Batch, 37°C for 8 days	2.06 times increase in CH_4 production	Tanaka et al. (1997)
WAS	pH=10 using $Ca(OH)_2$ at 100°C for 60 min	NR	Decrease in CST from 34 s to 22 s Increase in DS content from 28 to 46%	Neyens and Baeyens (2003)
WAS	7 g NaOH/L heated 121°C for 30 min	Batch, 37°C for 7 days	34.3% increase in CH_4 production 67.8% increase in sCOD removal	Kim et al. (2003)
WAS	1.65 g KOH/L (pH=10) heated at 130°C for 60 min	Batch, 35°C for 24 days	54% increase in biogas production	Valo et al. (2004)
WAS	pH=11 at 90°C for 10 h	Batch, 55°C for 15 days	CH_4 production of 0.28 L/g VSS_{in}	Vlyssides and Karlis (2004)
WAS	0.10 M NaOH at 90°C for 6 h	Batch,35°C for 21 days	73.9% increase in CH_4 production	Kim et al. (2013)

WAS: waste activated sludge; VSS: volatile suspended solids; sCOD: soluble chemical oxygen demand; AD: anaerobic digestion; CST: capillary suction time; DS: dry solids; NR: not reported

2.6.3 Characterization of Degraded Plastics

The degree of deterioration for plastics exposed to the stress factors mentioned earlier can be quantified by analyzing their physicochemical and mechanical properties, including bond cleavage, changes in chemical functionality, and material properties, as illustrated in Figure 2.11.

2.6.3.1 Physical Appearance

Properties related to appearance of plastics such as color, gloss, haze and yellowness are relatively easy to observe, and they are instrumentally analyzed by following standard methods provided by American Society for Testing and Materials (ASTM) and International Organization for Standardization (ISO). While color, haze and yellowness can be measured with a spectrophotometer, gloss is generally determined by a glossmeter (Zhang et al., 2021).

Topographical changes such as increased roughness, holes and cracks, as well as biofilm formation after fragmentation can be detected by SEM and atomic force microscopy (AFM) (Arkatkar et al., 2009).

2.6.3.2 Physicochemical Properties

Physicochemical structure of plastics including their surface properties, crystallinity, and thermal properties may undergo changes during degradation. Surface properties such as hydrophobicity, surface charge, surface area and porosity govern the interactions of plastics with microorganisms and other pollutants, thus essential to be measured in determination of the risk related to MPs in the environment.

Degradation causes decrease in hydrophobicity by the addition of hydrophilic groups (e.g., carbonyl group) to the chain (Arp et al., 2021). Surface charges may also change with the addition of functional groups during degradation, which can be measured by Zeta potential analysis. Besides, change in porosity and surface area of plastics is generally determined by the Brunauer-Emmett-Teller (BET) method (Sarkar et al., 2021).

Crystallinity, which is the degree of structural order in a polymer, can increase during the early stages of degradation by chain scission in amorphous region (Zhang et al., 2021). It can be measured either by FTIR or differential scanning calorimetry (DSC) (Arhant et al., 2019).

Glass transition temperature (T_g) and melting temperature (T_m) are thermal properties of plastics affecting polymer's transition from glass to rubbery state. Change in T_g and T_m, influenced by altered crystallinity after degradation can also be measured by DSC.

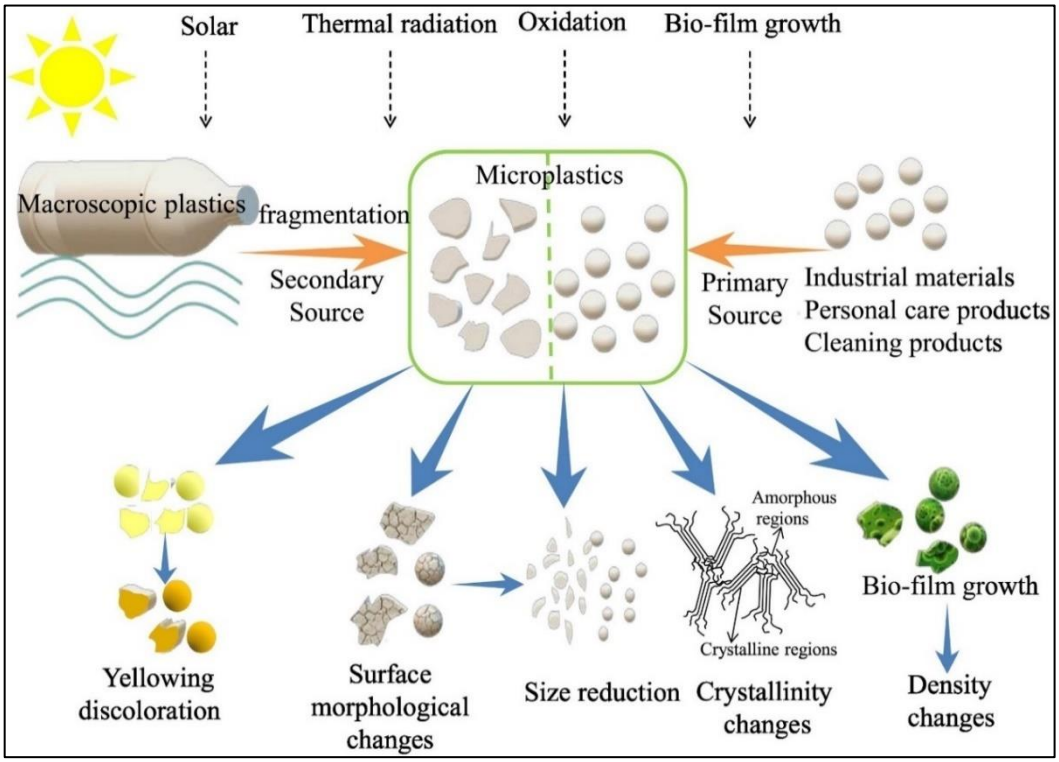

Figure 2.11. Change in characteristics of MPs after degradation (Guo and Wang, 2019)

2.6.3.3 Mass Loss

Quantifying the loss in mass is the most straightforward determinant of polymer degradation. It may either result from the volatilization of conversion products (CO_2 and H_2O) or loosing fragments from their surface such as MPs and mesoplastics. However, measuring the mass of plastics may not provide the accurate results at

initial stages of degradation due to oxygen attachment and accumulation of microorganisms and other debris on surface cracks (Chamas et al., 2020).

2.6.3.4 Chemical Composition

Depending on the degree of polymerization and additives used during their manufacturing, plastics may undergo reactions either in their polymer chain or in additives, resulting in altered chemical composition.

Both abiotic and biotic degradation processes can cause chain scission and cross-linking of polymers, which change their molecular weight. Generally, a decrease is observed during a degradation process. Gel Permeation Chromatography (GPC) is a method detecting molecular weight of a polymer by size exclusion (Albright and Chai, 2021).

As an indicator of oxidative degradation, polar functional groups such as ketones and ester C=O stretching (1715 and 1735 cm^{-1}, respectively) are generally analyzed using FTIR. Especially, change in carbonyl index, the ratio of absorbance at carbonyl bond to C-H bond, quantifies the extent of degradation for most polymer types (Chamas et al., 2020). Besides, elemental composition of polymers (specifically carbon and oxygen) is generally determined using Energy-dispersive X-ray spectroscopy (EDX) to observe surface oxidation (Alassali et al., 2018).

Degradation products and leaching additives can be measured using chromatographic techniques coupled with mass spectrometry (MS). While non-polar and volatile compounds are analyzed using gas chromatography mass spectrometry (GC/MS), polar and non-volatile compounds are generally measured using liquid chromatography mass spectrometry (LC/MS) (Zhang et al., 2021).

2.6.3.5 Mechanical Properties

Mechanical properties such as elongation at break and tensile modulus (Young's modulus) are detected when characterizing the physical deterioration such as formation of cracks and pores at the surface (Chamas et al., 2020). ASTM and ISO standard methods are generally followed to perform stress-strain test for deformed plastics. These properties are also associated with chemical composition, physicochemical properties as well as additives. Therefore, any change in chemical composition and physiochemical properties of plastics may affect mechanical properties as well (Zhang et al., 2021).

2.7 Techniques for Detection of Microplastics in Sewage Sludge

In order to better understand the extent of MP pollution in environmental samples including sewage sludge, properly applied sampling, pretreatment, and extraction methods, followed by effective identification and quantification are of great importance. Despite the rising concerns about MP pollution, there is no standard method that is accepted and applied globally for MP detection. It has to be mentioned that there are some recent efforts, such as the two standards published by ASTM in August 2020 for wastewaters with high, medium and low suspended solids, that cover the collection (ASTM D8332-20) (ASTM, 2020a) and preparation of samples (ASTM D8333-20) (ASTM, 2020b) to identify and quantify MPs in them. While these standards are addressing the sampling and pretreatment issues for drinking water, surface waters, wastewater influent and effluent (secondary and tertiary) and marine waters; sewage sludge has not been addressed in these documents. For sludge on the other hand, several different methods with varying levels of quality assurance have been reported (Okoffo et al., 2019). The lack of a standardized and globally accepted method made the comparison between studies difficult (WHO, 2019). Despite this fact, there is still a commonality in the flow of testing in many studies and involves the steps summarized in Figure 2.12.

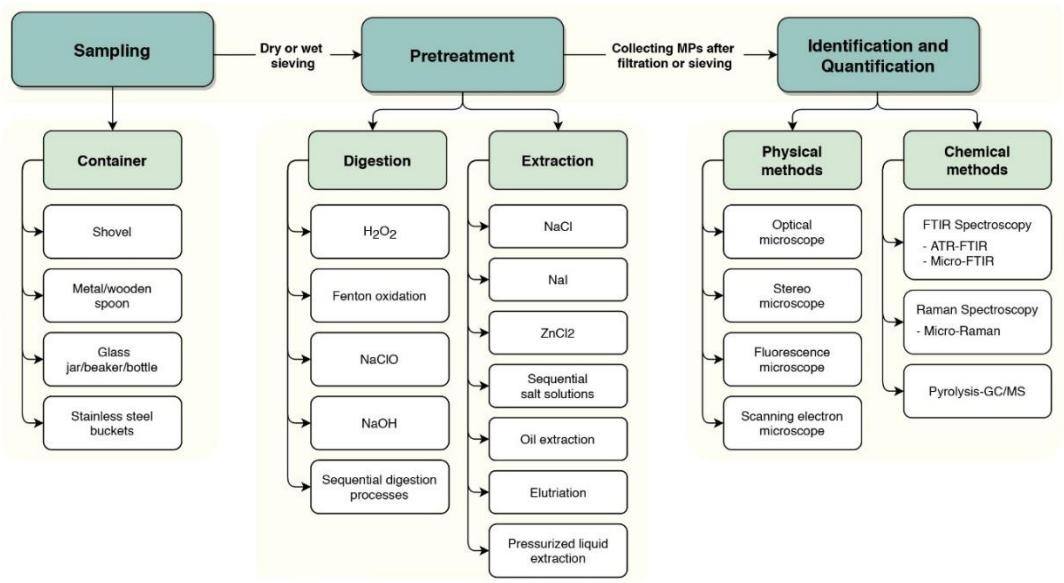

Figure 2.12. Flow chart summarizing the steps and the techniques used for detection of MPs in sewage sludge

2.7.1 Sampling, Pretreatment and Extraction

Categorization of the techniques used for sampling, pretreatment and detection of MPs in sewage sludge are collected from literature and presented in Figure 2.12. In addition, Table 2.6 lists the studies from around the world analyzing MPs in sewage sludge samples and summarizes the details of techniques used for sampling, pretreatment, extraction, and characterization. One can see that many of these methods are similar to the ones used for wastewater, even though the table is collected from studies involving only sludge.

Sewage sludge samples are typically collected by grab sampling method because high organic matter and solids content of sludge makes it rare to apply in-situ filtration coupled with size separation, which is the commonly used sampling method for effluent wastewaters (Nguyen et al., 2019; Okoffo et al., 2019). In other studies, composite samples are obtained by combining sludge collected from different points of the bulk material or at different times (Lusher et al., 2017; Q. Xu et al., 2020) to

overcome the potential variability resulting from heterogeneous nature of sludge and sampling time and to ensure better representativeness (Okoffo et al., 2019). Sample preparation steps varied based on the nature of sludge as well as how the sludge is collected. For example picking out large non-plastic substances was deemed necessary for some sludges (Jiang et al., 2020; Ren et al., 2020), softening the sludge by soaking it in water (Gies et al., 2018; Liu et al., 2019; Mahon et al., 2017), drying the sludge (Lares et al., 2018; Q. Li et al., 2019; Murphy et al., 2016; Q. Xu et al., 2020), and filtration of the wet/dried sludge through stacked sieves (Hongprasith et al., 2020; Magnusson and Norén, 2014; Mahon et al., 2017; Ren et al., 2020) were among the observed applications.

Sewage sludge has a viscous matrix consisting of microorganisms, organic materials, and inorganic particles posing attraction for polymer surfaces (X. Li et al., 2020; Zhang and Chen, 2020). EPS encapsulating these materials intervene the extraction of MPs and interfere with MP analysis. X. Li et al. (2020) have revealed that sewage sludge with EPS in the sludge floc had the lowest MP extraction efficiency compared with the other solid matrices such as cattle manure, soil, sediment and silicon dioxide. In addition, high organic matter content of sludge interferes with the identification and quantification of MPs. To facilitate identification and quantification, both the organic matter and EPS in sludge should be removed by pretreatment/digestion methods without disrupting the polymer integrity of MPs (Dyachenko et al., 2017; Sun et al., 2019). The most frequently applied methods to remove or reduce organic materials in sludge samples are hydrogen peroxide (H_2O_2) digestion and Fenton oxidation as indicated in Table 2.6. Studies not including any pretreatment method for organic matter removal, instead directly proceeding to MP extraction step; may experience increased filtering time and workload during identification (Kang et al., 2020; Leslie et al., 2017).

Among four commonly applied digestion techniques including Fenton oxidation, H_2O_2, NaOH, and KOH digestion, Lusher et al. (2017) found that Fenton oxidation was the most cost and time-effective method for the reduction of organic matter in sewage sludge samples. Similarly, Hurley et al. (2018) stated Fenton's reagent

ensured an effective organic matter removal without any observed damage to the tested polymers which were PP, low-density polyethylene (LDPE), high-density polyethylene (HDPE), PS, PET, polyamide 6,6 (PA-6,6), PC, and polymethyl methacrylate (PMMA). In reaching this conclusion, Hurley et al. (2018) tested the effectiveness of organic matter removal of four main protocols (i.e., Fenton oxidation, H_2O_2, NaOH and KOH) with the loss in mass of filter papers. Likewise, Bretas Alvim et al. (2020a) considered total suspended solids (TSS) removal while investigating Fenton and H_2O_2 oxidation in sewage sludge samples and determined H_2O_2 oxidation as the ideal protocol. Other than these studies, systematic control of organic matter removal efficiency in sewage sludge samples is generally overlooked in the literature. Instead, a visual inspection is widely applied in tracking the removal of organic matter in samples, as recommended by National Oceanographic and Atmospheric Administration (NOAA) for water and sediment samples (Masura et al., 2015). It is critically highlighted to standardize the protocol to demonstrate complete digestion process using parameters such as chemical oxygen demand (COD) that quantitatively represents organic matter content of the sample (Nguyen et al., 2019). Using this step is especially critical for sludge considering the high organic contents typically encountered.

The extraction of MPs from sludge samples has been most frequently carried out by a density-based approach, as is the case for all environmental samples (Table 2.6), where the low-density MPs are floated to the surface by the addition of saturated salt solutions of NaCl (1.2 g/cm^3), $ZnCl_2$ (1.5-1.7 g/cm^3) or NaI (1.6-1.8 g/cm^3) (Q. Li et al., 2019; Lv et al., 2019) to the samples. Q. Li et al. (2019) stated that there is a direct proportionality between the salt solution's density and the number of MPs extracted. According to their results, the amount of high-density polymers, which are PET and polyacrylonitrile (PAN), in NaI solution was higher than in NaCl solution. In a study comparing the extraction efficiencies of four different salt solutions (i.e., NaCl, NaBr, NaI, $ZnBr_2$), Quinn et al. (2017) showed the lowest recovery efficiency (< 85-95% and ~70% for MPs in sizes 200-400 μm and 400-800 μm, respectively) was for NaCl solution added into sediment samples.

Table 2.6. Reported sampling, pretreatment, extraction and characterization methods for sludge samples

Sampling point/ Sludge type	Sampling equipment/ sample amount	Sample preparation	Pretreatment/Digestion method	Extraction method	Identification and quantification methods	Reference
Sludge treatment[a]	NR	-	3% NaClO	NR	Microscope; FTIR	Carr et al. (2016)
Sludge treatment[a]	2 L glass jars/ 10-21 g wet weight	-	-	NaCl solution; Filtration over a GF/F (0.7 µm); Filtration over an Al_2O_3 filter (0.2 µm)	Light microscope; FTIR	Leslie et al. (2017)
Membrane filtration unit/ MBR sludge Aeration tank/ Activated sludge Anaerobic digestion	Stainless steel bucket/ 150-200 mL	Drying the sludge at 45°C for 18 h	-	Collection of particles with a tweezer	Optical microscope; micro-FTIR; micro-Raman	Lares et al. (2018)
Primary clarifier/ Primary sludge Secondary clarifier/ Secondary sludge	250 mL glass jars/ NR	Mixing the sludge with distilled water and refrigeration to allow solid organic matter to settle	30% H_2O_2 at room T for 10 days (for solid layer)	OEP (for liquid layer); Filtration over a polycarbonate membrane (1 µm)	Stereo microscope	Gies et al. (2018)
Primary clarifier/ Primary sludge Secondary clarifier/ Secondary sludge Centrifugation/ Biosolids	500 mL glass bottles/ 1 L Manual collection from conveyor/ 500 mL	Drying the sludge at 60°C for 24-72 h; Mixing the sludge with ultra-pure water to homogenize it	30% H_2O_2 at 60°C for 24-48 h (pre-digestion); Fenton's reagent at room T for 1-2 h (post-digestion)	NaI solution; Manual shaking and centrifugation; Filtering the buoyant part (25 µm); Staining with Rose Bengal	Dissecting microscope; micro-FTIR (for smaller particles); ATR-FTIR (for larger particles)	Ziajahromi et al. (2021)
Primary clarifier Secondary clarifier/ WAS	NR/ 5 L	-	15% H_2O_2 at 50°C for 2 days	NaBr solution; Filtering the supernatant; Transferring the particles onto a cellulose acetate membrane (0.45 µm) using a tweezer	Stereo microscope; micro-FTIR	Pittura et al. (2021)
Secondary clarifier/ RAS	NR	-	30% H_2O_2 at 70°C for 24 h	SNT; Filtration over cellulose acetate membrane filters (0.45 µm)	Confocal Raman microscopy	Sujathan et al. (2017)
Secondary clarifier/ RAS	Glass beaker/ 50 mL	-	15% H_2O_2 at room T for 3 days	NaCl solution; Filtration over a cellulose nitrate membrane (8 µm)	Stereo microscope; micro-FTIR	Magni et al. (2019)
Secondary clarifier/ RAS Sludge dewatering/ Sludge filter cake	Stainless steel barrel/ 2 kg	Picking out non-plastic substances; Drying the sludge at 60°C	30% H_2O_2 at 25°C for 7 days	NaCl solution; $ZnCl_2$ solution; Filtration	Stereo microscope; Tip enhanced laser confocal Raman spectroscopy	Jiang et al. (2020)

Table 2.6. Continued

Secondary clarifier/ WAS	NR/ 100 mL	Diluting the sludge with deionized water	Fenton's reagent	$ZnCl_2$ solution; Centrifugation; Filtering the supernatant over Grade 589/1 Black ribbon filter (12-25 µm)	Light microscope; micro-ATR-FTIR	Bilgin et al. (2020)
Secondary clarifier/ WAS	Plastic buckets/ 60 L	-	Fenton's reagent at 70°C for 30 min	Filtration through a series of stainless-steel sieves (2 mm, 1 mm, 250 µm); Staining with Rose Bengal (for retaining MPs); Centrifugation with NaI solution (for filtrate); Filtration over a cellulose filter disc (1.5 µm); Staining with Nile red	Stereo microscope; ATR-FTIR	Raju et al. (2020)
Secondary clarifier/ RAS+WAS	NR/ 1 kg	Sieving the sludge through 4.75 mm and 0.33 mm meshes	WPO (30% H_2O_2 with 0.05M Fe^{2+} solution at 75°C until organic matter is invisible)	Density separation; Manual collection of MPs; Drying the collected MPs at 75 °C for 24 h	Microscope; FTIR spectroscopy	Hongprasith et al. (2020)
Anaerobic digestion	NR	-	33% w/v H_2O_2 at 50°C for 20-24 h	NaCl solution; Filtration through a series of stainless steel meshes (375,104,25 µm)	Stereo microscope; micro-FTIR	Edo et al. (2020)
Anaerobic digestion	NR/ 30 g	Soaking the sludge in water to soften and homogenize it; Washing the sludge through 250, 212, 63, and 45 µm sieves	-	Elutriation column; Filtration over a 250 µm mesh; $ZnCl_2$ solution; Filtration over a GF/C (1.2 µm)	Stereo microscope; ATR-FTIR; SEM	Mahon et al. (2017)
Lime stabilization				Filtration over a GF/C (1.2 µm)		
Thermal drying		Softening the pellets in water for 1 week; Water-bath (30°C) for 24 h; End-over-end shaker for 12 h; Passing through 250,212, 63, and 45 µm sieves		Elutriation column; Filtration over a 250 µm mesh; $ZnCl_2$ solution; Filtration over a GF/C (1.2 µm)		
Composting plant/ Raw compost, semi-finished product, finished product	Glass bottles/ 2-3 kg	Manual collection of MPs (>0.5mm) with a metal tweezer	-	Ultrasonic treatment of MPs for 15 min; Drying the MPs at 50°C for 48h	Stereo microscope; micro-FTIR-MCT	Zhang et al. (2020)
Centrifugation Belt type pressure filtration Plate frame pressure filtration		Drying the sludge at 50°C for 24 h	30 wt % H_2O_2 at 65°C for 72h	$ZnCl_2$ solution; NaCl solution; Filtration through standard stainless-steel sieves (25 µm); Filtration with GF/F (0.45 µm)		

Table 2.6. Continued

Sampling point/ Sludge type	Sampling equipment/ sample amount	Sample preparation	Pretreatment/Digestion method	Extraction method	Identification and quantification methods	Reference
Co-composting plant Lagooning/ Fresh sludge Lagooning/ Sludge dewatering	NR/ 1 kg	-	Fenton's reagent	$ZnCl_2$ solution; Centrifugation; Filtration over a cellulose nitrate filter (0.45 µm)	Preliminary steps (Pyr-GC/MS and Fluorescent staining); Stereo microscope; Confocal Raman spectroscopy	El Hayany et al. (2020)
Sludge dewatering	NR/ 25 g wet weight	Sieving through a 300 µm filter	-	-	Stereo microscope; ATR-FTIR	Magnusson and Norén (2014)
Sludge dewatering	Shovel/ 500 g wet weight	-	10 M NaOH at 60°C for 24 h	NaCl solution; Filtration over a PA net (500 µm); Filtration over an Al_2O_3 filter (0.2 µm)	Stereo microscope; ATR-FTIR; FPA based micro-FTIR (for smaller MPs)	Mintenig et al. (2017)
Sludge dewatering	Metal or wooden spoon/ 5 – 10 grabs (each 100 g)	-	Fenton's reagent at room T for 2h	Filtered RO water + NaI solution; Filtration over GF/D filters	Stereo microscope; Hot needle test; FTIR	Lusher et al. (2017)
Sludge dewatering/ Sludge cake	Shovel/ NR	-	Fenton's reagent at 75°C for 30 min	$ZnCl_2$ solution; Sieving (300, 106 µm)	USB digital microscope; ATR-FTIR	Lee and Kim (2018)
Sludge dewatering	NR	-	30% H_2O_2 overnight	NaCl solution; Filtration through a sieve (37 µm); Filtration over GF filters	Stereo microscope; SEM; micro-FTIR	Li et al. (2018)
Sampling point/ Sludge type	Sampling equipment/ sample amount	Sample preparation	Pretreatment/Digestion method	Extraction method	Identification and quantification methods	Reference
Sludge dewatering	NR/ 30 g	Softening the sludge in pure water for 24 h; Water-bath (40°C) for 24 h; Centrifugation to collect supernatant	30% H_2O_2	NaCl solution; NaI solution; Filtration over a GF/F (0.8 µm)	Fluorescence microscope; micro-Raman	Liu et al. (2019)
Sludge dewatering	Shovel/ 2 kg	Drying at 60°C; Filtration through a 5 mm stainless steel filter	30% H_2O_2 at 60°C for 72h	$ZnCl_2$ solution; SDS solution; Filtration over a stainless-steel filter (5 µm)	Stereo microscope; Optical microscope; micro-FTIR	Xu et al. (2020)

[a] Sludge sampling point could not be understood from this article. NR: Not reported; RAS: Retum activated sludge; WAS: Waste activated sludge; GF: Glass microfiber filter paper; WPO: Wet peroxide oxidation; OEP: Oil extraction protocol; SNT: Sodium nitrate/sodium thiosulfate solution; SDS: Sodium dodecyl sulfate solution; Pyr-GC/MS: Pyrolysis- gas chromatography/mass spectrometry; FPA: Focal plane array detector; ATR: Attenuated total reflection mode

Thus, they needed three times wash of the sediment for NaCl solution while only a single wash was sufficient for NaI and $ZnBr_2$ solutions to extract MPs properly (Quinn et al., 2017). To separate both the low and high-density MPs and accurately determine their number, sequential extraction in NaI and $ZnCl_2$ are recommended despite the high price and relatively toxic properties of these two salts (Okoffo et al., 2019; Silva et al., 2018). The extraction procedure continues with the filtration of supernatant and separation of retained MPs on the filter for the following identification and quantification steps (Bretas Alvim et al., 2020b).

2.7.2 Identification and Quantification

Once MPs are extracted from sludge samples, they are subjected to various identification and quantification procedures based on physical and chemical techniques (Table 2.6). Physical identification techniques predominantly involve using a light microscope or stereo microscope for enumeration and visual categorization of MPs by size, shape, and color (Yang et al., 2021b; Zarfl, 2019). While the overall picture of MP abundance can be obtained quickly and conveniently through these microscopic techniques, their application is limited to large particles (Okoffo et al., 2019). Likewise, Gies et al. (2018) stated that only 32.4% of the suspected MPs under light microscope were later confirmed as plastic polymers by FTIR spectrometer. Therefore, majority of the studies initially identified MPs by visual techniques and then directed a representative portion of the suspected MPs to either FTIR or Raman spectroscopies alone or combination of them.

Moreover, for removing the degree of subjectivity in physical characterization, some studies have combined the visual inspection with a hot needle test or fluorescent staining to assist identification of suspected particles as plastics (Kang et al., 2020). As a low-cost, time-saving method facilitating the visual identification Prata et al. (2019) and Campo et al. (2019) isolated the MPs from sludge samples using fluorescent Rose Bengal dye and achieved MP recovery of up to 97%. Besides, Nile Red, which is another fluorescent dye, seems to be a promising staining tool for MPs.

However, its co-staining effect on partially degraded natural organic material such as cellulose, chitin, and microbial mass may hamper the identification using spectroscopical methods due to the fluorescence of particles (Raju et al., 2020). The reliability of successive staining and spectroscopic methods can be improved by removing absorbed dye and satisfactory degradation of natural organic materials in environmental samples (Shim et al., 2017). Thus, this procedure has been applied to a lesser extent for sludge samples with high organic content, which means that there is still much work to be done to recommend the staining method by itself.

Identifying MPs with diverse sizes, shapes, and types is challenging to handle using a single method (Shim et al., 2017). So far, studies have mostly applied chemical identification methods such as spectroscopic methods (i.e., FTIR and Raman spectroscopy) and thermoanalytical methods in conjunction with visual inspection to ensure the chemical composition of MPs identified reliably. FTIR spectroscopy is the most powerful and relatively fast method for analysis of MPs with its two modes prevailing in studies examining sludge samples: micro-FTIR and ATR-FTIR (Elert et al., 2017; Okoffo et al., 2019; Tagg et al., 2015). Micro-FTIR combines FTIR spectroscopy with microscopy (Wesch et al., 2016) to produce high-resolution for the particles down to 20 μm, with little/no sample preparation (Prata et al., 2019). The ATR-FTIR is efficient for the analysis of larger particle sizes (>500 μm) (Mintenig et al., 2017) and also applicable for the characterization of irregularly shaped particles (Hidalgo-Ruz et al., 2012). Compared to FTIR spectroscopy, Raman techniques are more sensitive tools for identification of MPs with an improved spatial resolution of down to 1 μm (Nguyen et al., 2019; Prata et al., 2019). A version of Raman spectroscopy standing out among studies analyzing MPs in sludge is called as micro-Raman, which can identify very small particles (down to 1 μm) (Ivleva et al., 2017; Wesch et al., 2016). So, complementing the FTIR imaging by micro-Raman can be a good attempt to properly account for a wide range of MP sizes (Araujo et al., 2018).

Size dependency of the previously mentioned methods may cause underestimating the number of plastics and hence reveals the necessity of mass-based identification

and quantification techniques. Pyrolysis-gas chromatography/mass spectrometry (Pyr-GC/MS), a thermoanalytical method analyzing polymer's thermal degradation products for identification, has been rarely reported in studies analyzing sewage sludge samples. Besides its fast identification mechanism, Pyr-GC/MS provides a quantitative estimation of MPs' mass independent of particle size (Mallow et al., 2020; Okoffo et al., 2019). Okoffo et al. (2020) applied single step pressurized liquid extraction (PLE) with double-shot Pyr-GC/MS to obtain mass concentrations of PE, PP, PVC, PMMA, and PS type MPs in biosolid samples, which provides a basis for uniform reporting of results. However, its destructive nature prevents subsequent analysis of MPs (Shim et al., 2017). Still, mass concentration data obtained from Pyr-GC/MS can complement the information gathered from FTIR and Raman spectroscopy, such as particle size, shape, and color.

CHAPTER 3

MATERIALS AND METHODS

Experimental work conducted throughout this study can be collected under three main headings: developing an analysis method for MPs in sludge, sludge disintegration studies and operating BMP reactors fed with alkaline-thermal disintegrated WAS spiked with PET type MPs. Method development studies cover gathering the most appropriate techniques together to obtain a repeatable and reliable method for the analysis of MPs. It continues with the validation of the developed method. The second part of the study investigates the relative solubilization efficiencies of alkaline, thermal, and alkaline-thermal sludge disintegration techniques. Following the determination of the prevailing disintegration technique based on its ability to solubilize the sludge and deteriorate PET MPs, BMP reactors are set-up and operated in the final part of the study.

3.1 Materials

3.1.1 Sludge Samples Used

Waste activated sludge (WAS) and anaerobically digested sludge (ADS) used in this study have been taken from the Central WWTP of Ankara located in Tatlar village, which is the largest WWTP in Turkey. It is an urban WWTP treating municipal wastewater by conventional activated sludge system with the capacity of 765,000 m^3/day. WAS sample was obtained from the sludge return line of secondary clarifier by grab sampling method. ADS used to seed the reactors was taken from the anaerobic digesters of the plant. Samples transported to the laboratory were stored at 4°C until their analysis. WAS and ADS were samples used throughout this study with different purposes as given in Table 3.1.

ADS samples, sterilized with the addition of mercury chloride ($HgCl_2$) at a concentration of 200 mg/g TSS and autoclaved for an hour for 2 consecutive days were used as inhibited seed in BMP test.

Table 3.1. Sludges used in this study and their usage areas

Sludge type	Area of use
WAS	- Method development studies for MPs - Recovery study of MPs - Sludge disintegration - BMP test
ADS	- BMP test (as the seed)
Inhibited ADS	- BMP test
Mixture of WAS and ADS	- MPs analysis

3.1.2 Model Microplastics Used

Three different types of MPs, that are frequently reported in sludge based on the literature review, were used in this study: PE, PA and PET. Physical properties of these plastics and usage areas are given in Table 3.2. While PE MPs were readily obtained in ground form from a water tank producer in Ankara, PET and PA type MPs were obtained by cutting water bottles and nylon fishing line in laboratory, respectively. Then, the particles were passed through a series of sieves to obtain MPs in the appropriate size range.

Table 3.2. Model MPs used and their usage areas

MP type	Size (μm)	Density (g/cm^3)	Shape	Area of use
PET	250 – 500	1.37 – 1.45	Film	- Sludge disintegration - Setting up of BMP reactors
PET	425 – 500	1.37 – 1.45	Film	- MPs recovery study
PE	250 – 500 425 – 500 500 – 1000	0.92 – 0.97	Fragment	- MPs recovery study
PA	425 – 500	1.02 – 1.05	Rod	- MPs recovery study

MPs recovery experiment involved the use of these three polymer types as they represent varying levels of density: PE (0.92-0.97 g/cm^3), PA (1.02-1.05 g/cm^3), and PET (1.37-1.45 g/cm^3). Moreover, PET MPs were spiked into WAS samples during sludge disintegration studies and BMP reactor set-up, as the model MP type.

3.2 Methods

3.2.1 Method Development and Validation Studies for Analysis of Microplastics in Sludge Samples

Method development involved optimization of each step of the scheme shown in Figure 3.1, which are sampling, pretreatment, extraction and identification and quantification. Then, the validity of this method for different polymer types and matrices was tested.

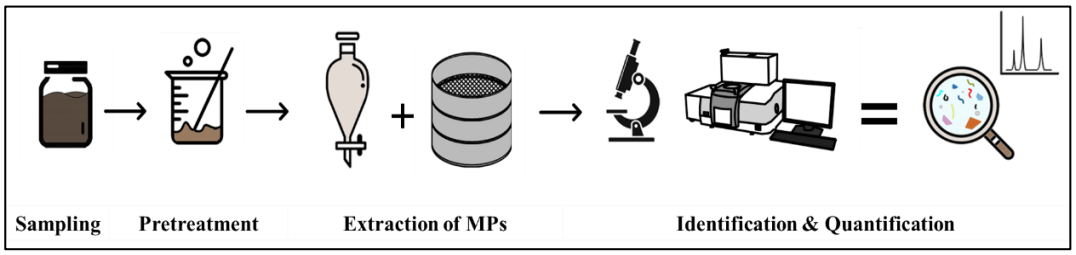

Figure 3.1. Experimental procedure developed for analysis of MPs in sludge

3.2.1.1 Method Development for Microplastics Analysis

WAS taken as grab-samples, were transported to the laboratory in glass jars having caps covered with aluminum foil to minimize plastic contamination. After sampling, Fenton Oxidation was employed to remove organic materials in WAS samples as much as possible to prevent any interfering effect of organics on chemical analysis of MPs (i.e., FTIR/Raman Spectroscopy). The generally accepted core reaction is shown in Equation 3.1.

$$Fe^{2+} + H_2O_2 \rightarrow Fe^{3+} + HO^{\cdot} + OH^{-} \qquad \text{(Equation 3.1)}$$

In this study, COD removal was used as the indicator of organic matter removal, first time in literature in MP analysis; so, the optimization studies have been carried out by monitoring the effects of different parameters of Fenton Oxidation on COD removal efficiency. The parameters tested were H_2O_2 dose, the molar ratio of H_2O_2 to Fe(II), and reaction time. The theoretically required amount of H_2O_2 to oxidize the total COD load of the sample can be calculated using Equation 3.2.

$$H_2O_2 \rightarrow H_2O + \frac{1}{2} O_2 \qquad \text{(Equation 3.2)}$$

According to Equation 3.2, 2.13 mg/L of H_2O_2 is needed to oxidize 1 mg/L of COD. Optimization studies consisted of testing the effectiveness of the theoretically required amount, as well as the excess amounts of H_2O_2 that were 2 and 5 times the theoretically calculated value. After fixing the optimal H_2O_2 dose at constant concentration of Fe(II) ($[H_2O_2]/[Fe(II)]=10$), the effective dose of Fe(II) ions was determined by applying different molar ratios of H_2O_2 to Fe(II) that were 10:1, 20:1 and 30:1.

During these tests the reaction time was varied from 15 min to 120 min and the COD removal efficiency was examined by taking 30 mL subsamples from the 300 mL continuously stirred reaction mixture in a regular pattern. The subsamples were immediately neutralized using 5 M NaOH solution to stop the reaction and let the samples sit for up to 6 h until Fe(III) flocs nicely settled down, as shown in Figure 3.2. pH was checked intermittently to ensure that it remained neutral.

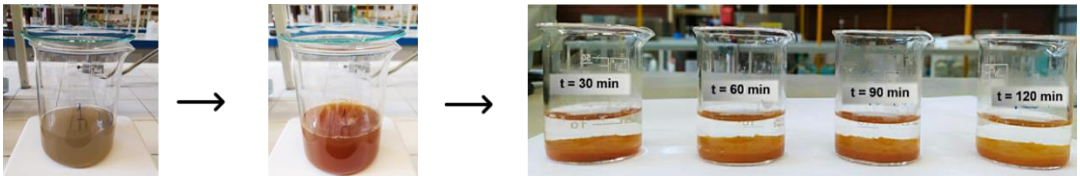

(a) **(b)** **(c)**

Figure 3.2. Steps of Fenton Oxidation: raw WAS (a); WAS during reaction (b); subsamples taken in a regular pattern at different reaction times (c)

Once the flocs settled, supernatant was collected both to measure COD values and the residual H_2O_2 that could interfere with the COD measurement. The amount of H_2O_2 remaining in the sample was determined by redox titration using potassium permanganate as the titrant. The redox reaction is given in Equation 3.3.

$$2KMnO_4\,(aq) + H_2O_2\,(aq) \rightarrow 2MnO_2\,(s) + 2O_2\,(g) + 2KOH\,(aq) \qquad \text{(Equation 3.3)}$$

Then the COD value was corrected using Equation 3.4 (Talinli and Anderson, 1992).

$$COD\ (mg/L) = COD_m - (d \times f) \qquad \text{(Equation 3.4)}$$

where,

d = H_2O_2 concentration remaining in the sample (mg/L)

f = correction factor = 0.25 (valid for 20 – 1000 mg/L H_2O_2)

COD_m = measured COD (mg/L)

Once this step was optimized, Fenton Oxidation for WAS samples, which was followed in the analysis of MPs throughout this study, was carried out as follows. A 300 mL of WAS sample diluted to a COD value of about 3000 mg/L was added 0.1 M Fe(II) solution prepared in H_2SO_4. Then the pH of the mixture was adjusted to 3 using 5 M NaOH solution. The reaction was started by adding theoretically required

amount of 35% H_2O_2 solution which also yielded $[H_2O_2]/[Fe(II)] = 10$, which is the determined optimal molar ratio. The system was mixed at 500 rpm at room temperature for 30 min, which was found to be the optimal duration for reaction. Finally, the reaction was terminated by neutralizing the pH using 5 M NaOH solution.

Samples cleaned from degradable organics were further treated to distinguish MPs from the remaining inorganic and recalcitrant organic materials. Extraction of MPs from sludge sample included density-based separation process followed by filtering through stack of sieves.

Two-step density-based separation process developed to float the MPs included the successive use of saturated NaCl and $ZnCl_2$ to ensure capturing high-density MPs. First, NaCl was added into the sample at a concentration of 5 M making the density of the mixture 1.15 g/cm^3. Salty solution mixed for an hour was transferred into a separatory funnel and let to settle overnight. The next day, $Fe(OH)_3$ flocs from the bottom was taken and added $ZnCl_2$ to obtain a concentration of 5 M (1.5 g/cm^3) and subjected to the same process in another separatory funnel as shown in Figure 3.3. The day after, uppermost portions of both funnels were collected and filtered through a stack of sieves with mesh sizes of 5 mm, 1 mm, 425 µm and 38 µm, respectively.

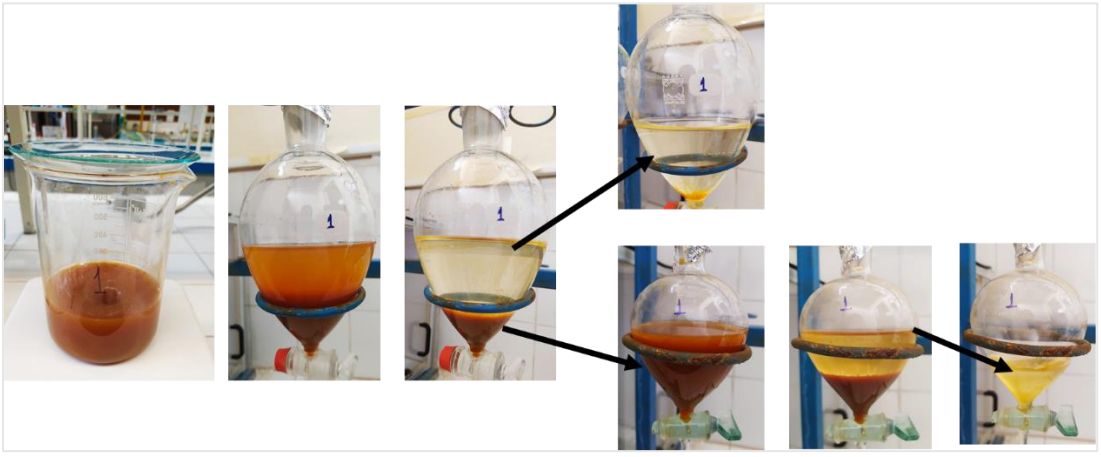

Figure 3.3. Two-step density-based separation of MPs

Particles trapped on the 5 mm-sized sieve were discarded since this size is out of the definition of MPs. The ones kept on the lower sized sieves were separately backwashed directly onto black Polycarbonate Track Etched (PCTE) membrane filters (1 μm pore size) using vacuum filtration unit. In order to distinguish MPs kept on the filters from the resembling non-plastic particles (e.g., recalcitrant natural organic materials, inorganic materials), samples on filters were stained by Nile Red, which is a hydrophobic fluorescent dye (Greyhound, FN11409). The staining protocol has been optimized by trying different solvent types to find the compatible one with the PCTE filter, incubation conditions including time and temperature, as well as the dye amount spread onto the filters. Furthermore, different filters such as Glass Fiber Filter (GF/A), Cellulose Nitrate (CN), qualitative filter paper (Whatman No 1) and Mixed Cellulose Ester (MCE) were tested for compatibility with Nile Red to assess the suitability.

Optimized protocol was used in the experiments as follows. Nile Red purchased in powder form was firstly dissolved in acetone to a concentration of 250 mg/L and then diluted to a concentration of 10 mg/L in n-hexane. Particles retained on filters were stained with 200 μL of Nile Red solution and incubated at room temperature for 15 minutes in dark. The filters incubated at proper conditions were inspected under ZEISS Axio Scope.A1 Fluorescence Microscope. Green Fluorescent Protein (GFP) is the optimal laser filter to clearly observe MPs and make natural organic materials relatively invisible. Shiny particles were reckoned as MPs, and they were counted under UV light and classified based on their size and shape. Sludge sample counting was then corrected by a blank analysis using distilled water.

3.2.1.2 Microplastics Recovery Experiment

The repeatability and reliability of the optimized method were ensured by conducting a series of experiments to calculate MPs recovery efficiency. For this purpose, plastic particles with different polymer types, shapes and sizes were spiked into different samples as given in Table 3.2. Moreover, three different matrices with varying levels

of complexity were used to understand the matrix effect on recovery efficiency, which are potassium hydrogen phthalate (KHP) solution, influent wastewater and WAS. KHP solution represents a simple organic matrix without visible suspended particles, while wastewater and especially WAS are viscous matrices consisting of microorganisms, organic materials, and inorganic particles.

First, PE type MPs in size ranges of 250 μm – 500 μm and 500 μm – 1.0 mm were spiked into KHP solution at a concentration of 25 MPs/300 mL in a series of trials. The model MPs were then extracted from the samples by following the entire MP analysis procedure developed in this study. The number of plastics with distinct shapes that enable them to be counted under Fluorescence Microscope was compared to those of added plastics to calculate the recovery rate in duplicates.

Once the reliability was ensured in KHP solution, the matrix used was switched to wastewater samples. PE type MPs in sizes of 250-500 μm were again spiked at the same concentration as the KHP solution. Then, for the WAS samples, the polymer types were diversified. PE, PA and PET MPs in sizes of 425-500 μm were spiked as a mixture containing 25 MPs of each type into a 300 mL of WAS sample with 1.5% of TS content and 3000 mg/L of COD value. The same extraction procedure given for the PE MPs in the KHP solution was then followed in determining the recovery rate in wastewater and sludge.

3.2.2 Sludge Disintegration

Studies conducted for sludge disintegration consisted of determining the optimal conditions for alkaline, thermal and combined techniques. Then, the efficacies of different methods were compared in terms of both sludge solubilization and level of deterioration on PET MPs.

3.2.2.1 Alkaline Disintegration

Four groups of studies were carried out for alkaline disintegration of WAS as shown in Figure 3.4.

Figure 3.4. Scope of alkaline disintegration studies

First, 200 mL of WAS samples with 2.0% TS content were disintegrated with the addition of 5 M NaOH solution at concentrations of 0.1, 0.2 and 0.5 M in separate vessels. The process was carried out in identical beakers in duplicates placed on magnetic stirrers at 250 rpm for 2 hours. To examine the change in solubilization of sludge in time, 30 mL of homogenous sludge portions were taken from the beakers at each 30 minutes. Subsamples were immediately neutralized using 5 M H_2SO_4 solution and centrifuged (Eppendorf 5810) at 4000 rpm for 15 minutes. Supernatants were filtered through 0.45 µm membrane filters. The filtrates, which are the soluble portion of WAS, were used for COD measurement. Then, soluble COD values of subsamples were compared to evaluate the performance of disintegration process. 0.5 M NaOH yielded the highest solubilization efficiency at the end of 2 hours.

Despite its prominence in sludge solubilization and possible deterioration of PET-MPs, 0.5 M NaOH application could inhibit microorganisms during anaerobic digestion due to inhibitory effect of Na ions. To reveal the ion effect resulting from the addition of 0.1, 0.2 and 0.5 M NaOH, a preliminary BMP test was carried out.

To prevent/minimize the inhibition (i.e., lag phase) observed with 0.5 M of NaOH during the preliminary BMP test, a combined dosing approach was developed (with individual doses of NaOH and KOH). This application aimed at delivering the same total alkali dose by adding it as the split doses of Na^+ and K^+ into the digesters. With this aim, KOH and NaOH solutions were added at concentrations of 0.10±0.02 and

0.38±0.02 M, respectively. The doses were selected to stay below the moderate inhibition level for microorganisms during anaerobic digestion, which was determined by McCarty (1964). Then, to assess the efficacy of combined application, combined dose as well as the individual doses of KOH (0.10±0.02 M) and NaOH (0.38±0.02 M) were applied on three different WAS samples. For preliminary demonstration purposes, disintegration process was carried out for 1 hour and COD solubilization was again used as the performance indicator.

The final set of studies for alkaline disintegration involves investigating the time effect as shown in Figure 3.4. The treatment was carried out in longer time periods such as in days in the presence of MPs with the purpose of maximizing both the solubilization of organics as well as the possible damage given to the plastics. With this purpose, WAS solubilization efficiency of combined alkali dosage (0.38±0.02 M NaOH and 0.10±0.02 M KOH) was tested for 5 consecutive days using 5 identical BMP bottles, to be destructively sampled each day to obtain the result of that particular day. The reason of doing this test in BMP bottles rather than in beakers, was to easily move the contents to BMP test without losing any MPs once the disintegration process was completed in later sets. Here the purpose was two-folds: one is to obtain the efficiency of combined solubilization, the other is to see the impact of this treatment on PET MPs. Towards this end, model PET MPs, details of which are given in Table 3.2, were added to each bottle at a concentration of 3 mg/g TS of sludge. The bottles, capped with a rubber septum, were placed into a shaker incubator at 25°C at 250 rpm. One bottle was terminated each day to measure the soluble COD, protein and carbohydrate value of WAS. Moreover, MPs were extracted from the sludge daily to further examine any change in their morphology.

3.2.2.2 Thermal Hydrolysis Process

The solubilization in THP depends on two main parameters: temperature and time of treatment. In an earlier study, 127°C was noted to be an effective temperature for the solubilization of COD (Arı-Akdemir, 2019). Thus, in this study, WAS samples

spiked with PET MPs (3 mg/g TS) were thermally hydrolyzed at 127°C in BMP bottles for 30, 60 and 120 minutes using an autoclave (Nüve SteamArt OT 90L). Following the hydrolysis, the samples were let to cool to room temperature and their final volumes were recorded to account for the loss in sludge volume during THP, while measuring soluble COD, protein and carbohydrate values in the supernatants. Then, the samples were centrifuged, and the supernatants were filtered through 0.45 μm membrane filters as in alkaline disintegration. Although extended treatment time did not significantly improve WAS solubilization, 120 min was selected to increase the impact on PET MPs.

3.2.2.3 Combined Disintegration

After deciding on optimal conditions for alkaline disintegration and thermal hydrolysis, which provide high sludge solubilization efficiency as well as conditions causing PET MPs to potentially deteriorate, a combined disintegration technique was employed. There are a few justifications in applying alkali addition prior to thermal hydrolysis (i) lipid content of WAS is better dissolved when alkali is added first (Mostafa et al., 2020); (ii) since THP releases organic acids in WAS, its application after alkaline disintegration decreases the amount of acid required for neutralization prior to anaerobic digestion (Toutian et al., 2021).

The main reason for the combined application is to enhance deterioration of PET MPs in sludge, rather than achieving further improvement in sludge solubilization. Therefore, three sets of PET MPs spiked WAS samples which had been alkaline disintegrated (0.5 M using KOH and NaOH combined) for 2, 4 and 5 days were autoclaved at 127°C in serum bottles for 120 minutes. Then the solubilization was measured by soluble COD, carbohydrate and protein analysis in the filtered samples. Soluble content of sludge was not significantly promoted over 2 days of alkaline disintegration. So, combined disintegration was reasonable to be applied when sludge is alkaline disintegrated for 2 days.

3.3 Installation and Operation of Anaerobic Reactors

In the third part of the study, both disintegrated and non-disintegrated BMP reactors were set-up and operated to investigate the fate and effects of MPs during anaerobic digestion of disintegrated and non-disintegrated sludges. Two different routes were followed for disintegrated and non-disintegrated sludge samples that are subjected to BMP tests as shown in Figure 3.5 and Figure 3.6.

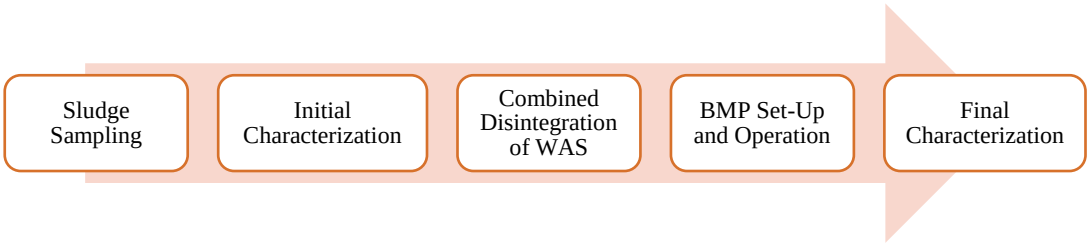

Figure 3.5. Flow diagram of disintegrated reactor sets

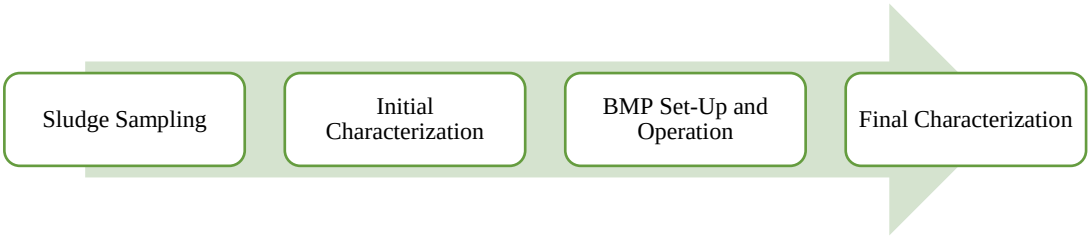

Figure 3.6. Flow diagram of reactor sets without sludge disintegration

To prepare the sludge for reactor set-up, first, the samples transported to the laboratory were left to settle for a few hours. The supernatants of the sludges were siphoned to concentrate them, and samples were mildly centrifuged if needed so that the TS concentration of 2% is achieved. TS, TSS, VS and VSS concentrations, total COD, soluble COD, protein, carbohydrate and pH values of each concentrated sludge were measured within 24 hours of sampling and used in determining the sludge volumes to be fed into the reactors. The characterization analyses performed in triplicate, are shown in Table 3.3 and Table 3.4.

Table 3.3. Characteristics of concentrated WAS used in BMP test

Parameter	Value
TS (g/L)	22.06±0.20
VS (g/L)	15.92±0.18
TSS (g/L)	20.66±0.11
VSS (g/L)	4.03±0.04
pH	7.3
tCOD (g/L)	23.64±0.57
sCOD (mg/L)	402.1±18.2
Soluble protein (mg/L)	64.8±2.9
Soluble carbohydrate (mg/L)	14.5±1.6

Table 3.4. Characteristics of concentrated ADS used in BMP test

Parameter	Value
TS (g/L)	17.98±0.05
VS (g/L)	9.48±0.05
TSS (g/L)	16.52±0.25
VSS (g/L)	8.82±0.11
pH	8.6
tCOD (g/L)	17.59±0.53
sCOD (mg/L)	670.6±26.1

Each amber bottle used as the BMP reactor had a total volume of 250 mL, of which 208 mL acted as the effective volume, and the rest as headspace. WAS and ADS samples were added into the reactors in such a way that F/M ratio and TS content of the mixtures were 1 (g VS WAS/g VSS ADS) and 2%, respectively.

3.3.1 Anaerobic Reactor Sets

BMP test was operated in 11 sets of triplicate serum bottles, details of which are given in Figure 3.7. In these sets, the reactors with disintegrated sludge having different doses of MPs (1, 3, 6 mg PET/g TS) are indicated by the letter P as in R0P, R1P, R3P, R6P. The reactors having sludge without disintegration and with no MPs (R0) were operated as control reactors of disintegration. Moreover, reactor sets

without disintegration (R1, R3, R6) were planned to control the sole impact of MPs on digestion efficiency. Abiotic reactors for both disintegrated (C3P) and non-disintegrated (C3) sludge with middle dose of MPs added were operated to observe the fate of MPs in the absence of microbial activity. Additionally, to account for the background methane production from the anaerobic seed culture, a seed control set was prepared (SM) with no WAS inside.

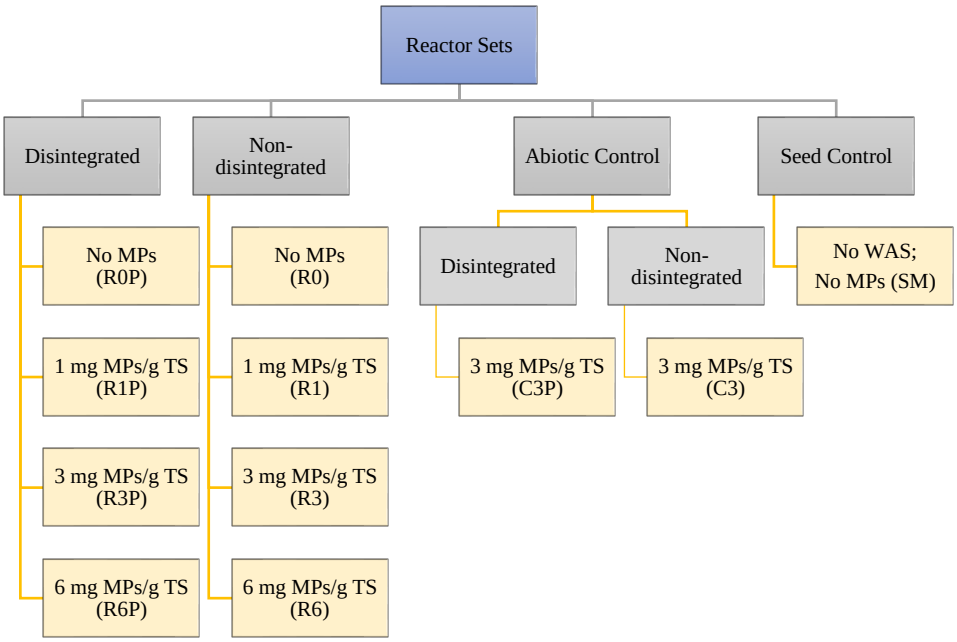

Figure 3.7. Reactor sets in BMP test

In addition to these 11 sets of triplicate reactors, two types of extra reactors (one for each) were planned for each set for the initial characterization of the system. Since the reactors were added with MPs as explained above, sampling from them would introduce a risk of disturbing the MPs and changing their concentration. So, two sets of extra reactors (E), with essentially representing characteristics of the relevant sets were established. Details of these are given in Table 3.5. Extra reactor #1 (E1), which do not have ADS inside, is the reactor used for examining the solubilization efficiency of the applied disintegration technique specifically at the time of reactor set-up with the presence of MPs (except for R0 sets). On the other hand, extra reactor #2 (E2) was added with ADS for initial characterization analyses of each set. Both

E1 and E2 reactors were not carried to the BMP set and terminated right after the initial analyses were completed. Table 3.6 shows all the reactors and their constituents.

Table 3.5. Details about the extra reactors of disintegrated sets at the stage of reactor initiation

	Extra reactors	
Label	E1	E2
Sludge content	WAS + MP	WAS + ADS + MP
Aim	- To determine WAS solubilizing efficiency of disintegration process - To characterize disintegrated WAS - To recover MPs after disintegration for characterization	- To characterize the mixed sludge in each set - To recover MPs after disintegration
Analysis	sCOD, sProtein, sCarbohydrate, TS, VS, TSS, VSS and pH of disintegrated WAS, observations on MP characteristics	sCOD, sProtein, sCarbohydrate, TS, VS, TSS, VSS and pH of the mixed sludge

3.3.1.1 Setting-up of Anaerobic Reactors

WAS samples at volumes of 71.3 mL and with 2% TS content were placed into 48 identical serum bottles (33 main reactors + 15 extra reactors). Then the prespecified amount of PET MPs (0, 1, 3, and 6 mg PET/g TS) were added into the triplicate reactors as shown in Figure 3.7 and Table 3.6. The reactors to be disintegrated were prepared as given below.

Disintegration reactors were prepared before all the other reactor sets. Each disintegration reactor set (R0P, R1P, R3P, R6P) containing the WAS and MP at the indicated concentration was added with the predetermined NaOH and KOH to yield an OH^- concentration of 0.5 M in WAS. The bottles, capped with a rubber septum, were placed into a shaking incubator at 25°C at 250 rpm for 2 days. The reactor sets prepared with identical properties but without disintegration (with no chemical

addition) were also sealed and left in the room temperature to keep both sets consistent. After two days, alkaline disintegrated reactors were autoclaved for 120 min at 127°C. Then, the disintegration process was terminated by neutralizing the sludges with 5 M HCl solution, using pH-indicator strips to prevent the loss of MPs added. The disintegrated WAS of extra reactors (i.e., E1 and E2), on the other hand, were neutralized with 5 M H_2SO_4 solution to ensure an optimal COD measurement without any chloride interference. Then the bottles were added by the necessary amount of ADS and went through the same procedure with the rest of the BMP reactors.

Once the disintegration step and all the required additions to the reactors were completed, the reactors were purged with 99% purity nitrogen gas for 10 minutes to eliminate oxygen remaining inside and immediately capped with rubber septa. The excess nitrogen gas was released using a syringe needle to equalize the pressure inside the bottles to atmospheric pressure. Finally, the reactors were incubated at 35°C in a shaking incubator at 100 rpm. Biogas productions and biogas compositions were measured daily for the first 19 days, once in two days in the next 14 days and once in four days in the last 27 days. BMP tests were terminated after 60 days of operation.

During reactor termination, contents of each reactor were subjected to the sludge-related analyses given in Table 3.7. Only two of the three replicates of each set having MPs were subjected to these analyses except tCOD and pH. The remaining reactors were only used for the determination of MPs recovery efficiency, tCOD and pH measurement.

The sludges from the third replicate of each set with MPs (R1-3, R3-3, R6-3, R1P-3, R3P-3, R6P-3, C3-3, C3P-3), which had been reserved for the determination of MPs recovery efficiency, were poured through a stack of sieves. PET MPs recovered were cleaned by applying H_2O_2 oxidation (1:1 v/v) for 24 h in a shaking incubator. Then the MPs were collected on filter papers and washed several times with distilled water under vacuum. This procedure was applied also for recovering the MPs

remaining in sludges of the first two reactors after conducting the analyses given in Table 3.8.

Table 3.6. Reactor sets and constituents at set-up

Reactor sets	Label	WAS, mL	ADS, mL	MPs added, mg/g TS	pH, average	Total Volume[a], mL
Non-disintegrated w/o MPs	R0	71.3	128.7	none	7.47	208.3
	R0 – E2	71.3	128.7	none	7.47	208.3[b]
Non-disintegrated w/MPs	R1	71.3	128.7	1	7.48	208.3
	R1 – E2	71.3	128.7	1	7.48	208.3[b]
	R3	71.3	128.7	3	7.48	208.3
	R3 – E2	71.3	128.7	3	7.48	208.3[b]
	R6	71.3	128.7	6	7.48	208.3
	R6 – E2	71.3	128.7	6	7.48	208.3[b]
Non-disintegrated abiotic w/MPs	C3	71.3	128.7	3	7.60	208.3
	C3 – E2	71.3	128.7	3	7.60	208.3[b]
Disintegrated w/o MPs	R0P	71.3	128.7	none	7.75	208.3
	R0P – E1	71.3	none	none	7.00	79.6[c]
	R0P – E2	71.3	128.7	none	7.75	208.3[b]
Disintegrated w/MPs	R1P	71.3	128.7	1	7.75	208.3
	R1P – E1	71.3	none	1	7.00	79.6[c]
	R1P – E2	71.3	128.7	1	7.75	208.3[b]
	R3P	71.3	128.7	3	7.75	208.3
	R3P – E1	71.3	-	3	7.00	79.6[c]
	R3P – E2	71.3	128.7	3	7.75	208.3[b]
	R6P	71.3	128.7	6	7.75	208.3
	R6P – E1	71.3	-	6	7.00	79.6[c]
	R6P – E2	71.3	128.7	6	7.75	208.3[b]
Disintegrated abiotic w/MPs	C3P	71.3	128.7	3	7.63	208.3
	C3P – E2	71.3	128.7	3	7.63	208.3[b]
Seed control	SM	none	128.7	none	8.07	208.3
	SM – E2	none	128.7	none	8.07	208.3[b]

[a] Further details of volumes added are given in Appendix B (Table B.1.)
[b] These reactors were used to characterize the sludges in each set and were not taken into further BMP test.
[c] In these reactors only the effect of pretreatment was studied and the reactors were not taken into further BMP test

Table 3.7. Parameters analyzed in each replicate when the reactors were terminated

Reactor sets	Label	Solids	tCOD	pH	ROS	sCOD, sProtein sCh	MP recovery and analysis	Biogas volume and composition[b]
Non-disintegrated w/o MPs	R0 – 1	+	+	+	+	+	-	+
	R0 – 2	+	+	+	+	+	-	+
	R0 – 3	+	+	+	+	+	-	+
Non-disintegrated w/ MPs	R1 – 1	+	+	+	+	+	+	+
	R1 – 2	+	+	+	+	+	+	+
	R1 – 3[a]	-	+	+	-	-	+	+
	R3 – 1	+	+	+	+	+	+	+
	R3 – 2	+	+	+	+	+	+	+
	R3 – 3[a]	-	+	+	-	-	+	+
	R6 – 1	+	+	+	+	+	+	+
	R6 – 2	+	+	+	+	+	+	+
	R6 – 3[a]	-	+	+	-	-	+	+
Non-disintegrated abiotic w/MPs	C3 – 1	+	+	+	-	+	+	+
	C3 – 2	+	+	+	-	+	+	+
	C3 – 3[a]	-	+	+	-	-	+	+
Disintegrated w/o MPs	R0P – 1	+	+	+	+	+	-	+
	R0P – 2	+	+	+	+	+	-	+
	R0P – 3	+	+	+	+	+	-	+
Disintegrated w/ MPs	R1P - 1	+	+	+	+	+	+	+
	R1P - 2	+	+	+	+	+	+	+
	R1P – 3[a]	-	+	+	-	-	+	+
	R3P – 1	+	+	+	+	+	+	+
	R3P – 2	+	+	+	+	+	+	+
	R3P – 3[a]	-	+	+	-	-	+	+
	R6P – 1	+	+	+	+	+	+	+
	R6P – 2	+	+	+	+	+	+	+
	R6P – 3[a]	-	+	+	-	-	+	+
Disintegrated abiotic w/MPs	C3P – 1	+	+	+	-	+	+	+
	C3P – 2	+	+	+	-	+	+	+
	C3P – 3[a]	-	+	+	-	-	+	+
Seed control w/o MPs	SM – 1	+	+	+	-	+	-	+
	SM – 2	+	+	+	-	+	-	+
	SM – 3	+	+	+	-	+	-	+

[a] As it was aimed to determine the MPs recovery efficiency, no solids analysis was performed in these reactors. The recovered MPs were further analyzed.
[b] Biogas measurements were conducted periodically until the reactors were terminated.
1, 2, and 3 define the name of each replicate.
Analysis of solids include TS, VS, TSS, and VSS.
ROS: Reactive oxygen species.

MPs gathered after disintegration and anaerobic digestion were morphologically and chemically analyzed to investigate any evidence for deterioration during these treatment processes, by comparing their properties with the raw PET MPs. The

plastics-related parameters analyzed for the collected particles, what they indicate, and their method of measurement are given in Table 3.8.

Table 3.8. Plastics-related parameters

Parameter	Indication	Measurement method
Crystallinity	Change in polymer density	FTIR
Carbonyl Index	Surface oxidation	FTIR
Mass	Change in mass of MPs	Gravimetric method
Surface morphology	Surface deterioration	Scanning Electron Microscopy (SEM)

3.4 Analytical Methods

The analytical methods used in this study are divided into two groups: methods used to measure the performance of BMP reactors and methods related to analysis of plastics.

3.4.1 Methods Used to Measure the Performance of BMP Reactors

Parameters given in Table 3.9 were measured at both reactor initiation and termination. Besides, biogas volume and composition were monitored periodically during reactor operation. The related information of each parameter is provided in sections below.

Table 3.9. Parameters analyzed at reactor initiation and termination and their purposes

Parameter	Method	Purpose
TS, VS	Standard Method 2540 G APHA, AWWA, and WEF (2017)	Sludge characterization, digester performance analysis
TSS, VSS	Standard Method 2540 D and 2540 E APHA, AWWA, and WEF (2017)	
pH	Standard Method 4500 H APHA, AWWA, and WEF (2017)	
Total COD	EPA approved digestion method Jirka and Carter (1975)	
Soluble COD	EPA approved digestion method Jirka and Carter (1975)	Sludge characterization, solubilizing effect of disintegration process and digester performance analysis
Soluble protein	Lowry et al. (1951)	
Soluble carbohydrate	Dubois et al. (1956)	
Reactive oxygen species*	Wei et al. (2019a; 2019c)	Understanding toxicity mechanism related to MPs in reactors

*Measured only at reactor termination

3.4.1.1 Solids Analyses

Set-up and termination steps of BMP test included triplicate analyses of TS, VS, TSS and VSS content of sludge samples according to Standard Methods. The method 2540G specialized for solid and semisolid samples was carried out for determining the TS and VS contents of WAS and ADS samples. Moreover, VSS content of ADS was measured by following the Methods 2540 D and 2540 E (APHA, AWWA, and WEF, 2017).

3.4.1.2 Chemical Oxygen Demand (COD)

COD content of samples during MPs analysis and BMP test was determined in triplicate according to EPA approved digestion method (COD range of 0-1500 mg/L) (Jirka and Carter, 1975). The samples were heated for 2 hours at 150°C using HACH COD Reactor. Following the digestion, samples cooled to room temperature were

spectrophotometrically measured by HACH DR/2800 Direct Reading. Calibration curve of COD plotted by using KHP solution is given in Appendix A (Figure A.1).

3.4.1.3 Soluble Chemical Oxygen Demand (sCOD)

sCOD was measured in triplicate during sludge disintegration studies to investigate the solubilizing efficiency of the applied techniques and BMP test as a digester performance indicator. Thirty mL of sludge samples were centrifuged, and the supernatant were filtered through a membrane filter with pore size of 0.45 μm. COD value of the filtrate which was measured using EPA approved digestion method gives the sCOD value of a sample.

3.4.1.4 Soluble Protein Analysis

Folin-Ciocalteu's Protein Measurement Method (Lowry et al., 1951) was applied to determine the soluble protein content of samples after sludge disintegration studies and BMP test on the 0.45 μm filtered samples. In this method, four different reagents (i.e., A, B, C, and D) were freshly prepared and Bovine serum albumin (BSA) was used as a standard solution in plotting the calibration curve given in Appendix A (Figure A.2). Reagent A was 2% w/v sodium carbonate which was dissolved in 0.1 N NaOH. Reagent B consisted of 1% w/v sodium potassium tartarate in 0.5 % w/v cupric sulphate. Reagent C was prepared by mixing the Reagent B and A to a ratio of 1:49. Finally, Reagent D was formed by diluting the Folin - Ciocalteu's phenol reagent 1:1 with distilled water.

Following the preparation of the reagents, 0.6 mL of samples with 0 – 200 μg protein content were put into 10 mL glass vials. Then, 3.0 mL of Reagent C was added onto the samples, the vials were mixed and let to stand for 10 minutes. Finally, 0.3 mL of Reagent D was added onto each vial, immediately vortexed and allowed to stand for another 30 minutes at room temperature. The intensity of the blue color obtained was read at 750 nm using HACH DR/2800 Direct Reading. Both the sample and standard

solutions were prepared in triplicates to minimize errors. Calibration curves were updated each time protein analysis was performed throughout the study.

3.4.1.5 Soluble Carbohydrate Analysis

As the soluble protein, soluble carbohydrate content of pretreated sludge samples was also analyzed for determining the solubilization efficiency of the applied pretreatment technique and their contribution to the released organics. It was also measured at reactor initiation and termination as an indicator of digester performance. Dubois Method (Dubois et al., 1956) was applied to determine the soluble carbohydrate content of sludge samples using the standard glucose solution, the calibration curve of which is given in Appendix A (Figure A.3).

First, 2 mL of samples containing 10 – 70 μg of carbohydrate were pipetted into 10 mL glass vials and 0.05 mL of 80% (w/w) Phenol solution was added. Then, 5 mL of concentrated H_2SO_4 solution was added rapidly onto each vial and they were allowed to stand for 10 minutes. The vials were vortexed and placed for 10 - 20 minutes in an incubator at 25 - 30°C. Readings were made at 490 nm using HACH DR/2800 Direct Reading. Both the sample and standard solutions were prepared in triplicates to minimize errors.

3.4.1.6 pH

pH was an inseparable parameter of this study as it was intensively used in analysis of MPs, sludge disintegration, as well as in anaerobic reactors. It was measured using Oakton pH/mV/°C meter Standard Method 4500 H (APHA, AWWA, and WEF, 2017).

3.4.1.7 Total Biogas Production

The volume of biogas produced in BMP reactors was measured using a water displacement unit. The method is based on equalizing the pressure inside the bottles to atmospheric pressure by releasing the gas accumulating in head space of the bottles via a needle connected to the water displacement unit. The volume of acidified water displaced in this unit reflects the amount of biogas produced.

3.4.1.8 Biogas Composition

The biogas composition of each reactor was analyzed by using Agilent Technologies 6890N Gas Chromatograph (Agilent Technologies, California, USA) with thermal conductivity detector (TCD). The device was equipped with a HP-Plot Q capillary column with dimensions of 30.0 m x 530 μm x 40.0 μm. The carrier gas of the device was helium with a velocity of 29 cm/s. Measurement was initated at a column temperature of 45°C maintained for the first minute, then the temperature was increased to 65°C at a rate of 10°C/min. Every time compositional measurement was carried out, the data obtained from the device was calibrated using standard curves plotted regularly. Two different calibration gas mixtures with varying compositions were used for this purpose, which are 65% methane, 25% carbon dioxide, 10% nitrogen and 25% methane, 55% carbon dioxide, 20% nitrogen. Following the calibration, composition of biogas produced in each reactor was measured daily using Hamilton gas tight syringe (#1710) with 100 μL volume.

3.4.1.9 Methane Yield Calculation

At reactor termination stage, experimental methane yield (Y_{Exp}) was calculated by using Equation 3.5. The substrate-specific theoretical methane yield (Y_{Theo}) was determined by the multiplier "a" added to the theoretical value based on COD removal at 35°C and 1 atm (395 mL CH_4/g COD) as shown in Equation 3.6 (Raposo et al., 2011). Moreover,

biodegradability (BD) of WAS based on the methane yield was determined by using Equation 3.7.

$$Y_{Exp} = \frac{\text{Experimental } CH_4 \text{ production (mL)}}{\text{VS of substrate added (g)}} \qquad \text{(Equation 3.5)}$$

$$Y_{Theo} = a \left(\frac{g\ COD}{g\ VS}\right) * 395 \left(\frac{mL\ CH_4}{g\ COD}\right) \qquad \text{(Equation 3.6)}$$

Where,

a = COD equivalent of 1 gram VS of WAS, which is 1.48 g COD/g VS based on data given in Table 3.3.

$$BD\ (\%) = \frac{Y_{Exp}}{Y_{Theo}} \qquad \text{(Equation 3.7)}$$

3.4.1.10 Reactive Oxygen Species

In order to assess the possible toxicity mechanism associated with MPs in reactors, intracellular ROS in sludge was measured once the reactors were terminated by a fluorescence-based method in which the signals are measured using a microplate reader, as shown in Figure 3.8.

2′,7′-Dichlorofluorescin diacetate (H2DCFDA, CAS: 4091-99-0) was prepared in absolute ethanol (≥ 99.5%) to a concentration of 10 mM and stored at -20°C until use. Different concentrations of H_2O_2 solution (35% w/w) ranging from 50 µm to 5

mM were prepared as standard solutions to adjust the settings for the measurement. Obtaining satisfactory fluorescent signals even at the lowest H_2O_2 concentration made the analysis procedure applicable for sludge samples. 1 mL of sludge was taken into a 1.5 mL microtube and centrifuged for 10 min at 10,000 rpm using TG16-W Microcentrifuge. While the supernatant obtained after centrifugation was decanted, the pellets were rinsed with phosphate buffer solution (pH=7.4) and resuspended. The suspension was centrifuged at 10,000 rpm for another 10 min. The supernatant was discarded and 5 µL of 10 mM H2DCFDA was added onto the pellets to a final concentration of 50 µM. The final volume of the mixture was adjusted to 1 mL with phosphate buffer solution. The mixture was vortexed well and incubated at 35±1 °C in dark for 30 min. Incubated sample was centrifuged, and the unbonded dye in supernatant was discarded. The pellets were resuspended in phosphate buffer, vortexed and transferred into 96-well plates in triplicate. The generated fluorescein dichlorofluorescein (DCF) was measured by Thermo Scientific Varioskan LUX Microplate Reader at excitation and emission wavelengths of 485 and 520 nm, respectively.

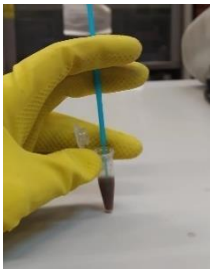

(a)

(b)

(c)

Figure 3.8. Sludge before fluorescent probe (a); sludge after incubation (b); microplate reader (c)

3.4.1.11 Statistical Analysis

To determine the effect of different PET-MPs doses on methane production and yield, One-way ANOVA method was applied both for disintegrated and non-disintegrated reactor sets. Furthermore, independent samples T-test was performed to determine the impact of disintegration and anaerobic digestion on mass of PET particles. The confidence level was taken as 95%. Both tests were carried out using SPSS v26.

3.4.2 Methods Related to MPs

PET MPs extracted from sludges in disintegration studies and anaerobic digestion were analyzed to investigate: (i) the effects of different sludge disintegration processes; (ii) the combined effect of disintegration and microorganisms after anaerobic digestion; (iii) the sole impact of microorganisms; and (iv) abiotic factors.

Before doing any analysis, PET MPs were cleaned by applying H_2O_2 oxidation (1:1 v/v) for 24 h in a shaking incubator, and then air-dried for overnight. Then, MPs were inspected both physically and chemically.

3.4.2.1 Chemical Analysis of MPs

MPs extracted from sludge samples were chemically characterized to investigate any evidence for deterioration both during sludge disintegration and anaerobic digestion by the calculation of crystallinity and carbonyl index from infrared spectra.

3.4.2.1.1 Crystallinity and Carbonyl Index

The infrared spectra, which were used for the determination of crystallinity and CI, were recorded by ATR-FTIR (Perkin Elmer 400) under spectral resolution of 4 cm^{-1},

sample scan of 16 and spectrum with wavelengths between 400 and 4000 cm^{-1}. This analysis was carried out at METU Central Laboratory.

Crystallinity index of PET was determined by taking the ratio of absorbances at 1340 cm^{-1}/1410 cm^{-1} (Donelli et al., 2010; Sammon et al., 2000). Similarly, carbonyl index of PET was calculated by dividing the absorbance of the carbonyl peak (1715 cm^{-1}) by that of a reference peak (1506 cm^{-1}) (Lessa Belone et al., 2021).

3.4.2.2 Surface Morphology

To analyze topographical properties of PET MPs QUANTA 400F Field Emission Scanning Electron Microscope (SEM) was used at METU Central Laboratory.

3.4.2.3 Mass Measurement

First, a linear graph was plotted for mass versus particle number of PET MPs in sizes of 250-500 μm, as given in Figure 3.9. The graph with its high R^2 value indicating uniformity of particles within the specified size range was used to obtain unit mass of untreated PET MPs.

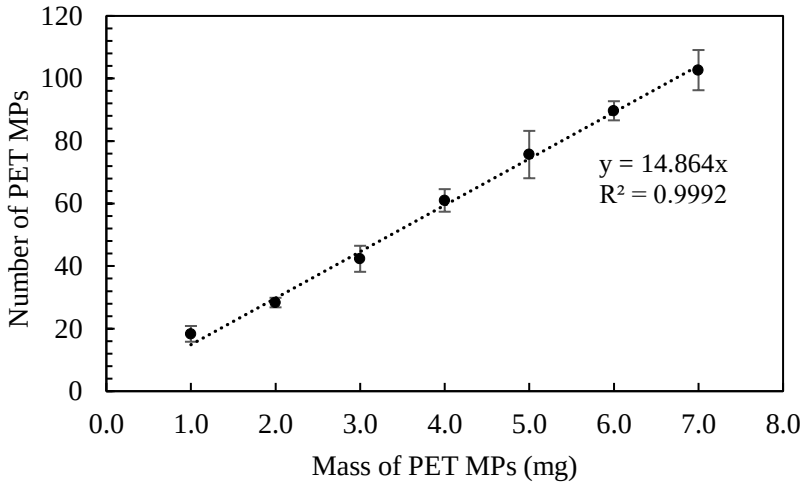

Figure 3.9. Mass versus number of PET MPs

Then, the treated PET MPs were counted and weighed in batches of 20 particles in triplicate using an analytical balance (accuracy of ±0.1 mg), thereby mass of each PET particle was determined. Change in mass of a unit PET MP exposed to different processes was determined by taking the untreated PET as the reference using Equation 3.8.

$$\% \text{ mass loss} = \frac{m_i - m_f}{m_i} \times 100 \qquad \text{(Equation 3.8)}$$

where m_i and m_f are the untreated and treated mass of unit PET particle (g), respectively.

CHAPTER 4

RESULTS AND DISCUSSION

This chapter covers the results and discussion of the three experimental steps, analysis of MPs in sludge, sludge disintegration, and BMP test.

4.1 Method Development and Results of Microplastics Analysis

Method development studies involved logically sequencing the commonly applied steps given in the literature for the analysis of MPs in water and wastewater and optimizing each step for sludge samples. The entire procedure developed consists of pretreatment, extraction, identification and quantification steps. Studies carried out under this heading continue with determining the efficacy (i.e., recovery rate) of the developed method and analysis of MPs in sludge.

4.1.1 Microplastics Analysis

As it is mentioned in Materials and Methods, MP analysis starts with the removal of organics that may interfere with the following steps of analyses. Figure 4.1 (a) shows the change of COD with time at different molar ratios (MR) of H_2O_2 to Fe(II) during the Fenton process and Figure 4.1 (b) shows the corresponding COD removal rates. Since the experiments were conducted at different days, the initial COD of samples were slightly different from each other. Figure 4.1 (a) shows that COD decreases as time proceeds at each MR with the sharpest reduction happening at the first 15 min. Then the reductions continue at a much smaller rate. Results show that MR: 10 with 90% COD removal is the most effective molar ratio as it provides the highest COD removal efficiency in the shortest time as given in Figure 4.1 (b). Providing the minimum time possible that yields high COD removal is important in analysis

because MPs are subjected to chemicals and oxidative conditions during pretreatment. Figure 4.1 shows most organics are oxidized at 15 minutes for all of the MR's employed. Though, the oxidation at MR:30 was generally slower due to lower Fe(II) amount, which acts as catalyst. Further removals can be observed at later times (90 or 120 mins), but the time of experiment is thought to be prohibitive and unnecessary. So, the best time of pretreatment was selected as 30 min.

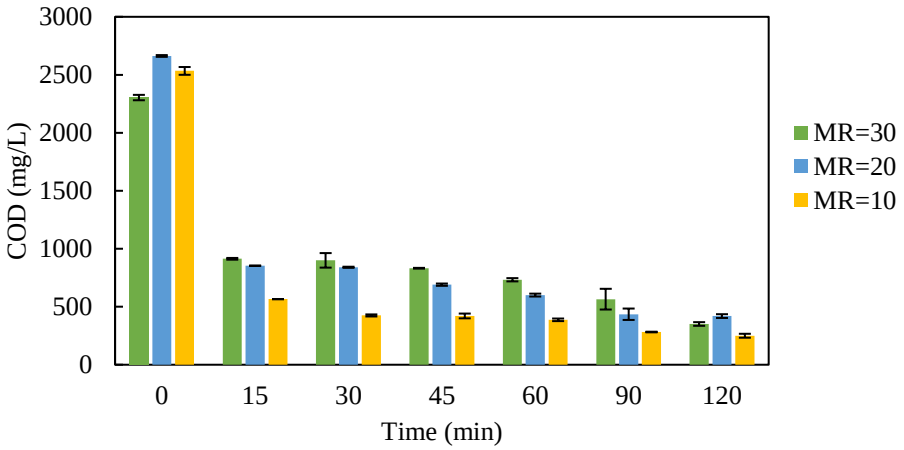

(a)

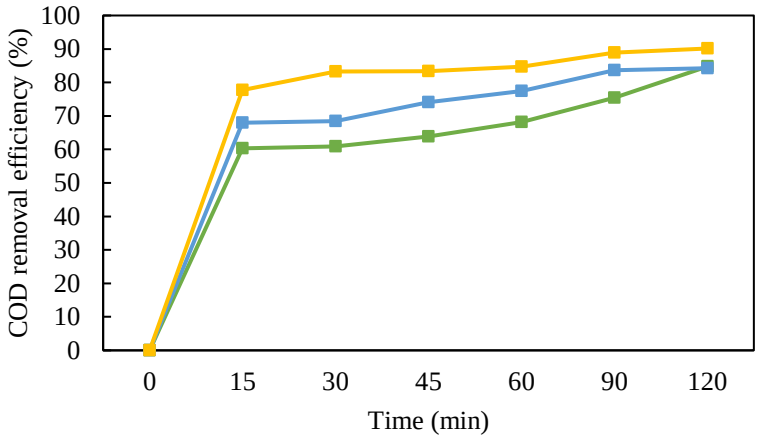

(b)

Figure 4.1. Change in COD of WAS during Fenton Oxidation (a); COD removal efficiency in time (b)

Following one-step (in saturated NaCl solution at 1.15 g/mL) and two-step (additionally in saturated $ZnCl_2$ solution at 1.5 g/mL) density separation, results

showed that two-steps provided better capture of MPs for two main reasons. First, some of MPs were trapped in $Fe(OH)_3$ flocs during settling, which caused an underestimation of the concentration of MPs in sample. Taking the settled flocs and remixing them with the addition of $ZnCl_2$ led those particles to become free and float upward. Hence, the floating portion of the sample better represented MPs content to be further analyzed. Second, the increase in density of sample achieved after NaCl addition was not sufficient to float MPs with high densities such as PVC, PET, PMMA, PU, PES which are among the most frequently reported polymer types in sludge. Adding $ZnCl_2$ ensures capturing all these polymers in sludge sample. Literature also recommends sequential extraction in NaI and $ZnCl_2$ to separate both the low and high-density MPs and accurately determine their number despite the high price and relatively toxic properties of these two salts (Okoffo et al., 2019; Silva et al., 2018).

The next step was to select the best solvent to dissolve the fluorescent dye, Nile Red. But at the same time the solvent selected had to be compatible with the filters (i.e., PCTE) used in the analysis. Among three different carrier solvents inspected (i.e., ultra-pure water, acetone and n-hexane), n-hexane was found as the best one for staining MPs without any damage to the PCTE filter. Acetone significantly destroyed the PCTE filter and ultra-pure water caused the dye to precipitate. Some pictures of the filters are given in Figure 4.2.

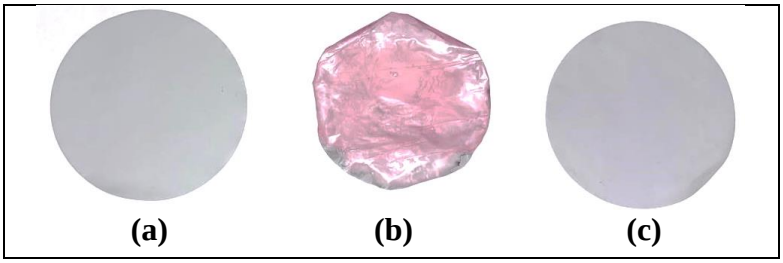

Figure 4.2. Picture of PCTE filters (a) without stain; and stained by (b) dye dissolved in acetone; and (c) n-hexane

Still, it was necessary to prepare the stock solution of dye in acetone due to its low solubility in n-hexane (Shim et al., 2016). Thus, Nile Red stock solution was prepared in acetone at 250 mg/L and diluted to 10 mg/L in n-hexane.

To find an alternative to PCTE, different filters such as Glass Fiber Filter (GF/A), Cellulose Nitrate (CN), qualitative filter paper (Whatman No 1) and Mixed Cellulose Ester (MCE) were tested for compatibility with Nile Red. As shown in Figure 4.3, all filters except MCE retained dye on their surfaces which caused high background fluorescence hampering visualization of MPs under Fluorescence Microscope. So, MCE filter could be the only alternative. Still, the PCTE filter was by far the best due to its perfectly flat black surface ensuring no background signal and no ridges.

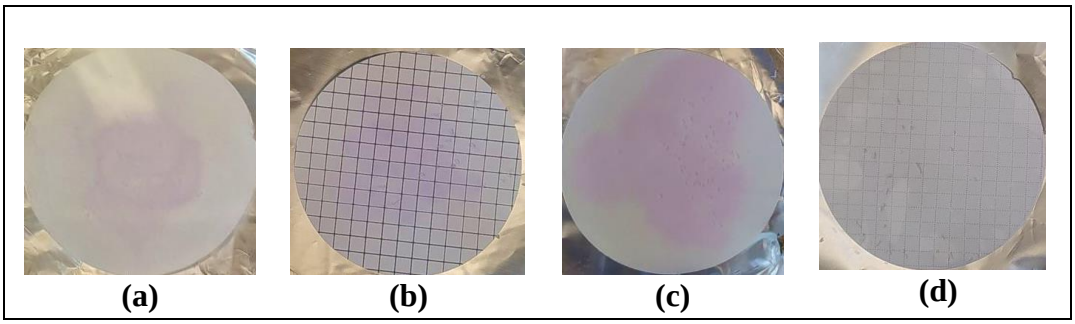

Figure 4.3. Compatibility test of different filter types with Nile Red: (a) GF/A; (b) CN; (c) qualitative filter paper; and (d) MCE

Moreover, the effectivity of staining procedure was tested on different types of MPs by changing the incubation conditions applied. Consequently, the most powerful fluorescence of MPs was achieved when 200 µL of the dye was added onto black PCTE filter and incubated at room temperature for 15 minutes in dark.

Following the incubation, filters were inspected under ZEISS Axio Scope.A1 Fluorescence Microscope using GFP filter. Shiny particles which are shown in Figure 4.4 were reckoned as MPs, and they were counted under UV light.

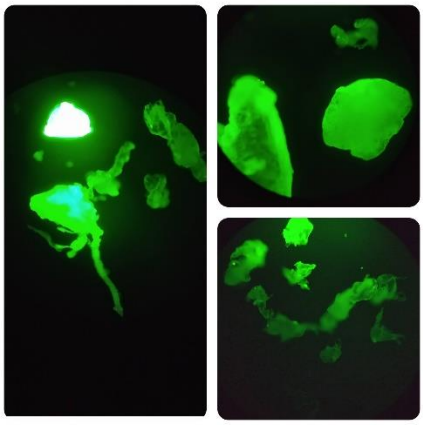

Figure 4.4. Example MPs under UV light at x10 magnification

Particles most commonly encountered and suspected to be MPs are shown under bright field in Figure 4.5.

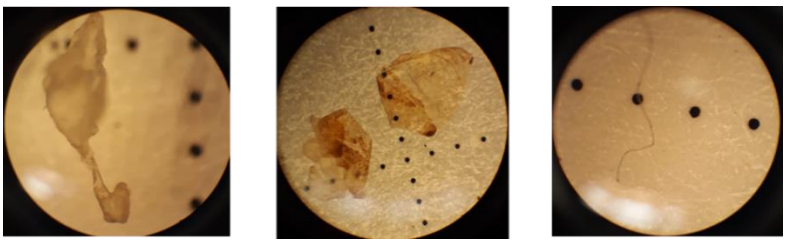

(a) **(b)** **(c)**

Figure 4.5. Most frequently encountered MP particles in sludge samples (taken under bright field): (a) fragment (x20 magnification); (b) film (x10 magnification); (c) fiber (x20 magnification)

The finalized method was schematically summarized in Figure 4.6. In short, Fenton process was first applied at a MR:10 of H_2O_2 and Fe(II) to remove organic materials in sample. Then MPs were extracted by applying a two-step density-based separation process using NaCl and $ZnCl_2$ in separatory funnels. Uppermost portions of both funnels were collected and sieved through stack of sieves with mesh sizes of 5.00 mm, 1.18 mm, 425 μm, and 38 μm. Particles kept on filters were stained with Nile Red solution and incubated for 15 min in dark. Following incubation, filters were

inspected under Fluorescence Microscope for counting and classification of MPs based on their size and shape.

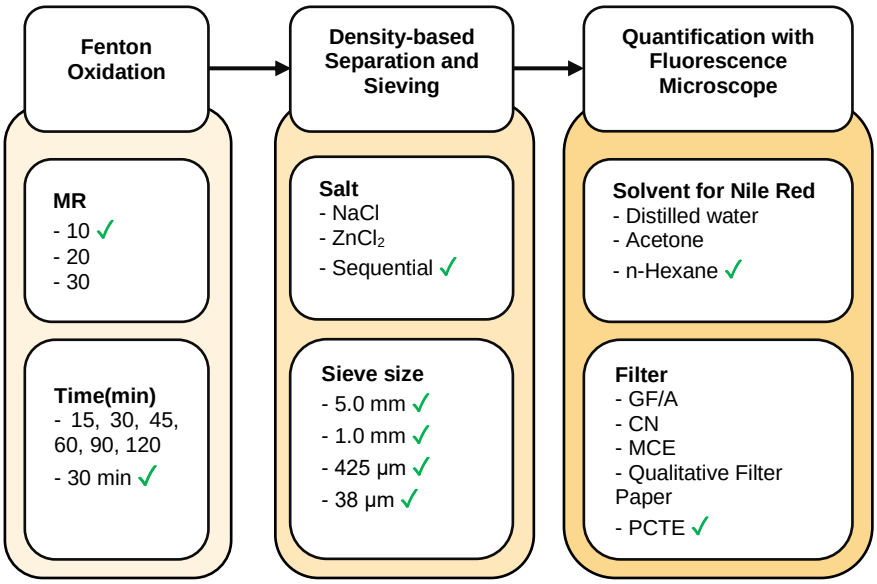

Figure 4.6. Optimized method for MPs analysis

4.1.2 Results of Recovery Experiment

To be able to check the effectiveness of the optimized method, known plastics at known concentrations were added into KHP (a simple organic matrix), wastewater and then to sludge (i.e., WAS). The entire MP analysis procedure presented in Figure 4.6 was then followed to recover spiked MPs.

Studying with different matrices, MP polymer types and sizes resulted in varying levels of recovery efficiencies as shown in Table 4.1. The initial COD values were around 700, 400, 3000 mg/L for KHP, wastewater and WAS, respectively. PE MPs in sizes of 500-1000 µm and 250-500 µm were spiked into the synthetic matrix made of KHP solution and 88±8% and 84% recovery efficiencies were achieved, respectively. So, the method works at a similar efficiency for PE MPs in the size range of 250-1000 µm.

Next, it was aimed to evaluate the efficacy of the method for complex matrices and compare it to a rather clean sample (KHP). Thus, PE MPs in sizes of 250-500 μm were added to a wastewater sample and 79±12% recovery was achieved. Then, a mixture of different polymers, which are among the most frequently reported ones in sludge and representing different density classes, was spiked into WAS. In WAS, PE, PA and PET MPs in sizes of 425-500 μm were recovered at a rate of 94, 80, and 80%, respectively. This result indicates that the density of plastics may be an important parameter affecting their recovery as the efficiency decreased with increasing density. Besides, in all cases, a removal rate of COD at a minimum of 86% was achieved.

Table 4.1. Summary of MPs recovery experiments

Polymer type	Size of MPs, μm	n	Matrix	# of MPs added	%MPs Recovery	%COD Removal
PE	500-1000	3	KHP	25	88±8	87±2
PE	250-500	2	KHP	25	84	
PE	250-500	3	Wastewater	25	79±1	87±3
PE	425-500	2	WAS	25	94	96±1
PA	425-500	2	WAS	25	80	
PET	425-500	2	WAS	25	80	

n: Number of replicates

All these results were deemed satisfactory with respect to literature, which states that MP recovery efficiencies higher than 70% are fairly acceptable (Cashman et al., 2020). The method also meets the 80% yield recommended by ASTM (2020). Thus, applying this method produces reliable data for both a clean sample (KHP) and complex matrices (wastewater and WAS). This achievement can be mainly attributed to two outstanding approaches integrated to the method. First, the optimized Fenton Oxidation provides such an effective organic removal efficiency (i.e., COD removal) that eliminates matrix effect in MPs analysis (Table 4.1). Second, two-step density-based separation process highly promotes the extraction efficiency of MPs (especially those with high densities) as the sample is mixed twice

in consecutive days, which allows MPs trapped in residuals of Fenton Oxidation to float upward.

4.1.3 Quantification Results of Microplastics in Sludge

The developed method was used to determine background MPs content of the sludge (mixture of WAS and ADS) added into BMP reactors. Sludge samples (WAS and ADS) used to set up the reactors were combined at the ratios used in reactors and this sample was subjected to the MP analysis with the optimized method shown in Figure 4.6 and Figure 4.7. Sludge sample counting was then corrected by a blank analysis using distilled water going through the same procedure.

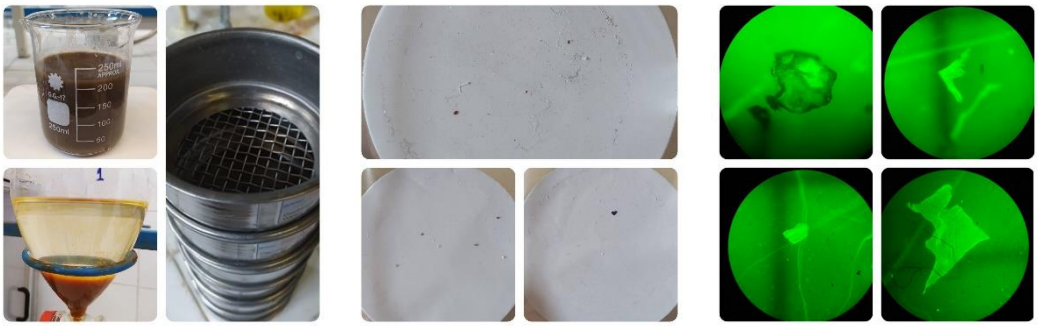

(a) **(b)** **(c)**

Figure 4.7. Photographs taken at different stages of the procedure: (a) pretreatment and extraction; (b) MPs retained on filters; (c) and sample MPs from sludge at x10 magnification

As shown in Figure 4.8 (a), MPs suspected in the sample were classified by number as fragment (62%), fiber (22%) and film (16%), which are the top three most reported MPs shapes in the literature. Moreover, particles were classified by number according to their sizes as follows: 38-425 µm (85%), 425-1180 µm (11%), 1180-5000 µm (4%) (Figure 4.8 (b)). The predominance of smaller sized MPs over the larger ones is in line with the findings of many studies which claim that smaller MPs

are removed at a higher rate via adsorption on sludge during sedimentation process (Liu et al., 2019; Magni et al., 2019; Mason et al., 2016; Talvitie et al., 2017).

The concentration of MPs determined was 270 MPs/g TS following blank correction (217 MPs/L of distilled water). It is close to the upper limit of the range, 1,000 – 240,300 MPs/g TS, given in literature for dewatered sludge and digested sludge (Table 2.1).

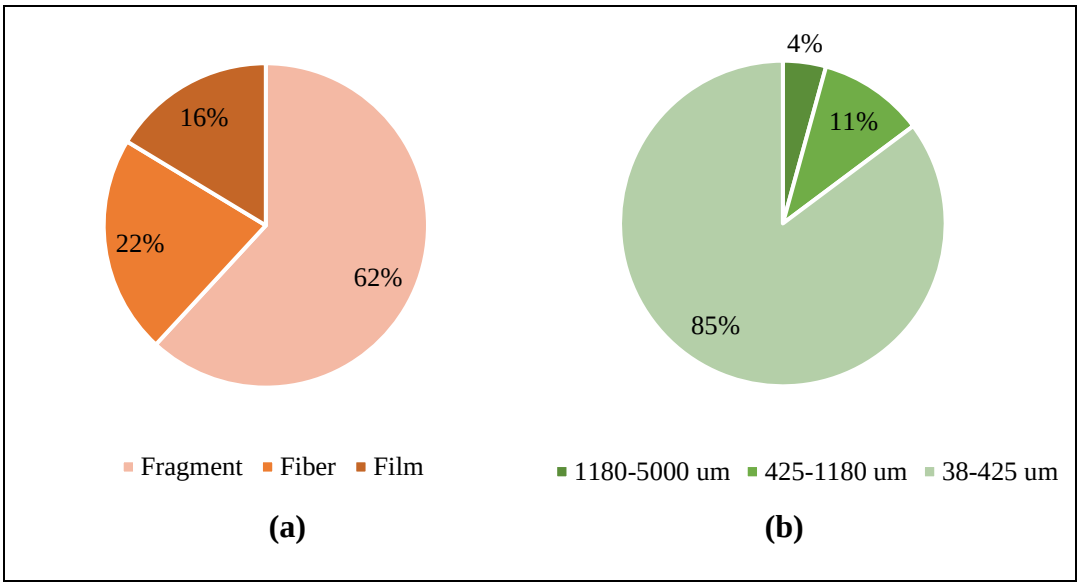

Figure 4.8. Shape (a); and size (b) distribution of MPs by number in a reactor

4.2 Sludge Disintegration

4.2.1 Alkaline Disintegration of Sludge

The first set of studies conducted for alkaline disintegration aimed to find the optimal NaOH concentration providing the highest sludge solubilization efficiency and deteriorative impact on PET MPs. Since highly alkaline conditions show significant deterioration on PET, as well as disintegrative effect on sludge, it was aimed to

increase alkali dose as much as possible. As shown in Figure 4.9, 0.5 M NaOH application in WAS was 24.5% and 15.1% more effective in COD solubilization (measured by relative increase of sCOD in relation to the value at time zero) compared to 0.1 and 0.2 M, respectively. 0.5 M NaOH increased sCOD content of WAS by 18.3-fold in 120 min. Despite observing an upward trend in solubilization with increasing alkaline dose, higher doses were not investigated due to toxicity concerns for anaerobic digesters (Kugelman and Mccarty, 1965; McCarty, 1964) which the samples are introduced into following the disintegration process.

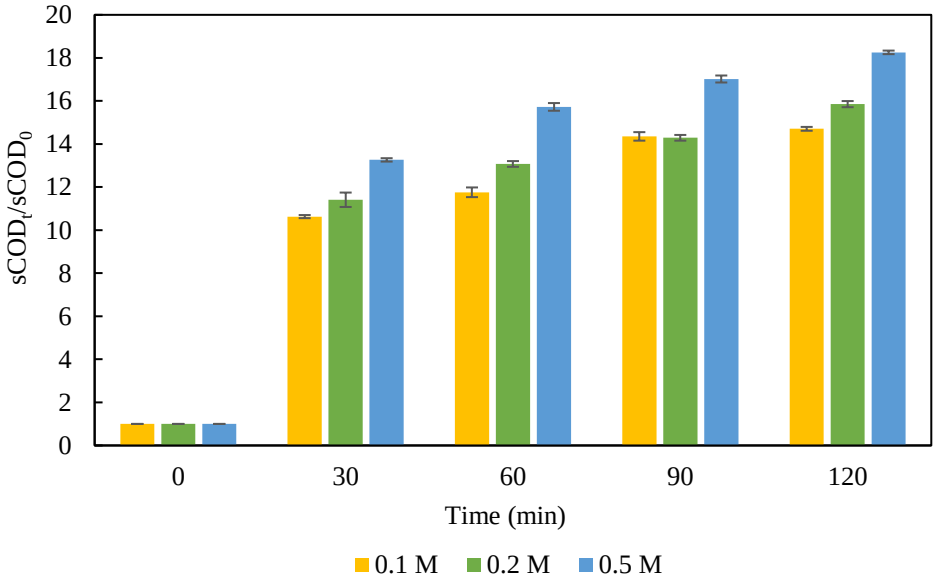

Figure 4.9. Comparative effectiveness of different NaOH concentrations in COD solubilization

Since anaerobic microorganisms are very sensitive to environmental conditions, it was important to keep the microorganisms uninhibited (due to the presence of high Na ions) while increasing the soluble substrate using alkaline disintegration. For that reason, a preliminary BMP test was set-up after alkaline disintegration and pH neutralization to check the inhibition situation. Since only the ion effect was investigated, the alkali doses were immediately neutralized and disintegrated effect was prevented. The preliminary BMP test investigating the ion effect on digestion efficiency showed that 0.1 M, 0.2 M and control reactors (with no NaOH) do not

differ much in cumulative methane generation (Figure 4.10). On the other hand, 0.5 M NaOH having 4123.8 mg/L Na^+ and 6441.5 mg/L Cl^- (introduced during pH neutralization) in a reactor causes retardation in methane production. These ion concentrations lie within the range of moderate inhibition (3500-5500 mg/L for Na^+ and >6000 mg/L for Cl^-) for anaerobic digestion process according to Appels et al. (2008) and McCarty (1964). In contrast to a long inhibition period observed, average cumulative methane yields of all reactors are similar. The yield values are 0.21, 0.21, 0.22, and 0.20 L CH_4/ g VS added for reactor sets with the addition of 0.1 M NaOH, 0.2 M NaOH, 0.5 M NaOH, and no extra ion addition (i.e., control), respectively.

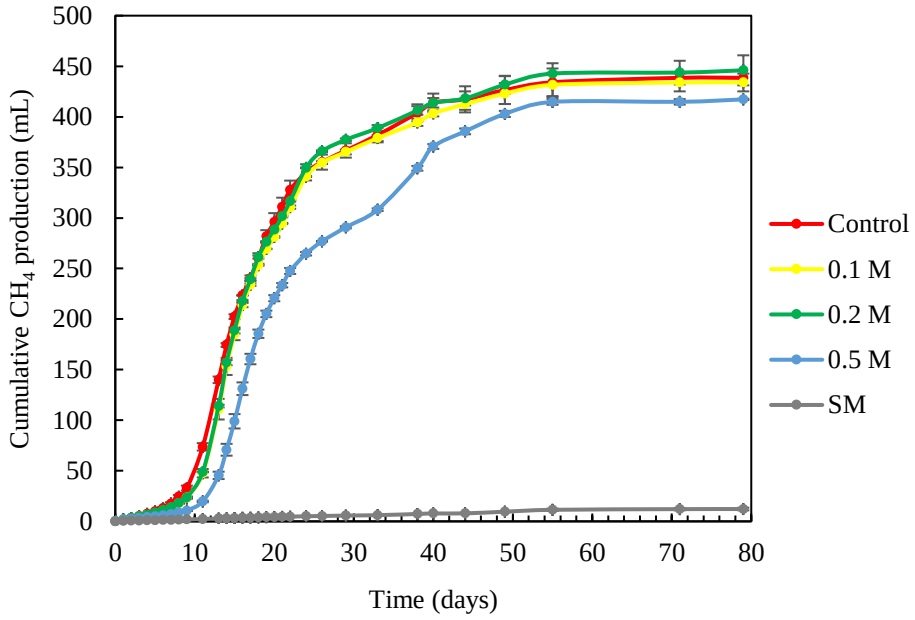

Figure 4.10. Average cumulative CH_4 production results for preliminary BMP test

Results of this preliminary BMP test necessitated decreasing Na^+ concentration to minimize inhibitory effect on microorganisms and hence the lag period observed. This goal was achieved in the next BMP test performed in this study by the combined use of NaOH and KOH, which provides antagonistic effect according to Kugelman and Mccarty (1965). This way, it was possible to keep the overall alkali dose constant at 0.5 M.

Based on the theory that the presence of one ion can significantly reduce the toxicity of the other cation, KOH and NaOH solutions were added at concentrations of 0.10±0.02 and 0.38±0.02 M, corresponding to Na^+ and K^+ concentrations of 3421.46 and 1595.5 mg/L in a reactor, respectively. These values are below the inhibitory levels determined by McCarty (1964).

The individual shares of NaOH (0.38±0.02 M) and KOH (0.10±0.02 M) in total WAS solubilization are shown in Figure 4.11. It was observed that their combined use promoted the solubilization along with alleviating the accumulation of single ion.

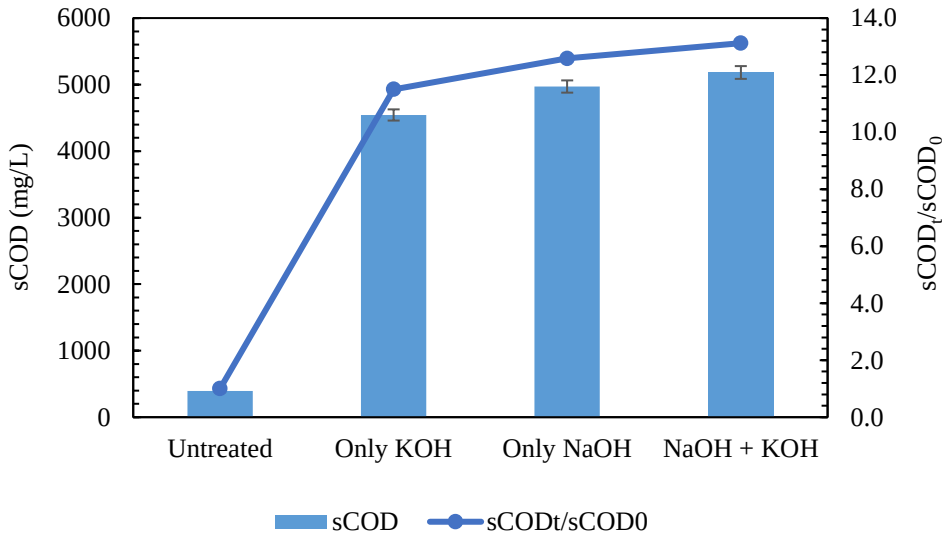

Figure 4.11. Individual and combined effect of KOH and NaOH on solubilization in 1 hour

After deciding on 0.5 M alkali application (combined dosing), the time effect was investigated; sludge solubilization results (as soluble COD, protein and carbohydrate) of which are in Figure 4.12 for five days. While COD continued to solubilize with a rate slowing down over the five days, carbohydrate and protein content of WAS did not further solubilize after the second day. Even one day was quite enough to solubilize most of carbohydrate and protein content of WAS. This concludes that the durations longer than two days do not provide any further positive impact. Therefore, two days of 0.5 M alkali (NaOH and KOH) disintegration

providing 47.8, 75.4 and 27.2-fold increase in soluble COD, protein and carbohydrate, respectively was observed to be the optimum condition and selected to be used in later studies. The choice of two days treatment was further justified in combined disintegration studies (Section 4.2.1). To increase the level of stress on PET MPs, subsequent thermal hydrolysis was adopted to the disintegration process.

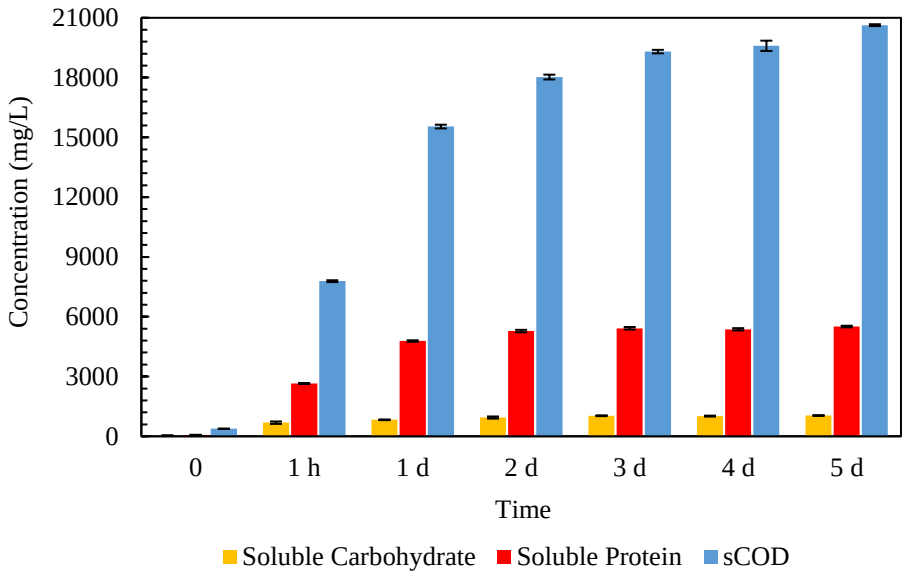

Figure 4.12. Solubilization of WAS with 0.5 M alkaline treatment in five consecutive days

4.2.2 Thermal Hydrolysis Process

Studies carried out for thermal hydrolysis involved examining the effect of time on WAS solubilization, since an earlier study suggested the temperature to be 127°C (Arı-Akdemir, 2019). As the duration of THP at 127°C was prolonged, the degree of COD solubilization slightly increased, as shown in Figure 4.13. Bougrier et al. (2006) also claimed that treatment time had little effect if higher than 30 min. Although there was no notable difference between the efficacy of treatment times studied, 120 min was selected as the main purpose was to expose MPs to stress conditions before anaerobic digestion rather than the sludge solubilization.

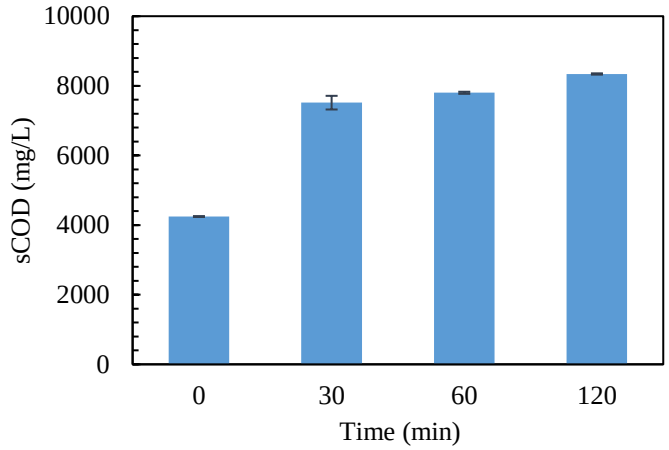

Figure 4.13. Change in sCOD of WAS at different pretreatment times

The initial sCOD value of WAS (~4000 mg/L) used in thermal hydrolysis was much higher compared to those (~450 mg/L) used in alkaline disintegration and combined disintegration. Although all samples used in sludge disintegration studies were taken from Ankara Central WWTP, sampling times were a little different. This variation in sludge characteristics might be due to an operational adjustment made at the plant. Still, the ultimate sCOD value reached at 120 minutes is almost the same with the results obtained during combined disintegration, which is shown in the next part.

4.2.3 Combined Disintegration

Following the optimization of individual applications of alkali and thermal disintegration techniques, their combined use was tested.

To justify the selection made on the alkali disintegration time (i.e., two days), COD solubilization efficacy of sludges disintegrated by alkali for two, four and five days and exposed to subsequent heating at 127°C for 120 min were examined. Figure 4.14 shows that two days of 0.5 M alkaline disintegration can be promoted with the addition of thermal hydrolysis. However, when sludge is disintegrated for more than two days, almost all degradable portion is dissolved, and integration of thermal

hydrolysis becomes useless. To take the advantage of heat application on sludge solubilization, two days of alkaline application is found to be sufficient.

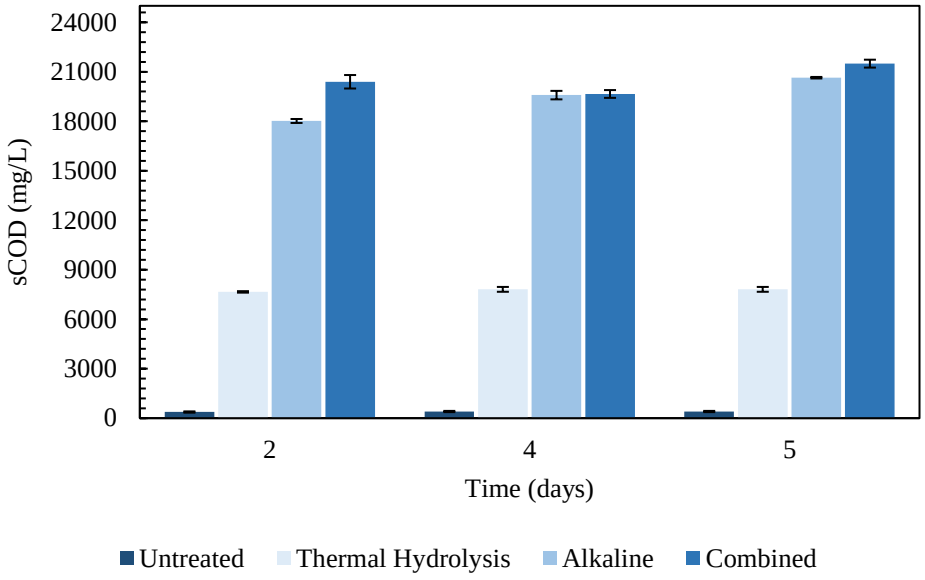

Figure 4.14. Effect of alkaline treatment time on solubilization of COD during single and combined disintegration applications

Consequently, application of 0.5 M alkaline disintegration for 2 days and thermal hydrolysis at 127°C for 120 min led to increase in soluble COD of WAS 48.4 and 20.6 times, respectively. Integrating these techniques provided an even greater improvement in COD solubilization (54.8-fold) compared to untreated WAS. As a result, sCOD of untreated WAS increased from 372.0 mg/L to 20,396 mg/L.

As shown in Figure 4.15, each three applications (i.e., alkaline, thermal, and combined) resulted in almost the same amount of carbohydrate solubilization (25.8-fold). Protein, on the other hand, was already solubilized with alkaline disintegration and the subsequent THP did contribute positively.

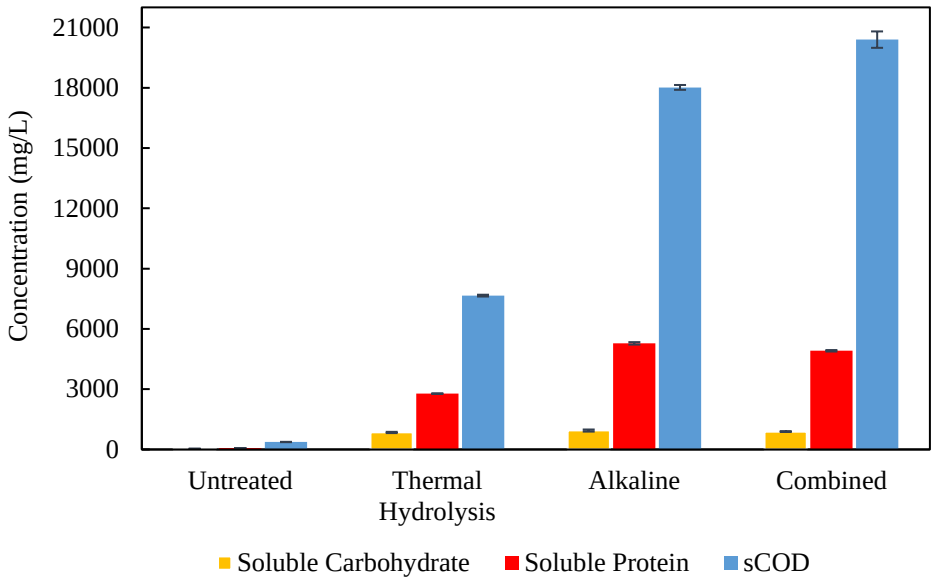

Figure 4.15. Individual and combined effects of two days of 0.5 M alkaline disintegration and thermal hydrolysis at 127°C for 120 min

Studies determining the sludge solubilization efficiency of disintegration techniques were finalized with a decision of applying combined disintegration that contains 0.5 M alkaline (NaOH+KOH) disintegration for two days followed by THP at 127°C for 120 min. The next step involves examining the fate of PET MPs exposed to sludge disintegration processes.

4.2.4 Characteristics of PET MPs After Sludge Disintegration

Potential changes occurred in PET MPs exposed to disintegration processes were quantified by measuring mass, crystallinity and carbonyl index; observing the FTIR spectra and qualified by visualizing under SEM. Both individual effects of alkaline disintegration (0.5M for 2 days) and THP (127°C for 120 min) as well as combined effect were comparatively investigated together with control samples.

4.2.4.1 Change in Mass

To determine the potential effect on mass, PET MPs recovered from WAS samples exposed to different disintegration processes were first washed and air-dried. These MPs were then counted and weighed in batches of 20 particles in triplicate, thereby mass of each PET particle was calculated. Figure 4.16 shows the changes in unit mass of PET MPs after disintegration processes including their individual and combined effects.

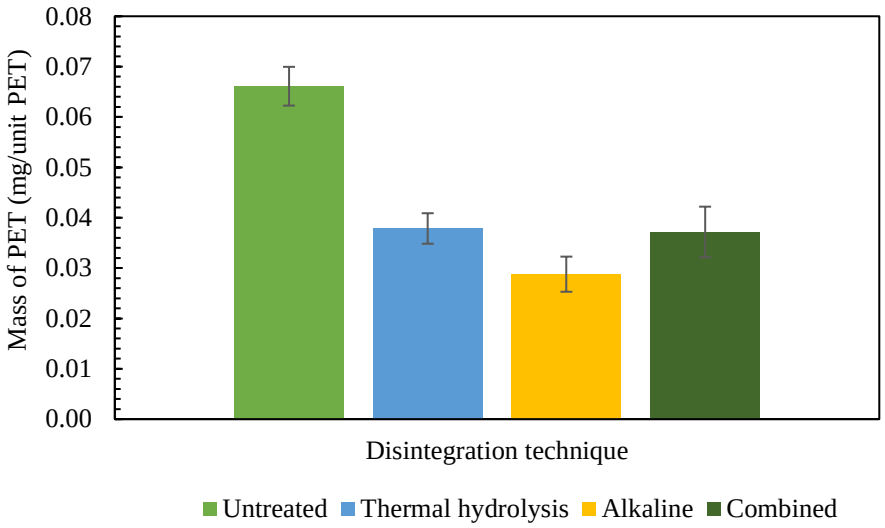

Figure 4.16. Change in mass of a unit PET MP during disintegration processes

One-way ANOVA test showed that mass of PET particles significantly decreased after disintegration. Also, there was a statistically significant difference in mass of PET particles subjected to different disintegration processes (Appendix D). The main reason of mass loss can be linked to the extraction of small and water soluble molecular fragments such as monomeric terephthalic acid and glycol formed near the chain ends by hydrolysis reactions including both alkaline disintegration and THP (Ballara and Verdu, 1989). Alkaline disintegration caused 56.5% decrease in mass of a PET particle compared to untreated PET MPs. This may also be due to surface peeling appeared on their surfaces resulting in loss of fragments. Moreover, the saponification process which occurs in ester linkages of PET with alkali added

is an important mechanism in loss of mass (Hurley et al., 2018). The impact observed in this study is much higher than that of X. Li et al. (2020), who reported a 30.2±6.2% decrease in mass after 1 M NaOH application. However, the length of the treatment applied in that study was one day, which is half of that in this study. Therefore, differences in treatment time, as well as shape and size of PET MPs studied are determinative factors affecting their vulnerability to lose their mass.

During thermal hydrolysis, PET MPs also experienced mass loss by 42.7% with a notable decrease in particle size. When combined, mass of MPs decreased to levels similar to that of thermal hydrolysis (43.8%), meaning that the effect of alkaline disintegration was overwhelmed by subsequent heat application. The cracks appeared on the surface of MPs after alkaline disintegration may provide sites for water absorption during thermal hydrolysis, which increases mass.

4.2.4.2 Change in Morphology

Figure 4.17 shows the surface morphology of PET MPs before and after exposure to sludge disintegration processes. It is evident from Figure 4.17 (d, e, f) that MPs exposed to alkaline environment experienced a strong surface peeling in comparison to plastic samples that were not subjected to disintegrated (Figure 4.17 a, b and c). This could possibly cause tiny particles to detach from their surfaces, supporting the findings of significant mass loss after alkaline disintegration.

THP in Figure 4.17 (g, h, i) appears to have caused a totally different kind of effect on surface morphology. As shown in Figure 4.17 (i), the applied heat caused the corners of the square-shaped MPs to expand outward compared to those of untreated MPs Figure 4.17 (c).

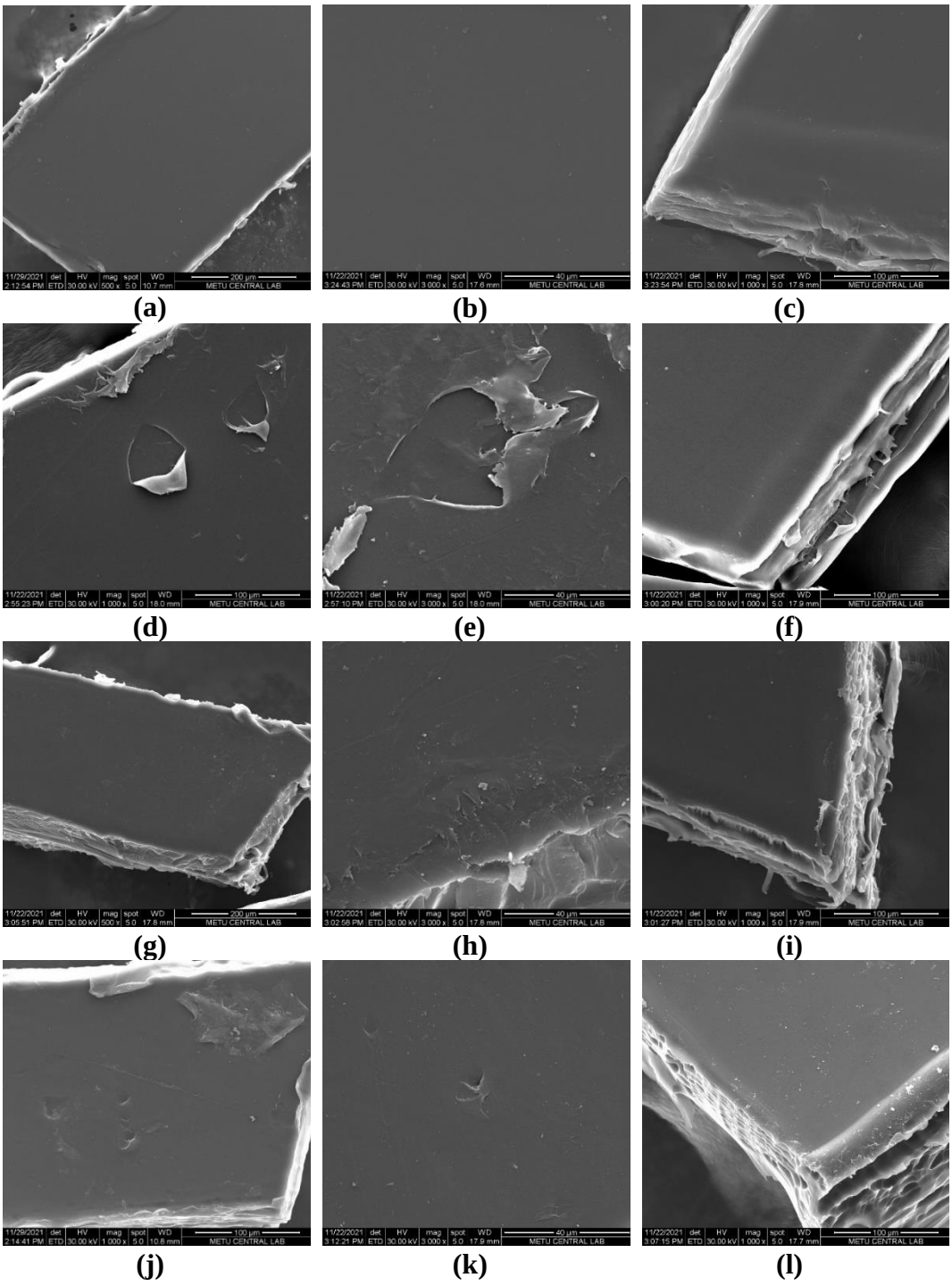

Figure 4.17. SEM images of PET MPs at x500, x3000 and x1000, respectively from left to right for each raw: untreated (a, b, c); alkaline disintegrated (d, e, f); thermally hydrolyzed (g, h, i) and combined disintegrated (j, k, l)

For combined disintegration, the notable peeling effect caused by alkaline disintegration diminished (Figure 4.17 j, k and l) due to the heat applied afterwards. As the heat is applied above the glass transition temperature of PET, MPs become ductile for the course of thermal hydrolysis (Shrivastava, 2018). At this stage, molecular mobility and hence the gap between molecular chains increases. The expanded MP lose the previous changes occurred on its surface and reforms. Still, the layers appeared after combined disintegration (Figure 4.17 l) is thought to be a remarkable change that may influence the fate of PET MPs during anaerobic digestion.

4.2.4.3 Change in Polymer Chemistry

FTIR spectra of untreated (i.e., non-disintegrated), alkaline disintegrated, thermally hydrolyzed and combined disintegrated PET samples, obtained in triplicate, were comparatively presented based on structural changes observed in three critical regions of PET as recommended in the literature (Sammon et al., 2000). These regions represent the O-H and C-H stretching (Figure 4.18), C=O stretching (Figure 4.19); CH_2 wagging and complex lower wavenumber regions containing ester bands (Figure 4.20).

Among the absorption bands of PET presented in these figures, the ones specific to PET at 1050 to 1100 cm^{-1} are assigned to C-O stretching and methylene group vibrations, 1300 cm^{-1} to ester group stretching, 1715-1725 cm^{-1} to ester carbonyl bond stretching and 2800-3100 cm^{-1} to aromatic and aliphatic C-H bond stretching (Chen et al., 2012; Prata et al., 2019).

The entire FTIR spectrum given in Appendix E (Figure E.1) was examined by taking the ratio of absorption intensities at specific regions mentioned to a reference peak at 1506 cm^{-1}, that remained unchanged during disintegration process. An overall decrease was noted in the intensity of PET (based on the ratio) with disintegration processes applied, especially in the region of C=O stretching. The relative intensities

of MPs exposed to different disintegration processes showed variety in different regions. For example, in the region of 2800 to 3100 cm^{-1}, alkaline disintegrated PET had almost the same intensity with the untreated PET, while thermally and combined disintegrated MPs appeared with a decreased intensity. When the regions of C=O stretching (Figure 4.18) and CH_2 wagging (Figure 4.20) were examined, alkaline and thermally disintegrated MPs were observed to be in similar levels, leaving the combined disintegrated PET with the lowest intensity.

There were only a few peaks appeared with an increasing intensity, mostly due to the effect of THP. For example, the largest increase in intensity (by 43%) was observed at 1960 cm^{-1} which is assigned to aromatic C-H bending. Combined disintegrated PET also experienced an increase at this peak, which was likely induced by thermal effects rather than the alkaline disintegration. Another prevailing difference was observed at peak 1577 cm^{-1}, assigned to C=C stretching after THP.

As a result, PET MPs exposed to different disintegration processes experienced varying levels of changes in different regions of the polymer structure.

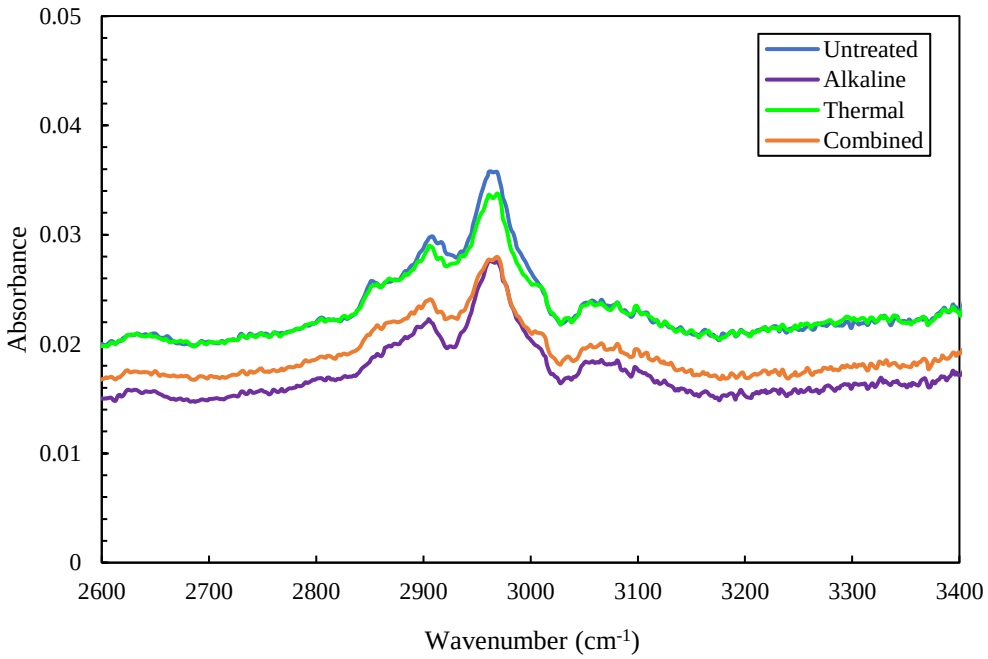

Figure 4.18. O-H and C-H stretching regions of PET

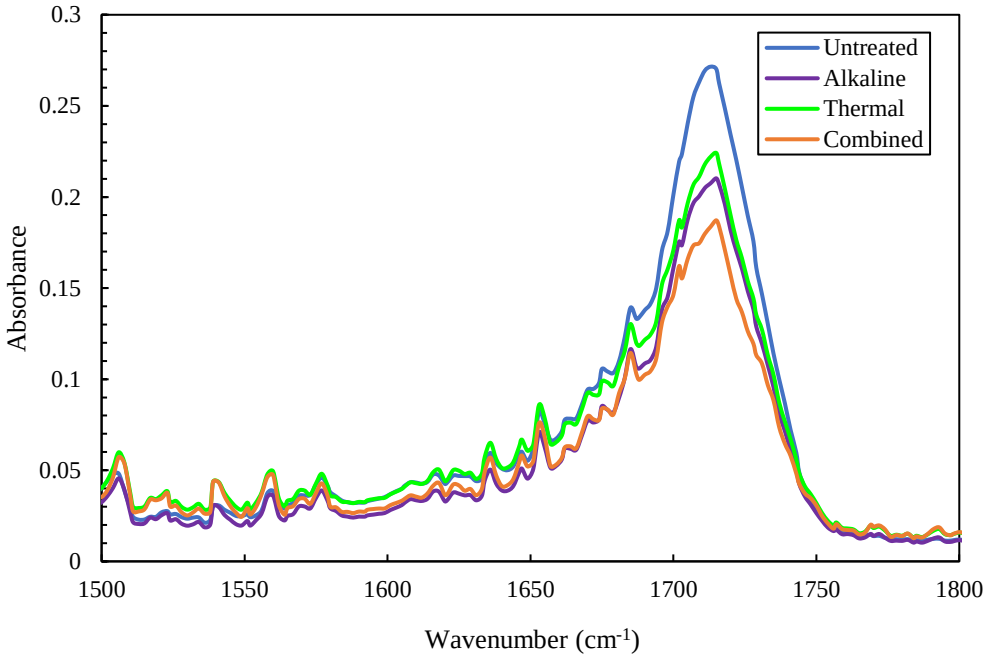

Figure 4.19. C=O stretching region of PET

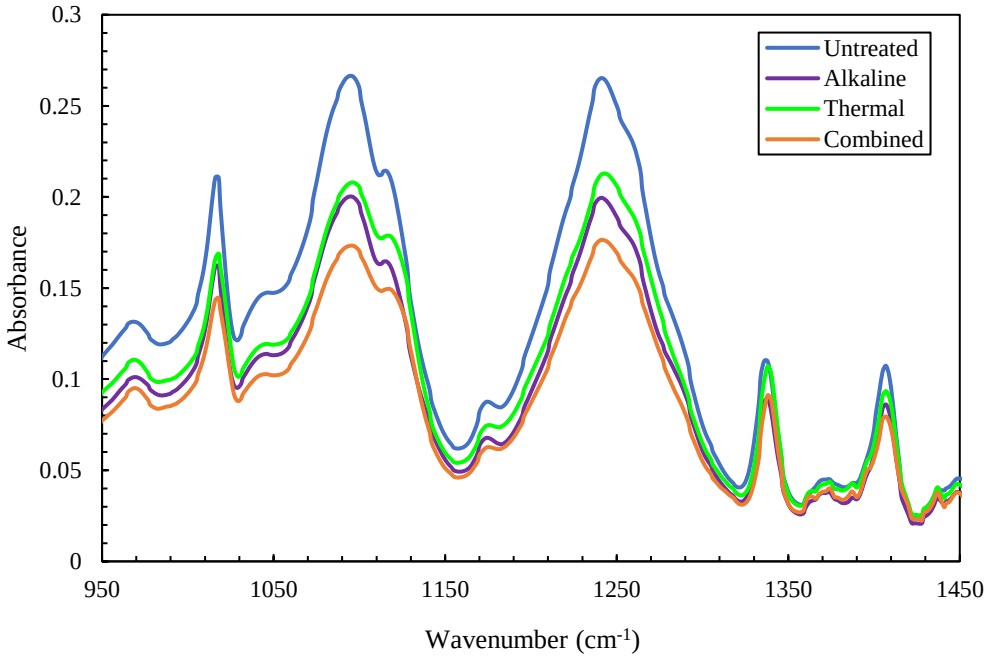

Figure 4.20. CH_2 wagging and ester band regions of PET

4.2.4.3.1 Change in Crystallinity and Carbonyl Index

Crystallinity in a material defines the degree ordering; so, as the crystallinity increases the density of a material increases. Same thing is valid for polymers as well. The more crystalline a polymer, the more regularly aligned its chains (Ballara and Verdu, 1989). On the other hand, the lower the crystallinity, the lower the polymer's density. Crystallinity index of the polymer, which is calculated by the ratio of absorbances at 1340 cm^{-1}/1410 cm^{-1}, is shown in Figure 4.21.

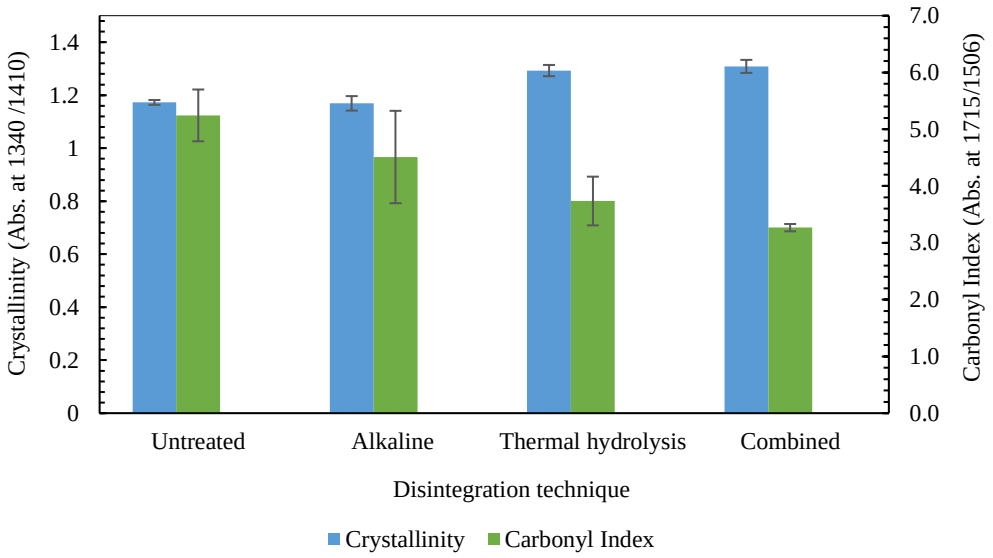

Figure 4.21. Change in crystallinity and carbonyl index (on the secondary axis) of PET MPs

It is seen that crystallinity increased with disintegration, with the highest increase for combined disintegration, followed by thermal hydrolysis. Alkaline disintegration, on the other hand, did not cause any change in crystallinity of untreated PET. This is in line with Donelli et al. (2010) arguing that the alkaline treatment alters only surface properties and leaves the bulk properties of PET unchanged. Therefore, heat application is thought to be the mechanism governing the increase in crystallinity of combined treated PET. This could be possibly due to formation of new crystalline zones in polymer's structure from the breakdown of branches in backbone and

bending on themselves as also mentioned by Martínez-Romo et al. (2015). In other words, partial melting and the recrystallization of the amorphous region of the polymer can be the reason of increase in crystallinity (Alassali et al., 2018). Another reason of the increase can be the extraction of water soluble and low molecular weight compounds formed after the degradation of amorphous phase, which is in line with the results of gravimetric analysis (Ballara and Verdu, 1989).

Change in carbonyl index of PET MPs, determined by diving the absorbance of the carbonyl peak (1715 cm^{-1}) by that of a reference peak (1506 cm^{-1}) is shown in Figure 4.21. Untreated PET has already an inherent strong peak at 1715 cm^{-1}, leading it to have the highest carbonyl index value. This value decreased with each disintegration technique applied, with the lowest achieved for the combined disintegration. The decrease in intensity of carbonyl stretching band could result from the destruction of ester carbonyl bond of PET by disintegration processes applied (Donelli et al., 2010).

4.3 Results of BMP Reactors

Fate and effects of PET MPs during anaerobic digestion were investigated by setting up combined disintegrated and non-disintegrated BMP reactors. Any correlation was scrutinized between doses of PET MPs added and methane yields obtained. In reaching this conclusion, results were evaluated in terms of (i) the sole impact of disintegration process (R0 and R0P) (ii) the sole impact of PET MPs doses (R0, R1, R3, and R6) and (iii) the combination of these two impacts (R0, R1, R3, R6, R0P, R1P, R3P, and R6P).

The entire BMP test lasted for 60 days in triplicates for both disintegrated and non-disintegrated reactor sets. Biogas production and its composition were measured daily for the first 19 days when the biogas production was intense, once in two days in the next 14 days and finally once in four days in the last 27 days, with relatively low levels of biogas production. Both at the reactor set-up and termination, sludges from the reactors were analyzed for TS, VS, TSS, VSS, tCOD, pH, biogas volume

and composition, soluble COD, protein and carbohydrate to evaluate the performance of digestion process.

4.3.1 Biogas and Methane Productions

The source of difference between disintegrated and non-disintegrated reactor sets is the altered soluble content of substrate (i.e., WAS) added into reactors. As shown in Table 4.2, combined disintegration process involving 2 days of 0.5 M alkali (as combined NaOH and KOH) application and a subsequent thermal hydrolysis at 127°C for 120 min has led WAS to substantially solubilize prior to anaerobic digestion. This means that the disintegrated reactor sets were fed with a substrate soluble COD, protein and carbohydrate content of which was increased by 47.3±0.7, 93.0±4.8, and 56.7±5.1 fold, respectively, compared to non-disintegrated reactor sets. These significantly increased indicators of soluble substrate are due to the pretty strong treatment applied on WAS to both improve biogas production as well as to deteriorate MPs to some degree.

Table 4.2. Soluble substrate content of WAS before and after combined disintegration

Parameter*	Non-disintegrated WAS, mg/L	Disintegrated WAS, mg/L
sCOD	402.1±18.2	19,025±624
sProtein	64.8±2.9	6,020±106
sCarbohydrate	14.5±1.6	817±41

*These measurements were performed in E1 reactors.

Daily and cumulative biogas production of each reactor set are shown in Figure 4.22 and Figure 4.23, respectively. The values presented are the averages of three replicate reactors where error bars demonstrate standard deviations of the three replicates.

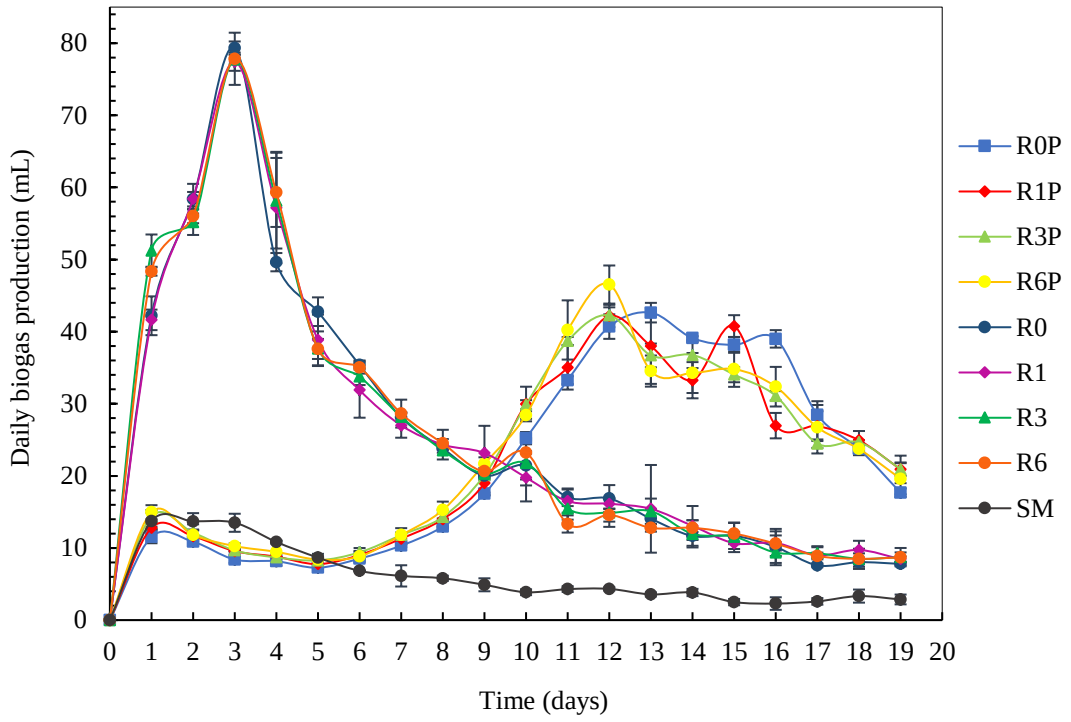

Figure 4.22. Daily biogas production graph of each set of reactors (R0P, R1P, R3P, R6P are disintegrated reactors with 0, 1, 3, 6 mg PET/g TS, respectively; R0, R1, R3, R6 are non-disintegrated reactors with 0, 1, 3, 6 mg PET/g TS, respectively; SM is seed control reactors and C3, C3P are non-disintegrated and disintegrated abiotic control reactors with 3 mg PET/g TS, respectively.)

From Figure 4.22, it is seen that untreated reactors without making much difference whether they have MPs or not reached about 80 mL of biogas at about the 3rd day. The peak of the biogas amount was reached sharply and again biogas decreased pretty sharply after the 3rd day. On the other hand, as seen in Figure 4.22, there is an absolute lag period taking approximately 5 days in each disintegrated reactor set for the biogas production to begin. During the first 5-day period, biogas production was even lower than that of seed control. This can be attributed to possible inhibition caused by ions added during disintegration of WAS, even though the ion concentrations were selectively kept lower than moderate inhibition levels, which are shown in Table 4.3. Another distinct difference of non-disintegrated and

disintegrated reactors in Figure 4.22 is the longer time the biogas volume to stay in its peak region for the disintegrated reactors. The biogas amount was about 35-40 mL for about a week before it started to gradually decrease. This behavior is clearly different than the sharp rise and decrease demonstrated by the non-disintegrated reactors.

Table 4.3. Concentrations of ions added during disintegration

Ion added	Concentration in a reactor (mg/L)	Moderate inhibition level (mg/L)	Reference
Na^+	3421.46	3500-5500	McCarty et al. (1964)
K^+	1595.47	2500-4500	McCarty et al. (1964)
Cl^-	6169.8	>6000	Appels et al. (2008)

Indeed, this lag phase was estimated and observed before setting up the reactors (Figure 4.10). To protect microorganisms from inhibition, an antagonistic approach (combined use of Na^+ and K^+) was followed, which was suggested to reduce the toxicity (Kugelman and Mccarty, 1965). Hence, microorganisms adopted to conditions and started to produce biogas after the 5th day, without further delay. Then they reached the peak point on day 13. Unlike the non-disintegrated reactor sets, peak points are not exactly on the same days for disintegrated sets with different PET MPs doses. For example, the first peak was observed on day 12 for each set except R0P, which reached its peak point the next day. The second peaks occured around 15^{th} and 16^{th} days. After these days, a gradual decrease was observed in biogas production until day 19.

Non-disintegrated reactors, on the other hand, were ready to consume organic matter present in sludge. Similar shapes of the curves representing reactors with different doses of PET MPs (0, 1, 3, 6 mg/g TS) indicate that none of the reactors experienced problems with acclimation. Also, zero lag phase can be due to the use of fresh seed and the available soluble degradable organics in each WAS sample. Therefore, these reactors produced the highest amount of biogas on day 3 and experienced a sharp decrease in production for the remainder of the test. Little humps can be observed

from Figure 4.22 on days 6 and 10, indicating biogas production following hydrolysis of different fractions of organics. Even though the disintegrated sets (R0P) never reached that much high daily biogas production, their cumulative biogas productions exceeded that of non-disintegrated ones (R0) by 14.2% at reactor termination, as shown in Figure 4.23. This finding revealed that, contrary to the literature, gas production can be enhanced by 0.5 M of alkaline disintegration (Li et al., 2012). This is thought to be achieved by combined application of NaOH and KOH into WAS, decreasing the accumulation of one type of ion in digester.

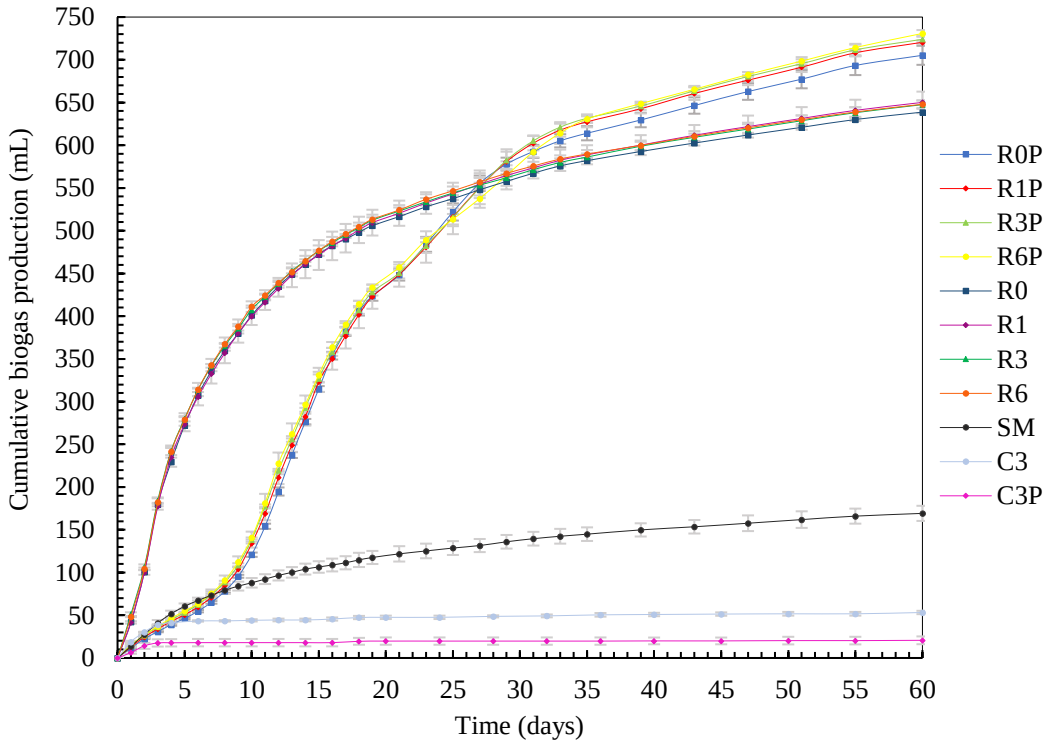

Figure 4.23. Cumulative biogas production graph of each reactor sets

Figure 4.23 shows the cumulative biogas production during the reactor operation time. In this figure, it is seen that the biogas production in disintegrated reactors were higher than that of non-disintegrated reactors in more than half of the reactor operation time. The lowest cumulative biogas production within their own group occurred in reactors without PET MPs (R0 and R0P). Although not drastically, the

production increased with the MPs dose added within disintegrated sets, especially at R6P. This was also supported by statistical analyses that MPs dose led to a significant impact on cumulative biogas production within disintegrated reactor sets. Non-disintegrated sets, on the other hand, did not significantly differ from each other at the 95% confidence level.

When methane content of biogas is examined, the difference between the sets with different doses became more distinguishable in non-disintegrated sets as shown in Figure 4.24. On the contrary, the disintegrated reactors lost the difference observed between MP doses when cumulative methane productions are evaluated (Figure 4.24). Disintegration, especially at later reactor operation times enhanced the methane production. As expected, in cumulative methane plot, methane content of reactors was observed to change the trends seen in biogas, for example R0P with the lowest biogas production was compensated with its relatively higher methane content. This resulted in all disintegrated reactor sets yielding similar cumulative methane production. The methane production values of disintegrated reactors showed no statistically significant difference from each other at 95% confidence interval. Besides, the methane amount produced for all the disintegrated reactors showed significantly different values compared to non-disintegrated reactors.

Figure 4.24 shows that R0 produced the lowest amount of methane since the early stages of digestion. Moreover, even though not directly correlated, cumulative methane production increased with the addition of PET MPs. R3 yielded the highest methane production, which was followed by R6, R1 and R0, in decreasing order. The doses other than R3 in non-disintegrated sets did not significantly differ from each other ($p>0.05$). Potential reason for this can be due to PET MPs inducing stress and causing floc fragmentation. Adding 250-500 μm sized PET MPs may decrease sludge particle size enhancing the sludge solubilization during digestion, which facilitates the hydrolysis step up to a certain dosage of PET (3 mg/g TS). In a study simulating a biological wastewater treatment system, Wei et al. (2021) reported a decrease in sludge particle size in the presence of PET MPs and attributed this to a lower surface hydrophobicity and less negative surface charge. The increase in

methane production can also be ascribed to that MPs may provide surfaces for microbial growth and biofilm formation. When PET dose reaches 6 mg/g TS, on the other hand, the positive effect may start to decrease potentially due to leakage of additives from plastics.

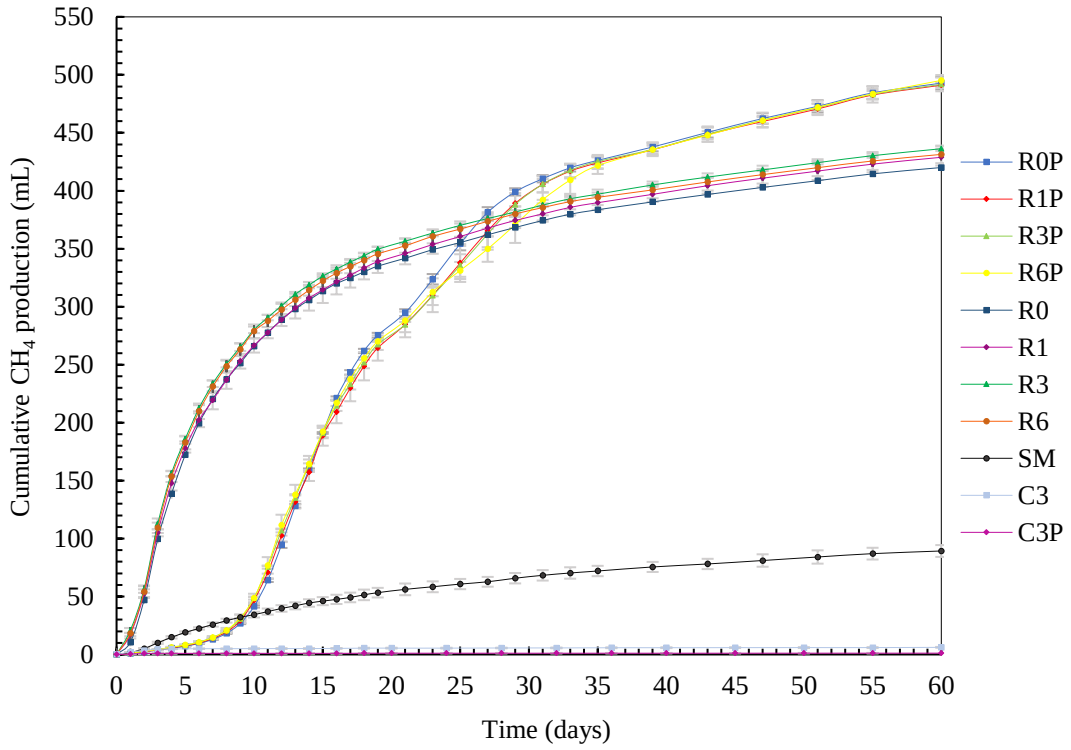

Figure 4.24. Cumulative methane production of both disintegrated and non-disintegrated reactor sets

As shown in Figure 4.24 disintegrated reactors follow a rather dynamic trend over 60 days compared to non-disintegrated reactors and yielded 22.0% higher cumulative methane production at reactor termination. It seems that methane production in disintegrated reactors follows three distinctly different rates all throughout reactor operation. The first and possibly the highest rate is observed between day zero and 18; the second highest rate was observed between days 18 and 30; and the lowest production rate was observed from day 30 till the reactor termination. Additionally, in the first 15 days, reactors with different PET MPs doses produced quite similar amounts of methane. For the next 20 days, R0P dominated in

cumulative methane production, R6P left with the lowest production and R1P and R3P lied in between. In the last 25 days, each reactor set had almost the same amount of cumulative methane production. The differentiation in methane production of the reactors in the middle stages of BMP test may be due to different effects such as possible toxicity induced by PET MPs in R1P, R3P and R6P reactor sets. The reason for seeing this impact only in disintegrated reactors, but not in non-disintegrated reactors may originate from the deterioration of MPs during disintegration process. Combined alkaline and thermal disintegration provides a harsh environment for PET MPs inducing changes in their physical and chemical properties, which may further increase their potential for leaching chemicals. If toxicity is the case, Figure 4.24 shows that microorganisms recover after a short acclimatization period. Consequently, the impact of PET MPs on cumulative methane production seen in non-disintegrated reactors were not observed in disintegrated reactors. This was attributed to the solubilization efficiency of the disintegration process exerting a predominant effect over that of PET MPs. The average cumulative gas production in each reactor set at reactor termination, are shown in Table 4.4.

Table 4.4. Gas production in each reactor set

Reactor set	Cum. CH_4. (mL)[a]	Cum. biogas (mL)[a]
R0	330.8±1.6	469.6±4.4
R1	339.6±7.1	480.9±12.6
R3	347.0±2.0	478.3±4.9
R6	342.1±7.6	478.8±4.6
R0P	403.5±5.5	536.0±11.2
R1P	401.8±2.0	551.3±2.1
R3P	402.4±5.9	554.8±4.0
R6P	405.9±4.6	561.6±3.9

[a]Volume of gas produced in seed control set (SM) was subtracted from that of each sample reactor.

The increase in methane production with MPs dose for non-disintegrated reactors shown in Table 4.4 has been observed only for PA in literature and it was attributed to the leaching of monomer CPL, which enhances the enzyme activity up to a certain MPs dosage (H. Chen et al., 2020). On the other hand, studies examining PET during alkaline anaerobic fermentation (Wei et al., 2019c) and up-flow anaerobic sludge

blanket (UASB) treating wastewater (Y. T. Zhang et al., 2020) have reported only adverse effects associated with MPs which originate mainly from leaching of additive DBP and excessive ROS formation. Both studies were limited to DBP measurement but the additive content of PET materials varies depending on the usage area which may cause different impact mechanisms to dominate during anaerobic digestion. Thus, further studies should expand the list of mechanisms to be explored. PET MPs used in this study were from water bottles and their phthalate content is restricted by Turkey's regulation on plastic materials and articles intended to come into contact with food due to health concerns. The limit values for di-2-(ethyl hexyl) phthalate (DEHP), DBP and benzyl butyl phthalate (BBP) are 1.5, 0.3, and 30 mg/kg, respectively (Türk Gıda Kodeksi, 2013). Phthalate concentrations in bottled waters exposed to varying storage conditions all over the world have been reported to reach 94.1 μg/L, 109.0 μg/L, 222.0 μg/L, 34.2 μg/L and 61.3 μg/L for DEHP, BBP, DBP, diethyl phthalate (DEP) and dimethyl phthalate (DMP), respectively (Luo et al., 2018). These are the highest reported values and the most frequently reported average values indeed are generally less than those measured in sludge leaching from MPs during anaerobic digestion.

4.3.2 BMP Reactor Performance Indicators

The characteristics of sludges at reactor set-up and termination, which indicate digester performance, are given in Table 4.5 and Table 4.6.

Both at the reactor initiation and termination stages, TS content of disintegrated reactors are about 1.8-fold higher than those of non-disintegrated reactors. VS content, on the other hand, are at similar levels between the disintegrated and non-disintegrated reactors. The difference in TS originates from the ions (i.e., Na^+, K^+, Cl^-) added to WAS during alkaline disintegration. This causes VS/TS ratio of disintegrated reactors to be almost half of the non-disintegrated reactor sets. Furthermore, abundance of ions in reactors caused the observation of a slightly lower TS removal efficiency in disintegrated reactors compared to the non-disintegrated

ones. On the other hand, VS removal efficiency increased from 32.7% (R0) to 38.7% (R0P) in the reactors where combined disintegration process applied relative to non-disintegrated reactors. These results are consistent with those of Wang et al. (2016) in which thermal-alkaline disintegration of WAS provided an increase in VS reduction from around 32.0% in control to 43.2% after thermal-alkaline disintegration. Similarly, Kim et al. (2003) observed an increase in VS reduction of WAS from 20.5% in control to 46.1% after thermochemical disintegration application.

Examining the non-disintegrated reactors, TS and VS removal efficiencies did not differ significantly between R0, R1 and R3. In contrast, R6 with the highest PET MPs content experienced lower VS removal and hence lower TS removal efficiency. The adverse effect associated with increasing PET levels in non-disintegrated reactor set (R6) was not observed in disintegrated ones. The difference observed in the VS removal in the presence of 6 mg PET/g TS and that of other reactors is negligibly small ($p>0.05$). One can state that the possible negative effect of MPs had been overwhelmed by the effect of enhanced solubilization of substrate in disintegrated reactor sets. Furthermore, abiotic reactor sets (C3 and C3P) showed up with a negative TS and VS removal. This is an artifact, originating from additional amount of $HgCl_2$ solution injection into abiotic reactors to kill microorganisms that revived at some point during the digestion period.

All the pH values in biotic reactors are in the optimal range for anaerobic microorganisms, which means that a healthy digestion has taken place. These reactors experienced the typical slight increase in pH between reactor initiation and termination. At reactor termination, abiotic reactors had relatively lower pH. There can be two reasons for this; one is the obvious absence of microbial activity not yielding the typical slight increase in pH as in the case of biotic reactors. The second reason could be the addition of excess $HgCl_2$ in abiotic reactors and its possible effect on pH.

Table 4.5. Evaluation of sludge characterization parameters during digester set-up and termination

Reactor set	TS_i, g/L	TS_f, g/L	% TS removal	VS_i, g/L	VS_f, g/L	% VS removal	$tCOD_i$, g/L	$tCOD_f$, g/L	% tCOD removal	pH_i	pH_f
R0	18.50±0.33	14.65±0.07	20.73	10.96±0.15	7.37±0.14	32.7	16.21±0.30	12.02±0.12	25.8	7.47	7.68
R1	18.80±0.08	14.66±0.17	22.02	11.35±0.04	7.70±0.16	32.2	16.15±0.46	12.58±0.17	22.1	7.48	7.52
R3	18.80±0.08	14.77±0.03	21.44	11.45±0.02	7.75±0.08	32.3	16.81±0.47	11.85±0.04	29.5	7.48	7.61
R6	18.20±0.13	14.94±0.31	17.93	10.95±0.08	7.68±0.03	29.9	15.44±0.08	12.00±0.57	22.3	7.48	7.64
C3	18.53±0.05	19.63±0.43	-5.98	11.33±0.47	11.99±0.49	-5.9	18.82±0.86	17.42±0.32	7.4	7.6	6.01
R0P	32.9±0.42	26.32±0.08	19.99	10.89±0.00	6.67±0.20	38.7	19.22±0.23	13.85±0.77	28.0	7.75	7.63
R1P	31.79±0.20	25.65±0.21	19.31	10.74±0.08	6.70±0.01	37.6	19.13±0.40	14.07±0.34	26.5	7.75	7.54
R3P	32.32±0.03	25.72±0.19	20.43	11.00±0.10	6.63±0.01	39.7	19.01±0.46	13.84±0.34	27.2	7.75	7.60
R6P	32.61±0.01	26.26±0.08	19.48	11.12±0.01	6.66±0.15	40.1	18.17±0.57	14.10±0.26	22.4	7.75	7.59
C3P	31.98±0.05	32.03±0.37	-0.16	10.61±0.10	11.39±0.27	-7.4	22.51±0.73	21.60±0.90	4.0	7.63	6.92
SM	11.28±0.22	9.77±0.27	13.39	5.97±0.14	4.69±0.11	21.5	10.63±0.06	8.94±0.13	15.9	8.07	7.63

"i" and "f" indicate initial and final value of parameters, respectively.

tCOD removal efficiencies vary in the range of 22.1-29.5% in non-disintegrated and 22.4-28.0% in disintegrated reactor sets, without any obvious trend with respect to MP dose. Normally tCOD is the second parameter next to VS to indicate the organic removal efficiency in digesters. However, tCOD is not a good indicator in this study because of the excessive amount of chloride ions in disintegrated reactors and the spiked MPs, both of which interfere with COD analysis. Preliminary studies have shown that PET MPs in sizes of 250-500 μm get oxidized in COD solution during 2 hours of incubation at 150°C, with the observation of unexpectedly strong change in color of COD digestion solution. As there is potential for the added MPs in sludge to be transferred into COD vials, this study even though measured, refrained from relying on COD-based removal efficiency evaluations.

The detailed listing and evaluation of suspended fraction of reactors (TSS and VSS) are shown in Appendix C (Table C.1). Initial TSS and VSS values of disintegrated reactors are lower than those of non-disintegrated ones as suspended particles in WAS are largely solubilized with the disintegration process. Unexpectedly, the disintegration process decreases the TSS and VSS removal efficiency. The examination of PET MPs' dose effect on TSS and VSS removal resulted in a fluctuation within a small range both in disintegrated and non-disintegrated reactor sets.

Table 4.6 shows the soluble fractions of reactors in terms of sCOD, soluble carbohydrates and proteins. Obviously, sCOD removal (as well as those for carbohydrates and proteins) are not parameters used in determining the digestion efficiency; therefore, they may attain a positive or negative value. For this reason, the removals shown in the table are just for demonstration purposes. Evaluating the results in Table 4.6, it is obvious that the disintegrated reactors are richer in soluble substate content at reactor set-up compared to non-disintegrated reactors. This is strikingly obvious for all three parameters. Results also show that the effluents of reactors at reactor take down had some amount of soluble organics remaining as observed in most digesters, especially in disintegrated digesters. The increase in COD solubilization was likely promoted by the proper temperature and constant

mixing applied during 60 days of digestion process as it was in studies of Çelik Çağlar (2021) and Kalaycıoğlu (2020). Similarly, soluble protein content of the reactors increased (except R6) meaning that the biodegradation rate of protein is slower than that of solubilization during the incubation period. In contrast, soluble carbohydrate was readily destroyed in each set due to its easily degradable nature. As opposed to the non-disintegrated ones, disintegrated reactors experienced an absolute decrease in sCOD, carbohydrate and protein during the digestion. It can be due to the fact that the combined disintegration has already solubilized a large portion of organics in WAS prior to the digestion, making them readily consumable by microorganisms. In general, reduction in organic content was the highest in R0P as shown in Table 4.6.

Table 4.6. Evaluation of soluble fraction at digester set-up and operation

Reactor set	$sCOD_i$, mg/L	$sCOD_f$, mg/L	% sCOD removal	$sCarbohydrate_i$, mg/L	$sCarbohydrate_f$, mg/L	% sCarbohydrate removal	$sProtein_i$, mg/L	$sProtein_f$, mg/L	% sProtein removal
R0	526.0±60.3	630.7±27.4	-19.9	20.3±0.6	13.6±0.3	33.1	81.1±1.6	90.1±10.1	-11.1
R1	505.4±0.7	622.4±7.0	-23.1	23.9±0.3	14.5±0.4	39.3	92.7±4.2	97.2±5.2	-4.9
R3	521.8±5.3	639.7±3.0	-22.6	19.8±0.1	13.9	30.1	82.5±0.9	87.4±0.9	-5.9
R6	479.2±2.0	630.8±18.9	-31.6	26.5±0.4	15.5±1.2	41.7	91.4±3.7	88.2±3.0	3.5
C3	1720.3±35.0	3632.2±86.6	-111.1	98.2±0.8	90.2±1.4	8.2	478.8±3.7	712.6±26.1	-48.8
R0P	7850.8±212.0	4191.3±114.3	46.6	308.4±1.0	61.3±5.4	80.1	2715.1±13.9	819.6±32.7	69.8
R1P	6305.0±119.2	4253.9±146.1	32.5	271.5±9.5	60.3±4.2	77.8	2675.8±23.2	817.6±2.5	69.5
R3P	6295.7±132.5	4188.2±219.1	33.5	254.7±13.3	58.7±0.2	77.0	2679.1	704.3±2.6	73.7
R6P	6033.3±477.0	4206.9±112.9	30.3	240.9±6.2	61.4±7.4	74.5	2603.8±23.2	788.5±59.5	69.7
C3P	8478.0±349.8	8488.9±575.0	-0.1	357.5±7.6	343.0±20.1	4.1	3262.1±74.1	3273.1±75.9	-0.3
SM	395.8±28.5	285.9±6.0	27.8	25.4±0.7	13.7±0.5	46.1	70.3±0.2	62.2±2.3	11.4

“i” and “f” indicate initial and final value of parameters, respectively.
sCarbohydrate: Soluble carbohydrate
sProtein: Soluble protein

Table 4.7 shows the experimental methane yield and biodegradability of each reactor set. Experimental methane yield was calculated based on methane production from VS of WAS added into a reactor (Equation 3.5). The theoretical methane yield of WAS used in this study was 586.5 mL CH_4/g VS added, calculated by using Equation 3.6.

Non-disintegrated reactor sets had experimental methane yields that could only reach half of the theoretical yield. Adding combined disintegration process increased methane yield of WAS by 22.0%. The yield significantly rose with increasing PET MPs doses in non-disintegrated reactor sets up to R3. Disintegrated sets, on the other hand, did not differ from each other due to their overwhelming methane production, resulting in no statistically significant difference at 95% confidence level ($p>0.05$). Detailed results of statistical analyses are given in Appendix D.

Table 4.7. Experimental cumulative methane yield and biodegradability of each reactor set

Reactor set	Experimental methane yield (mL CH_4/g VS added)	Biodegradability (%)
R0	291.4±1.4	49.7±0.2
R1	299.2±6.3	51.0±1.2
R3	305.7±1.8	52.1±0.3
R6	301.4±6.7	51.4±1.1
R0P	355.5±4.8	60.6±0.8
R1P	354.0±1.8	60.4±0.3
R3P	354.5±5.2	60.5±0.9
R6P	357.6±4.1	61.0±0.7
SM	n/a	n/a

n/a: not applicable

4.3.3 Effects of PET MPs on ROS Formation

Figure 4.25 shows the amount of ROS in disintegrated and non-disintegrated reactor sets relative to control, which is the reactor set without PET MPs addition (i.e., R0 and R0P). PET MPs appeared to induce the formation of ROS, regardless of whether there is disintegration process. The literature attributes this mechanism to the

interaction of MPs' electron donor active sites with molecular dioxygen, which presents at submicromolar concentrations in digesters. The electrons captured by oxygen produces ROS molecules such as superoxide radicals and hydrogen peroxide (Wei et al., 2019a; Y. T. Zhang et al., 2020).

In this study, non-disintegrated reactor sets produced up to 16% higher ROS compared to the control and R6 was the only reactor set breaking the upward trend. Disintegrated reactor sets got to a point of 23% increase in ROS production with the highest PET MPs dose.

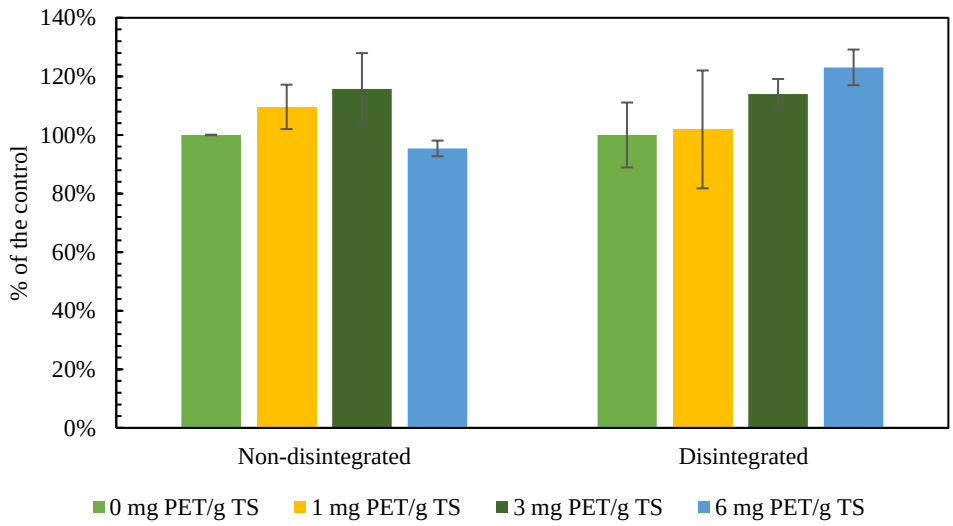

Figure 4.25. Amount of ROS in each reactor set relative to control

In contrast to the literature, increasing level of ROS could not be linked to a decrease in methane production in this work. This might be due to moderate ROS concentrations that microorganisms can protect themselves through inherent antioxidant system. Since oxidative stress causes cell death, measurement of an endocellular enzyme (e.g., Lactate dehydrogenase (LDH)), which is released upon damage of cell membrane could be useful to better understand the mechanism. Besides, live/dead cells count assay would support the findings of ROS measurement (Y. T. Zhang et al., 2020).

4.3.4 Characteristics of PET MPs After Anaerobic Digestion

4.3.4.1 Change in Mass

Figure 4.26 shows the change in mass of PET MPs during anaerobic digestion. Please note that the y-axis is calculated mass per particle obtained as dividing the total mass by number of particles. In non-disintegrated reactor sets, mass of a PET particle significantly decreased (9.2%) at the end of 60 days compared to untreated MPs (the ones did not enter the digestion process) and statistical results are given in Appendix D. This might either result from the volatilization of conversion products (CO_2 and H_2O) or loosing fragments from surface of MPs. PET MPs in abiotic reactors, on the other hand, did not experience a loss but instead a gain by 3.7%. This reflects that, factors affecting MPs during anaerobic digestion are not limited to microorganisms, but also the matrix and incubation conditions.

In disintegrated reactor sets, the control was the mass of PET MPs subjected to combined disintegration prior to digestion. It is seen that the initial mass is already less than the mass of untreated PET MPs by 43.8%, potential reasons of which are already discussed in Section 4.2.4.1. The figure and independent samples t-test results showed that digestion process did not provide a statistically significant further loss in mass (Appendix D). Instead, cracks that appeared on the surface of MPs after disintegration likely provided additional sites for accumulation of microorganisms and other debris, resulting in weakness to measure the mass. Moreover, water absorption may be another mechanism governing the increase in mass observed especially in disintegrated PET MPs due to the increased roughness providing additional site.

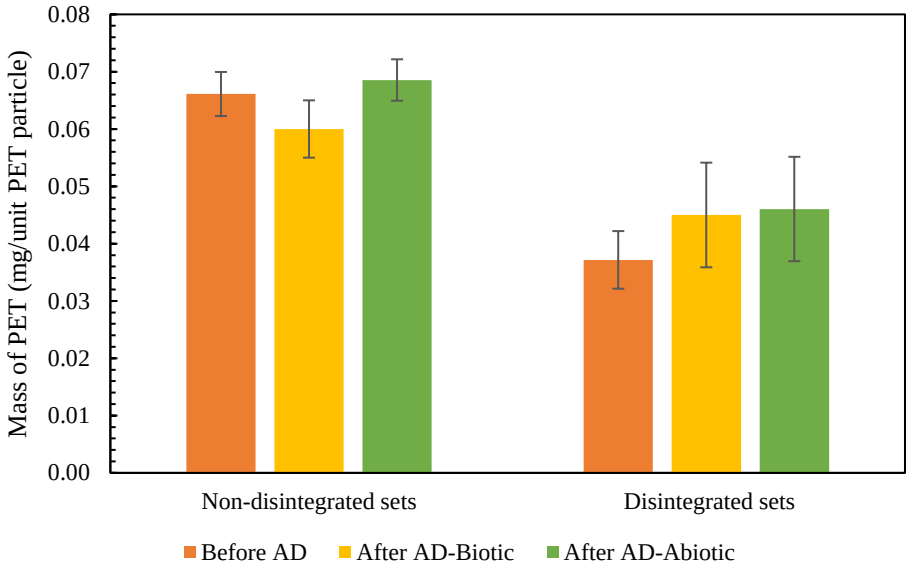

Figure 4.26. Change in mass of a PET MP during anaerobic digestion

Furthermore, MPs extracted from abiotic reactors had a similar mass with those of biotic reactors, indicating that the effect on mass might originate from an abiotic factor other than microbial action.

4.3.4.2 Change in Morphology

Change in morphology of PET MPs after anaerobic digestion was analyzed using SEM. Potential impact of microbial action was evaluated by comparing PET MPs from reactors with the control samples. Figure 4.27 compares the PET MPs recovered from a reactor with untreated PET MPs. It is obvious that PET MPs digested for 60 days experience fragmentation on their surface, resulting in micro or nano sized flakes to break off from their surface. This loss may further cause decrease in mass of PET MPs, supporting the results of mass measurement given in previous part.

In Figure 4.28, images of PET MPs from a disintegrated reactor and a disintegrated WAS (i.e., control) are compared. The dominant effect of digestion on disintegrated

MPs is more like a smash rather than fragmentation on surface, which mostly appeared on surface of MPs from non-disintegrated reactors.

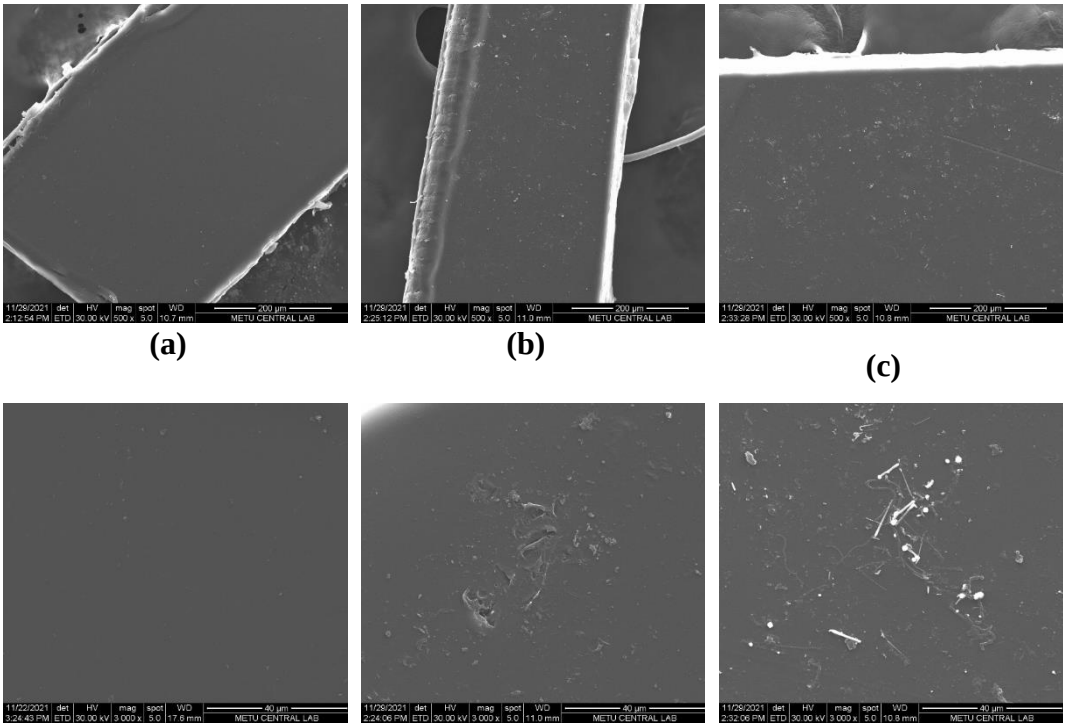

(a) **(b)** **(c)**

(d) **(e)** **(f)**

Figure 4.27. SEM images of untreated PET MPs at x500 (a) and x3000 (d); untreated PET MPs after anaerobic digestion at x500 (b) and x3000 (e); and untreated PET MPs after abiotic anaerobic digestion at x500 (c) and x3000 (f)

Figure 4.27 and Figure 4.28 both also show the fate of MPs after abiotic anaerobic digestion to demonstrate abiotic mechanisms responsible for changes on morphology of PET MPs, eliminating microbial action. Unexpectedly, an intense fragmentation was observed on surface of MPs after abiotic anaerobic digestion as shown in Figure 4.27 (c; f). This may be due to the interaction of MPs with $HgCl_2$ added into reactors to create an inhibitory environment for microorganisms. Another reason for the needle shaped fragments on the surface can be the accumulation of insoluble mercury salts. Morphological changes on disintegrated PET MPs after abiotic digestion, on the other hand, was not so strong as shown in Figure 4.28 (c; f).

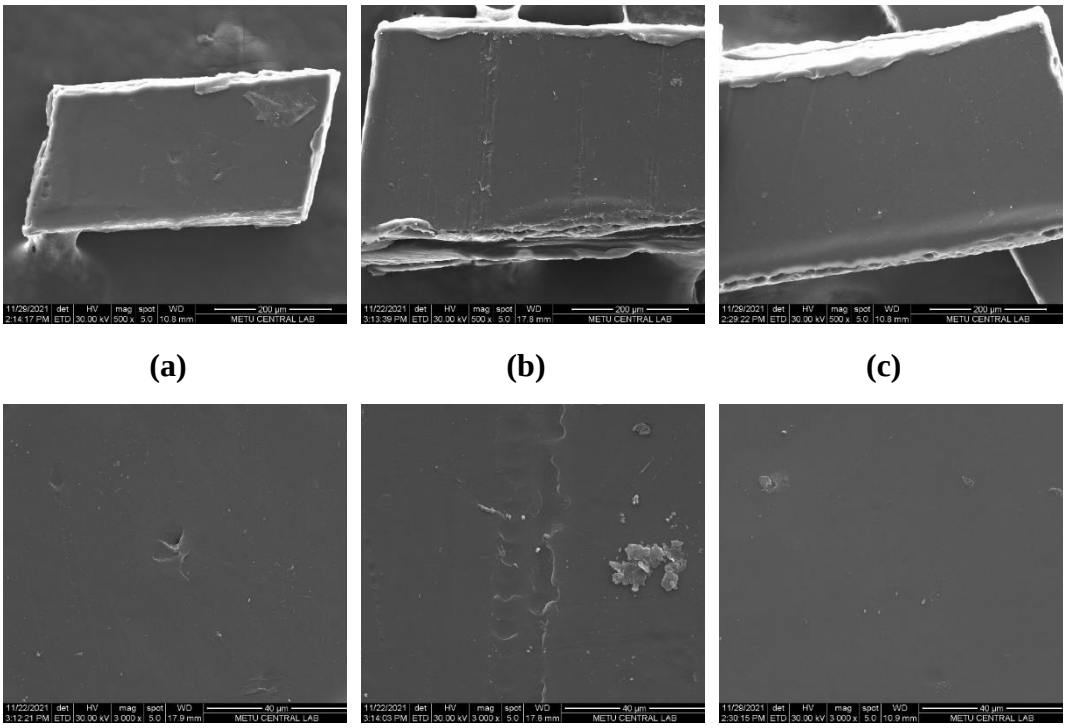

(a) **(b)** **(c)**

(d) **(e)** **(f)**

Figure 4.28. SEM images of combined disintegrated PET MPs at x500 (a) and x3000 (d); combined disintegrated PET MPs after anaerobic digestion at x500 (b) and x3000 (e); and combined disintegrated PET MPs after abiotic anaerobic digestion at x500 (c) and x3000 (f)

4.3.4.3 Change in Polymer Chemistry

FTIR spectra of PET MPs after anaerobic digestion were evaluated based on changes occurred on various bands specific to PET polymer, such as formation/disappearance, increase/decrease and displacement. To interpret the sole impact of anaerobic digestion, changes were determined by taking non-disintegrated (i.e., untreated) PET and disintegrated PET as reference, for non-disintegrated and disintegrated digested reactor sets, respectively.

Structural changes observed in three critical regions of PET were examined as it was in Section 4.2.4. These regions are O-H and C-H stretching (Figure 4.29), C=O

stretching (Figure 4.30); CH_2 wagging and complex lower wavenumber regions containing ester bands (Figure 4.31).

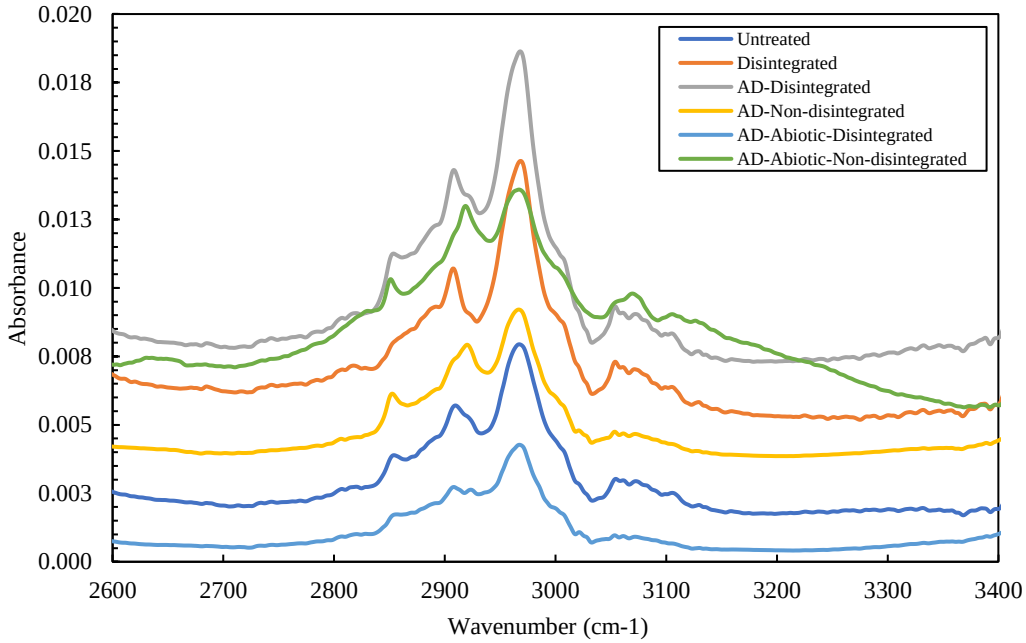

Figure 4.29. O-H and C-H stretching regions of PET

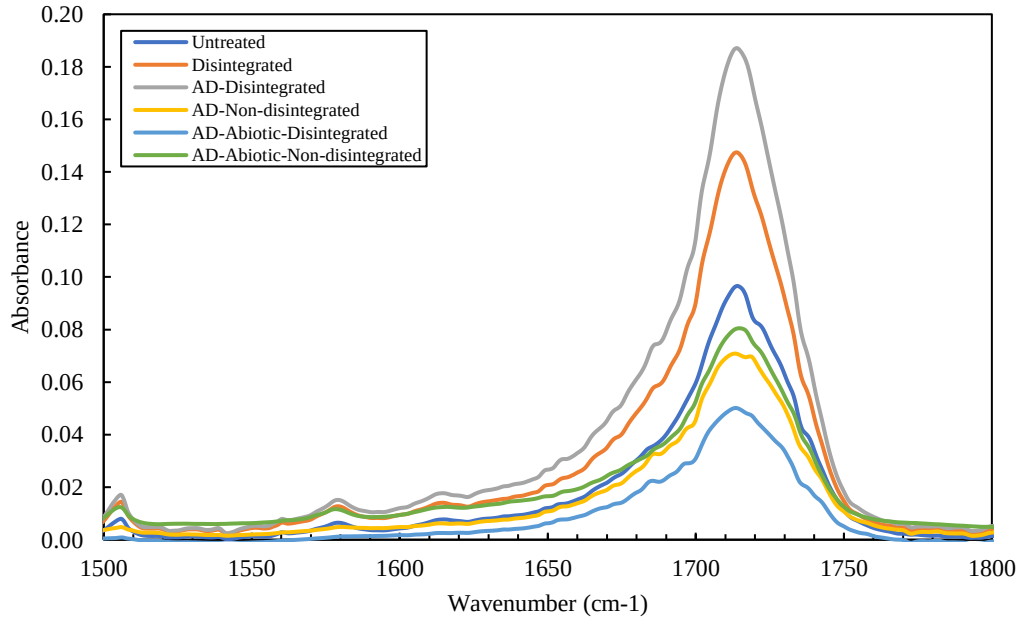

Figure 4.30. C=O stretching region of PET

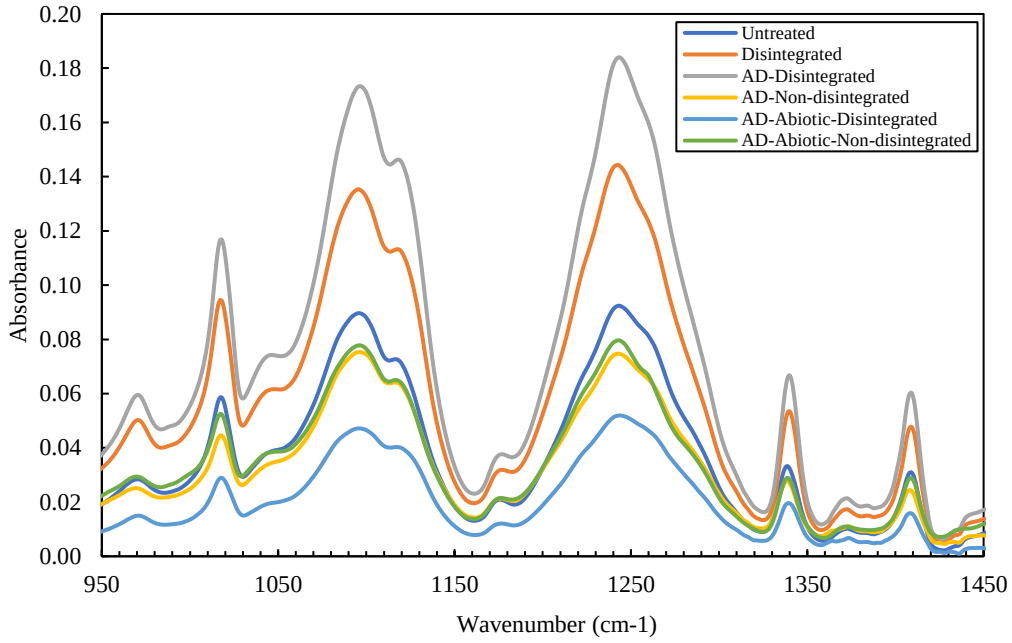

Figure 4.31. CH_2 wagging and ester bond regions of PET

As it was in Section 4.2.4., changes in spectra of PET MPs were determined by taking the ratio of absorption intensities at specific regions to that of a reference peak at 1506 cm^{-1}. Among the three regions examined, the highest changes were observed between 2800-3100 cm^{-1}, which is assigned to C-H stretching. As shown in Figure 4.29, peak shifting, disappearance and intensity change were the mechanisms observed. The regions shown in Figure 4.30 and Figure 4.31, on the other hand, experienced mostly changes in absorption intensity.

Since this section of the study primarily aimed at understanding the impact of anaerobic digestion rather than the disintegration, the focus was on two groups of spectra consisting of (1) Untreated, AD-Non-disintegrated and AD-Abiotic-Non-disintegrated, and (2) Disintegrated, AD-Disintegrated and AD-Abiotic-Disintegrated. With this purpose, structural changes between these polymers were compared within their own groups.

It can be observed from the comparison of the first group of spectra, anaerobic digestion caused an intensity decrease in all three regions in the presence of

microorganisms. Besides, this process also led to a shift in peak wavelength at 2910 cm^{-1} (Figure 4.29). In the absence of microbial activities, anaerobic digestion again produced similar effects on both the intensity and wavelength of polymers. However, the impact in the C-H stretching region was more intense with changes observed in shape of the peak at around 3600 cm^{-1} (Figure 4.29).

The second group of spectra, taking the disintegrated PET as reference, showed that digestion process carried out in the presence of microbial activity increased the intensity in most of the bands, especially those in Figure 4.30 and Figure 4.31. Moreover, the peak disappeared after the disintegration at 2852 cm^{-1} was regenerated after the digestion. When there were no microorganisms alive, on the other hand, the intensity of disintegrated MPs were substantially reduced.

These findings concluded that the impact of digestion may significantly vary depending on the polymer's existing structure prior to processing. For the further examination, one can see the entire FTIR spectrum of PET between 400 to 4000 cm^{-1} in Appendix E (Figure E.2).

4.3.4.3.1 Change in Crystallinity and Carbonyl Index

Figure 4.32 shows the change in crystallinity of PET MPs after anaerobic digestion. The ratio of absorption intensities at 1340 cm^{-1}/1410 cm^{-1} showed that crystallinity of untreated PET MPs increased by 7.2% during digestion. The increase in crystallinity was attributed to local structural rearrangement of PET due to hydrolysis. This is because hydrolytic attack can cause chain shortening leading to recrystallization from short polymeric chain segments in the amorphous region (Donelli et al., 2010). When PET MPs were disintegrated beforehand, anaerobic digestion did not further improve their crystallinity and even a 0.9% decrease was observed. This decrease may be insignificant or may be the sign of destruction in crystalline regions of the polymer.

When the change in crystallinity was determined for both PET MPs extracted from non-disintegrated reactors and disintegrated reactors relative to untreated PET MPs, it is seen that the process leading to recrystallization differs. Already recrystallized disintegrated MPs started to lose their integrity during anaerobic digestion, indicating that the polymer reached to the further stages of degradation. Untreated MPs, on the other hand, were in the stage of recrystallization the loss had not started during anaerobic digestion, meaning that the degradation was in early stages.

These results conclude that the crystallinity level increased by combined disintegration applied is reduced after digestion. On the other hand, when PET was directly introduced into anaerobic digestion, its crystallinity increased, but the level achieved at the end of both cases reached about the same crystallinity level.

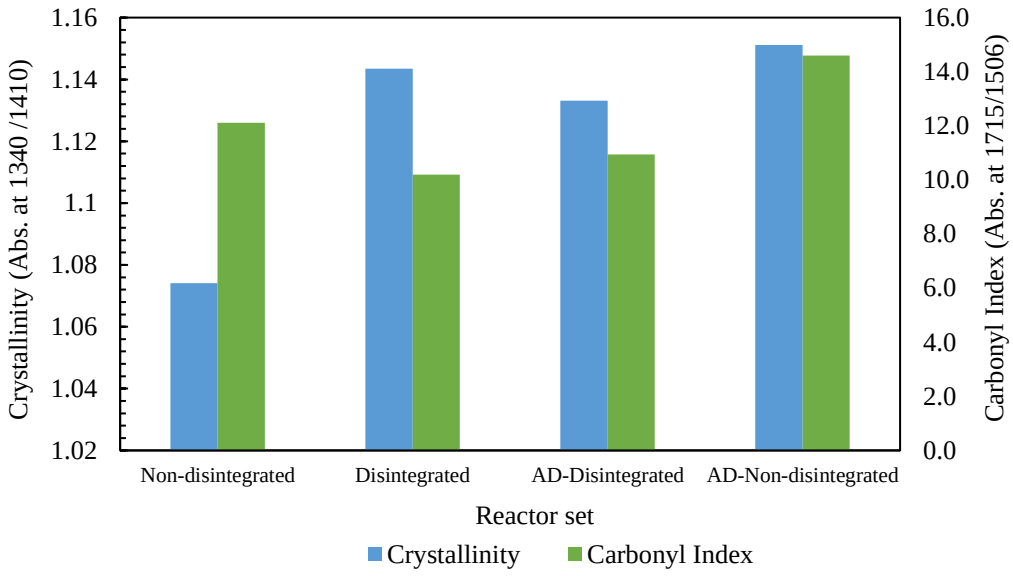

Figure 4.32. Change in crystallinity and carbonyl index (on the secondary axis) of PET MPs

The ratio of absorption intensities at 1715 cm^{-1}/1506 cm^{-1} showed that anaerobic digestion increases carbonyl index of PET MPs regardless of whether there is disintegration process (Figure 4.32). However, the level of impact differs. When there is no disintegration process, carbonyl index of untreated PET increases by

20.4% after 60 days of anaerobic digestion. PET MPs those disintegrated beforehand, however, experience only 7.3% increase in carbonyl index after incubation period. This increase validated the microbial interactions with the polymer as also reported by Torena et al. (2021). Unlike disintegration, digestion process involves the activity of microorganisms. Their extracellular enzymes are the key to increase the hydrophilicity of the polymers by converting them to functional groups (e.g., carbonyl or alcohol groups), which enhances the microbial attachment and further biodegradation (Miri et al., 2022). Therefore, increase in carbonyl index after digestion can be attributed to formation of carboxylic acid end groups as the degradation product and hence the carbonyl bonds (Beltrán-Sanahuja et al., 2020).

When the change in carbonyl index was calculated by taking untreated PET MPs as the only reference material, the impact of anaerobic digestion appears to differ depending on the presence of disintegration process beforehand. In this scenario, which also takes into account the impact of disintegration, carbonyl index of PET from disintegrated reactors decreases by 9.7%. The decrease most likely originates from the disintegration process rather than the anaerobic digestion.

As a result, the chemical changes detected by FTIR analysis confirmed that PET was biodegraded to some degree after anaerobic digestion process. Even though not measured in this study, the contribution of some other parameters can also be mentioned. For instance, chain scissions increasing the concentration of alcoholic and acidic chain end groups likely increased the hydrophilicity of PET MPs, which facilitates the microbial activities on the surface of MPs. Also, most studies in literature undoubtedly associated changes in crystalline structure of polymers with a decrease in molecular weight, which also very likely enhanced the microbial attachment.

CHAPTER 5

CONCLUSION

The aim of this study was two-folds: first, to develop a reliable and repeatable analysis method for MPs in sludge; and second, to investigate fate and effects of PET MPs during anaerobic digestion of alkaline-thermal disintegrated sludge. Creating an appropriate analysis method for MPs consisted of logically sequencing the steps given in the literature for the analysis of MPs and optimizing each step for sludge samples, which was further supported by determining the recovery efficiency of the method. Next, different sludge disintegration techniques were tested for solubilizing WAS and deteriorating PET MPs. The prevailing technique was integrated with anaerobic digestion to scrutinize combined effect on PET MPs and the corresponding impact of MPs on methane yield, by also taking into account MP dose.

Based on the results obtained, the conclusions reached for MPs analysis are as follows.

- Fenton Oxidation applied at theoretical amount of H_2O_2 dosage and MR:10 for 30 min satisfactorily removed organic content of WAS (based on COD) with minimum deteriorative impact on MPs. The following two-step density-based separation provided capturing MPs with densities up to 1.5 g/cm^3. MPs were best visualized under fluorescence microscope when they were retained on PCTE filter and stained by Nile Red, which was prepared in acetone and diluted to 10 mg/L with n-hexane, and incubated for 15 min in dark.
- The developed method ensured recovery of PE, PA and PET MPs in sizes of 425-500 μm from sludge at a rate of 94, 80, and 807%, respectively. So, the method meets the 80% efficiency recommended by ASTM (2020).

- The concentration of MPs in digester sludge was 270 MPs/g TS following blank correction, which is in line with the values reported in literature for dewatered sludge and digested sludge.

The developed method is unique in that it ensures high organic removal efficiency in the sample, for the first time in literature, using a wastewater and sludge specific parameter (i.e., COD). Hence, this method is thought to facilitate further handling of MPs, such as identification and quantification.

The next step in this study consisted of finding the best sludge disintegration technique providing improved WAS solubilization and a deteriorative environment for PET MPs. In reaching these goals, the following conclusions were achieved:

- WAS solubilization was observed to be in positive correlation with treatment time and alkali concentration up to a certain point. A 0.5 M NaOH application to WAS for 120 min was 24.5% and 15.1% more effective in COD solubilization, compared to 0.1 and 0.2 M, respectively. When the 0.5 M alkali application was prolonged, COD continued to solubilize with a rate slowing down over the five days and carbohydrate and protein content of WAS did not further solubilize after the second day.
- As the duration of thermal hydrolysis at 127°C was prolonged to 120 min, the degree of COD solubilization slightly increased.
- Individual applications of 0.5 M alkaline disintegration for two days and thermal hydrolysis at 127°C for 120 min led to increase in soluble COD of WAS 48.4 and 20.6 times, respectively. Combining these techniques provided an even greater improvement in COD solubilization (54.8-fold) compared to untreated WAS. As a result, sCOD of untreated WAS increased from 372.0 mg/L to 20,396 mg/L.
- 0.5 M alkaline disintegration for two days caused a strong peeling effect on surface of PET MPs due to saponification process occurring in ester linkages of the polymer, resulting in 56.5% decrease in mass compared to untreated PET MPs (i.e., control). At the end of two days, alkaline disintegrated PET

had the same level of crystallinity and decreased carbonyl index compared to the control sample.

- Unlike alkaline disintegration, THP at 127°C for 120 min caused an impact on lateral view of PET MPs which is expansion of the particle layers. THP also induced mass loss by 42.7% compared to the control. Although not quantitatively measured, this process caused color change, as well as particle size reduction. Moreover, thermally hydrolyzed PET experienced more distinguishable changes in its chemistry: first, their crystallinity increased by 10%, possibly due to chain scission leading chemi-crystallization; and second, carbonyl index decreased by 29% due to destruction of carbonyl band.
- Combining these techniques did not necessarily pose exaggerated impact on PET MPs. For example, mass reduction was 43.8% compared to the control, meaning that THP did not cause further decrease on alkaline disintegrated PET, potentially due to water absorption on PET surface with many cracks. Similarly, combined disintegration did not further improve the crystallinity of thermally hydrolyzed PET. In contrast, an enhanced decrease was observed in carbonyl index of PET by 37.7% compared to the control, which is higher than the individual impacts.

After the disintegration studies had been completed, anaerobic reactors with disintegrated and non-disintegrated substrates were installed. The conclusions obtained from the BMP test are as follows:

- Disintegrated reactor sets produced statistically higher amounts of methane than non-disintegrated ones regardless of PET MPs dose. More specifically, R0P achieved 22.0% higher methane yield compared to R0.

In contrast to the limited findings in literature demonstrating negative impacts of PET MPs on digestion efficiency, this study revealed an increasing trend in methane yield with MPs dose. Statistical analysis showed that the dose of PET MPs significantly affected the methane yield of non-disintegrated reactor sets. It increased

up to the dosage of 3 mg PET/g TS. However, applying disintegration process ruled out the difference achieved in methane yields of reactors with varying levels of MPs. This means that the disintegration process overwhelmed the impact of MPs on digesters, which was one of the research questions of this study.

- In general, PET MPs induced the formation of ROS, which is consistent with the literature. However, increasing levels of ROS could not be associated with methane yield in none of the reactor sets studied. This might be potentially due to formation of ROS at moderate levels that microorganisms can protect themselves.
- Disintegration process affected the way of impact posed on PET MPs by anaerobic digestion. For example, in non-disintegrated reactor sets, unit mass of PET MPs decreased by 9.2% at the end of 60 days compared to untreated PET MPs, which is also supported by SEM images showing fragmentation on the surface. In disintegrated sets, on the other hand, digestion process did not provide further loss in mass of already disintegrated PET MPs. Instead, water absorption to deteriorated surface of PET MPs caused an increase by 21.6%. Moreover, during anaerobic digestion, crystallinity of untreated MPs increased by 7.2% while it decreased for disintegrated MPs by 0.9%. In contrast, the digestion process increased the carbonyl index of both untreated (by 20.4%) and disintegrated (by 7.3%) PET MPs but at different rates.
- Abiotic reactors revealed the impact of abiotic and biotic factors on fate of PET MPs during anaerobic digestion. Disintegrated PET MPs exposed to abiotic digestion experienced similar level of increase in mass with biotic digestion, indicating that the disintegration process overwhelms the impact of microorganisms. When untreated PET MPs were abiotically digested, their mass increased by 4.5% contrarily to biotically digested MPs, indicating the role of microorganisms.

With these findings it is concluded that combined alkaline thermal disintegration provides a significant improvement in anaerobic digestibility of WAS. Moreover, this treatment has such a great effect on PET MPs that their physical and chemical

properties are substantially altered, as well as their impacts on digester performance are no longer observed.

CHAPTER 6

RECOMMENDATIONS FOR FUTURE STUDIES

Based on the literature review and the results of the laboratory work carried out in this study, following recommendations can be made for future studies.

The concentration of MPs has been mostly reported in particle numbers per unit mass or volume of sludge, both in the literature and in this study. However, treatment units may lead MPs to be broken down, as it was observed during alkaline disintegration in this study. This may result in an inaccurate comparison of MP concentrations in samples taken from different units of a WWTP. Therefore, the reporting of MPs should be reconsidered to be expressed on mass basis.

There is a possibility that Nile Red overestimates MP concentration due to its co-staining effect on residual organic matter in the sample. Therefore, the recovery efficiency of this dye should be tested by chemically analyzing a representative amount of shiny particles on filter using a spectroscopic technique. Then, the MP concentration determined using Nile Red should be corrected with this multiplier. Furthermore, coapplication of a second dye which binds only to biological materials such as 4′,6-diamidino-2-phenylindole (DAPI) or Methylene Blue can be useful to distinguish non-plastic particles.

Excessive ion concentrations due to alkali application caused disintegrated reactors of this study to face with a lag period. Therefore, the ion effect caused to underestimate the methane yield, which was actually highly promoted by combined disintegration. Further studies should set up control reactors to correct the yield by subtracting the delay caused by the ion effect.

The sequence of combined disintegration applied in this study is recommended to be switched to thermal-alkaline treatment. Thus, the strong peeling effect observed on

the surface of MPs after alkali application will not be suppressed by THP. Hence, the increased surface area may facilitate microbial attack during anaerobic digestion.

Hydrolytic degradation causes chain scission at ester linkages of PET resulting in the formation of carboxyl and hydroxyl end groups. Therefore, analyzing the concentration of end groups can be a method to understand the rate of polymer degradation.

Molecular weight of polymers is strongly influenced by the chain scission mechanism and thus the crystallinity. Therefore, it would be good to measure it using GPC to support the findings about change in crystallinity and degradation.

The level of chemicals leaching from PET both during disintegration and anaerobic digestion can be measured to understand if there is a toxicity and/or stimulatory mechanism associated with them. Moreover, a correlation can be investigated between the dose and effect of leaching chemicals.

There are no studies encountered investigating the fate of MPs under thermophilic anaerobic conditions. Prolonged exposure to an environment close to glass transition temperature can yield totally different results, both in terms of methane yield and polymer-related properties.

REFERENCES

Al-Sabagh, A.M., Yehia, F.Z., Eshaq, G., Rabie, A.M., ElMetwally, A.E., 2016. Greener routes for recycling of polyethylene terephthalate. Egypt. J. Pet. 25, 53–64. https://doi.org/10.1016/j.ejpe.2015.03.001

Alassali, A., Moon, H., Picuno, C., Meyer, R.S.A., Kuchta, K., 2018. Assessment of polyethylene degradation after aging through anaerobic digestion and composting. Polym. Degrad. Stab. 158, 14–25. https://doi.org/10.1016/j.polymdegradstab.2018.10.014

Alavian Petroody, S.S., Hashemi, S.H., van Gestel, C.A.M., 2021. Transport and accumulation of microplastics through wastewater treatment sludge processes. Chemosphere 278, 130471. https://doi.org/10.1016/j.chemosphere.2021.130471

Alavian Petroody, S.S., Hashemi, S.H., van Gestel, C.A.M., 2020. Factors affecting microplastic retention and emission by a wastewater treatment plant on the southern coast of Caspian Sea. Chemosphere 261, 128179. https://doi.org/10.1016/j.chemosphere.2020.128179

Albright, V.C., Chai, Y., 2021. Knowledge Gaps in Polymer Biodegradation Research. Environ. Sci. Technol. 55, 11476–11488. https://doi.org/10.1021/acs.est.1c00994

Ali, S.S., Elsamahy, T., Al-Tohamy, R., Zhu, D., Mahmoud, Y.A.G., Koutra, E., Metwally, M.A., Kornaros, M., Sun, J., 2021a. Plastic wastes biodegradation: Mechanisms, challenges and future prospects. Sci. Total Environ. 780, 146590. https://doi.org/10.1016/j.scitotenv.2021.146590

Ali, S.S., Elsamahy, T., Koutra, E., Kornaros, M., El-Sheekh, M., Abdelkarim, E.A., Zhu, D., Sun, J., 2021b. Degradation of conventional plastic wastes in the environment: A review on current status of knowledge and future perspectives

of disposal. Sci. Total Environ. 771, 144719. https://doi.org/10.1016/j.scitotenv.2020.144719

Alimi, O.S., Claveau-Mallet, D., Kurusu, R.S., Lapointe, M., Bayen, S., Tufenkji, N., 2022. Weathering pathways and protocols for environmentally relevant microplastics and nanoplastics: What are we missing? J. Hazard. Mater. 423. https://doi.org/10.1016/j.jhazmat.2021.126955

Allen, N.S., Edge, M., Mohammadian, M., Jones, K., 1991. Hydrolytic degradation of poly(ethylene terephthalate): Importance of chain scission versus crystallinity. Eur. Polym. J. 27, 1373–1378. https://doi.org/10.1016/0014-3057(91)90237-I

Andrady, A.L., Neal, M.A., 2009. Applications and societal benefits of plastics. Philos. Trans. R. Soc. B Biol. Sci. 364, 1977–1984. https://doi.org/10.1098/rstb.2008.0304

APHA, AWWA, WEF, 2017. Standard Methods for the Examination of Water and Wastewater, 23rd ed. American Public Health Association, American Water Works Association, Water Environment Federation, Washington, DC.

Appels, L., Baeyens, J., Degrève, J., Dewil, R., 2008. Principles and potential of the anaerobic digestion of waste-activated sludge. Prog. Energy Combust. Sci. 34, 755–781. https://doi.org/10.1016/j.pecs.2008.06.002

Araujo, C.F., Nolasco, M.M., Ribeiro, A.M.P., Ribeiro-Claro, P.J.A., 2018. Identification of microplastics using Raman spectroscAraujo, C.F., Nolasco, M.M., Ribeiro, A.M.P., Ribeiro-Claro, P.J.A., 2018. Identification of microplastics using Raman spectroscopy: Latest developments and future prospects. Water Res. 142, 426–440. ht. Water Res. 142, 426–440. https://doi.org/10.1016/j.watres.2018.05.060

Arhant, M., Le Gall, M., Le Gac, P.Y., Davies, P., 2019. Impact of hydrolytic degradation on mechanical properties of PET - Towards an understanding of microplastics formation. Polym. Degrad. Stab. 161, 175–182.

https://doi.org/10.1016/j.polymdegradstab.2019.01.021

Arı-Akdemir, E., 2019. Investigation of biogas production potential of three different sludges after thermal hydrolysis, MS Thesis, Middle East Technical University.

Arkatkar, A., Arutchelvi, J., Bhaduri, S., Uppara, P.V., Doble, M., 2009. Degradation of unpretreated and thermally pretreated polypropylene by soil consortia. Int. Biodeterior. Biodegrad. 63, 106–111. https://doi.org/10.1016/j.ibiod.2008.06.005

Arp, H.P.H., Kühnel, D., Rummel, C., Macleod, M., Potthoff, A., Reichelt, S., Rojo-Nieto, E., Schmitt-Jansen, M., Sonnenberg, J., Toorman, E., Jahnke, A., 2021. Weathering Plastics as a Planetary Boundary Threat: Exposure, Fate, and Hazards. Environ. Sci. Technol. 55, 7246–7255. https://doi.org/10.1021/acs.est.1c01512

ASTM International, 2020a. D8332-20 Standard Practice for Collection of Water Samples with High, Medium, or Low Suspended Solids for Identification and Quantification of Microplastic Particles and Fibers. https://doi.org/https://doi.org/10.1520/D8332-20

ASTM International, 2020b. D8333-20 Standard Practice for Preparation of Water Samples with High, Medium, or Low Suspended Solids for Identification and Quantification of Microplastic Particles and Fibers Using Raman Spectroscopy, IR Spectroscopy, or Pyrolysis-GC/MS. https://doi.org/https://doi.org/10.1520/D8333-20

Ballara, A., Verdu, J., 1989. Physical aspects of the hydrolysis of polyethylene terephthalate. Polym. Degrad. Stab. 26, 361–374. https://doi.org/10.1016/0141-3910(89)90114-6

Beltrán-Sanahuja, A., Casado-Coy, N., Simó-Cabrera, L., Sanz-Lázaro, C., 2020. Monitoring polymer degradation under different conditions in the marine environment. Environ. Pollut. 259. https://doi.org/10.1016/j.envpol.2019.113836

Bilgin, M., Yurtsever, M., Karadagli, F., 2020. Microplastic removal by aerated grit chambers versus settling tanks of a municipal wastewater treatment plant. J. Water Process Eng. 38, 101604. https://doi.org/10.1016/j.jwpe.2020.101604

Bläsing, M., Amelung, W., 2018. Plastics in soil: Analytical methods and possible sources. Sci. Total Environ. 612, 422–435. https://doi.org/10.1016/j.scitotenv.2017.08.086

Bougrier, C., Delgenès, J.P., Carrère, H., 2006. Combination of thermal treatments and anaerobic digestion to reduce sewage sludge quantity and improve biogas yield. Process Saf. Environ. Prot. 84, 280–284. https://doi.org/10.1205/psep.05162

Bretas Alvim, C., Bes-Piá, M.A., Mendoza-Roca, J.A., 2020a. Separation and identification of microplastics from primary and secondary effluents and activated sludge from wastewater treatment plants. Chem. Eng. J. 402, 126293. https://doi.org/10.1016/j.cej.2020.126293

Bretas Alvim, C., Mendoza-Roca, J.A., Bes-Piá, A., 2020b. Wastewater treatment plant as microplastics release source – Quantification and identification techniques. J. Environ. Manage. 255. https://doi.org/10.1016/j.jenvman.2019.109739

Cambi Group AS., 2019. USA, Washington DC, Blue Plains [WWW Document]. URL https://www.cambi.com/media/1999/cambi-plant-washington-dc-blue-plains.pdf

Campo, P., Holmes, A., Coulon, F., 2019. A method for the characterisation of microplastics in sludge. MethodsX 6, 2776–2781. https://doi.org/10.1016/j.mex.2019.11.020

Carr, S.A., Liu, J., Tesoro, A.G., 2016. Transport and fate of microplastic particles in wastewater treatment plants. Water Res. 91, 174–182. https://doi.org/10.1016/j.watres.2016.01.002

Carrère, H., Dumas, C., Battimelli, A., Batstone, D.J., Delgenès, J.P., Steyer, J.P., Ferrer, I., 2010. Pretreatment methods to improve sludge anaerobic degradability: A review. J. Hazard. Mater. 183, 1–15. https://doi.org/10.1016/j.jhazmat.2010.06.129

Cashman, M.A., Ho, K.T., Boving, T.B., Russo, S., Robinson, S., Burgess, R.M., 2020. Comparison of microplastic isolation and extraction procedures from marine sediments. Mar. Pollut. Bull. 159, 111507. https://doi.org/10.1016/j.marpolbul.2020.111507

Çelik Çağlar, T., 2021. The investigation of methane production from an agricultural waste, corncob, and its enhancement via co-digestion and pretreatment, MS Thesis, Middle East Technical University.

Chamas, A., Moon, H., Zheng, J., Qiu, Y., Tabassum, T., Jang, J.H., Abu-Omar, M., Scott, S.L., Suh, S., 2020. Degradation Rates of Plastics in the Environment. ACS Sustain. Chem. Eng. 8, 3494–3511. https://doi.org/10.1021/acssuschemeng.9b06635

Chatterjee, S., Sharma, S., 2019. Microplastics in our oceans and marine health. F. Actions Sci. Rep. 2019, 54–61.

Chen, H., Tang, M., Yang, X., Tsang, Y.F., Wu, Y., Wang, D., Zhou, Y., 2020. Polyamide 6 microplastics facilitate methane production during anaerobic digestion of waste activated sludge. Chem. Eng. J. 127251. https://doi.org/10.1016/j.cej.2020.127251

Chen, W., Yuan, D., Shan, M., Yang, Z., Liu, C., 2020. Single and combined effects of amino polystyrene and perfluorooctane sulfonate on hydrogen-producing thermophilic bacteria and the interaction mechanisms. Sci. Total Environ. 703, 135015. https://doi.org/10.1016/j.scitotenv.2019.135015

Chen, Y., Jiang, S., Yuan, H., Zhou, Q., Gu, G., 2007. Hydrolysis and acidification of waste activated sludge at different pHs. Water Res. 41, 683–689. https://doi.org/10.1016/j.watres.2006.07.030

Chen, Z., Hay, J.N., Jenkins, M.J., 2012. FTIR spectroscopic analysis of poly(ethylene terephthalate) on crystallization. Eur. Polym. J. 48, 1586–1610. https://doi.org/10.1016/j.eurpolymj.2012.06.006

Chen, Z., Zhao, W., Xing, R., Xie, S., Yang, X., Cui, P., Lü, J., Liao, H., Yu, Z., Wang, S., Zhou, S., 2020. Enhanced in situ biodegradation of microplastics in sewage sludge using hyperthermophilic composting technology. J. Hazard. Mater. 384, 121271. https://doi.org/10.1016/j.jhazmat.2019.121271

Corradini, F., Meza, P., Eguiluz, R., Casado, F., Huerta-Lwanga, E., Geissen, V., 2019. Evidence of microplastic accumulation in agricultural soils from sewage sludge disposal. Sci. Total Environ. 671, 411–420. https://doi.org/10.1016/j.scitotenv.2019.03.368

Crawford, C.B., Quinn, B., 2016. Microplastic Pollutants, Microplastic Pollutants. https://doi.org/10.1016/c2015-0-04315-5

de Sousa, T.A.T., do Monte, F.P., do Nascimento Silva, J.V., Lopes, W.S., Leite, V.D., van Lier, J.B., de Sousa, J.T., 2021. Alkaline and acid solubilisation of waste activated sludge. Water Sci. Technol. 83, 2980–2996. https://doi.org/10.2166/wst.2021.179

Doğan, I., Sanin, F.D., 2009. Alkaline solubilization and microwave irradiation as a combined sludge disintegration and minimization method. Water Res. 43, 2139–2148. https://doi.org/10.1016/j.watres.2009.02.023

Donelli, I., Freddi, G., Nierstrasz, V.A., Taddei, P., 2010. Surface structure and properties of poly-(ethylene terephthalate) hydrolyzed by alkali and cutinase. Polym. Degrad. Stab. 95, 1542–1550. https://doi.org/10.1016/j.polymdegradstab.2010.06.011

Dubois, M., Gilles, K.A., Hamilton, J.K., Rebers, P.A., Smith, F., 1956. Colorimetric Method for Determination of Sugars and Related Substances. Anal. Chem. 28, 350–356.

Dyachenko, A., Mitchell, J., Arsem, N., 2017. Extraction and identification of microplastic particles from secondary wastewater treatment plant (WWTP) effluent. Anal. Methods 9, 1412–1418. https://doi.org/10.1039/c6ay02397e

Edo, C., González-Pleiter, M., Leganés, F., Fernández-Piñas, F., Rosal, R., 2020. Fate of microplastics in wastewater treatment plants and their environmental dispersion with effluent and sludge. Environ. Pollut. 259, 113837. https://doi.org/10.1016/j.envpol.2019.113837

El Hayany, B., El Fels, L., Quénéa, K., Dignac, M.F., Rumpel, C., Gupta, V.K., Hafidi, M., 2020. Microplastics from lagooning sludge to composts as revealed by fluorescent staining- image analysis, Raman spectroscopy and pyrolysis-GC/MS. J. Environ. Manage. 275, 111249. https://doi.org/10.1016/j.jenvman.2020.111249

Elalami, D., Carrere, H., Monlau, F., Abdelouahdi, K., Oukarroum, A., Barakat, A., 2019. Pretreatment and co-digestion of wastewater sludge for biogas production: Recent research advances and trends. Renew. Sustain. Energy Rev. 114, 1–23. https://doi.org/10.1016/j.rser.2019.109287

Elert, A.M., Becker, R., Duemichen, E., Eisentraut, P., Falkenhagen, J., Sturm, H., Braun, U., 2017. Comparison of different methods for MP detection: What can we learn from them, and why asking the right question before measurements matters? Environ. Pollut. 231, 1256–1264. https://doi.org/10.1016/j.envpol.2017.08.074

Eubeler, J.P., Zok, S., Bernhard, M., Knepper, T.P., 2009. Environmental biodegradation of synthetic polymers I. Test methodologies and procedures. TrAC - Trends Anal. Chem. 28, 1057–1072. https://doi.org/10.1016/j.trac.2009.06.007

Fang, W., Zhang, P., Zhang, G., Jin, S., Li, D., Zhang, M., Xu, X., 2014. Effect of alkaline addition on anaerobic sludge digestion with combined pretreatment of alkaline and high pressure homogenization. Bioresour. Technol. 168, 167–172.

https://doi.org/10.1016/j.biortech.2014.03.050

Filho, W.L., Salvia, A.L., Bonoli, A., Saari, U.A., Voronova, V., Klõga, M., Kumbhar, S.S., Olszewski, K., De Quevedo, D.M., Barbir, J., 2021. An assessment of attitudes towards plastics and bioplastics in Europe. Sci. Total Environ. 755, 142732. https://doi.org/10.1016/j.scitotenv.2020.142732

Fotopoulou, K.N., Karapanagioti, H.K., 2015. Surface properties of beached plastics. Environ. Sci. Pollut. Res. 22, 11022–11032. https://doi.org/10.1007/s11356-015-4332-y

Fu, S.F., Ding, J.N., Zhang, Y., Li, Y.F., Zhu, R., Yuan, X.Z., Zou, H., 2018. Exposure to polystyrene nanoplastic leads to inhibition of anaerobic digestion system. Sci. Total Environ. 625, 64–70. https://doi.org/10.1016/j.scitotenv.2017.12.158

Galloway, T.S., Cole, M., Lewis, C., 2017. Interactions of microplastic debris throughout the marine ecosystem. Nat. Ecol. Evol. 1, 1–8. https://doi.org/10.1038/s41559-017-0116

Gao, D., Li, X. yu, Liu, H. tao, 2020. Source, occurrence, migration and potential environmental risk of microplastics in sewage sludge and during sludge amendment to soil. Sci. Total Environ. 742, 140355. https://doi.org/10.1016/j.scitotenv.2020.140355

Gatidou, G., Arvaniti, O.S., Stasinakis, A.S., 2019. Review on the occurrence and fate of microplastics in Sewage Treatment Plants. J. Hazard. Mater. 367, 504–512. https://doi.org/10.1016/j.jhazmat.2018.12.081

Gewert, B., Plassmann, M.M., Macleod, M., 2015. Pathways for degradation of plastic polymers floating in the marine environment. Environ. Sci. Process. Impacts 17, 1513–1521. https://doi.org/10.1039/c5em00207a

Geyer, R., Jambeck, J.R., Law, K.L., 2017. Production, use, and fate of all plastics ever made. Sci. Adv. 3, 25–29. https://doi.org/10.1126/sciadv.1700782

Gies, E.A., LeNoble, J.L., Noël, M., Etemadifar, A., Bishay, F., Hall, E.R., Ross, P.S., 2018. Retention of microplastics in a major secondary wastewater treatment plant in Vancouver, Canada. Mar. Pollut. Bull. 133, 553–561. https://doi.org/10.1016/j.marpolbul.2018.06.006

Gong, J., Xie, P., 2020. Research progress in sources, analytical methods, eco-environmental effects, and control measures of microplastics. Chemosphere 254, 126790. https://doi.org/10.1016/j.chemosphere.2020.126790

Guo, X., Wang, J., 2019. The chemical behaviors of microplastics in marine environment: A review. Mar. Pollut. Bull. 142, 1–14. https://doi.org/10.1016/j.marpolbul.2019.03.019

Gurjar, B.R., Tyagi, V.K., 2017. Sludge Management, Angewandte Chemie International Edition, 6(11), 951–952. CRC Press, London.

Hardesty, B.D., Good, T.P., Wilcox, C., 2015. Novel methods, new results and science-based solutions to tackle marine debris impacts on wildlife. Ocean Coast. Manag. 115, 4–9. https://doi.org/10.1016/j.ocecoaman.2015.04.004

Hidalgo-Ruz, V., Gutow, L., Thompson, R.C., Thiel, M., 2012. Microplastics in the marine environment: A review of the methods used for identification and quantification. Environ. Sci. Technol. 46, 3060–3075. https://doi.org/10.1021/es2031505

Hongprasith, N., Kittimethawong, C., Lertluksanaporn, R., Eamchotchawalit, T., Kittipongvises, S., Lohwacharin, J., 2020. IR microspectroscopic identification of microplastics in municipal wastewater treatment plants. Environ. Sci. Pollut. Res. 27, 18557–18564. https://doi.org/10.1007/s11356-020-08265-7

Hurley, R.R., Lusher, A.L., Olsen, M., Nizzetto, L., 2018. Validation of a Method for Extracting Microplastics from Complex, Organic-Rich, Environmental Matrices. Environ. Sci. Technol. 52, 7409–7417. https://doi.org/10.1021/acs.est.8b01517

Hurley, R.R., Nizzetto, L., 2018. Fate and occurrence of micro(nano)plastics in soils: Knowledge gaps and possible risks. Curr. Opin. Environ. Sci. Heal. 1, 6–11. https://doi.org/10.1016/j.coesh.2017.10.006

Ioakeimidis, C., Fotopoulou, K.N., Karapanagioti, H.K., Geraga, M., Zeri, C., Papathanassiou, E., Galgani, F., Papatheodorou, G., 2016. The degradation potential of PET bottles in the marine environment: An ATR-FTIR based approach. Sci. Rep. 6, 1–8. https://doi.org/10.1038/srep23501

Iram, D., Riaz, R., Iqbal, R.K., 2019. Usage of Potential Micro-organisms for Degradation of Plastics. Open J. Environ. Biol. 4, 007–015. https://doi.org/10.17352/ojeb.000010

Ivleva, N.P., Wiesheu, A.C., Niessner, R., 2017. Microplastic in Aquatic Ecosystems. Angew. Chemie - Int. Ed. 56, 1720–1739. https://doi.org/10.1002/anie.201606957

Jahan, S., Strezov, V., Weldekidan, H., Kumar, R., Kan, T., Sarkodie, S.A., He, J., Dastjerdi, B., Wilson, S.P., 2019. Interrelationship of microplastic pollution in sediments and oysters in a seaport environment of the eastern coast of Australia. Sci. Total Environ. 695, 133924. https://doi.org/10.1016/j.scitotenv.2019.133924

Jiang, J., Wang, X., Ren, H., Cao, G., Xie, G., Xing, D., Liu, B., 2020. Investigation and fate of microplastics in wastewater and sludge filter cake from a wastewater treatment plant in China. Sci. Total Environ. 746, 141378. https://doi.org/https://doi.org/10.1016/j.scitotenv.2020.141378

Jin, B., Wang, S., Xing, L., Li, B., Peng, Y., 2016. Long term effect of alkali types on waste activated sludge hydrolytic acidification and microbial community at low temperature. Bioresour. Technol. 200, 587–597. https://doi.org/10.1016/j.biortech.2015.10.036

Jirka, A.M., Carter, M.J., 1975. Micro Semi-Automated Analysis of Surface and Wastewaters for Chemical Oxygen Demand. Anal. Chem. 47, 1397-1402.

https://doi.org/10.1021/ac60358a004

Kalaycıoğlu, N.N., 2020. Energy production from yard wastes via one-stage and two-stage anaerobic digestion and investigation of pretreatment effect, MS Thesis, Middle East Technical University.

Kang, P., Ji, B., Zhao, Y., Wei, T., 2020. How can we trace microplastics in wastewater treatment plants: A review of the current knowledge on their analysis approaches. Sci. Total Environ. 745, 140943. https://doi.org/10.1016/j.scitotenv.2020.140943

Kawai, F., Kawabata, T., Oda, M., 2019. Current knowledge on enzymatic PET degradation and its possible application to waste stream management and other fields. Appl. Microbiol. Biotechnol. 103, 4253–4268. https://doi.org/10.1007/s00253-019-09717-y

Khanh Nguyen, V., Kumar Chaudhary, D., Hari Dahal, R., Hoang Trinh, N., Kim, J., Chang, S.W., Hong, Y., Duc La, D., Nguyen, X.C., Hao Ngo, H., Chung, W.J., Nguyen, D.D., 2021. Review on pretreatment techniques to improve anaerobic digestion of sewage sludge. Fuel 285, 1–13. https://doi.org/10.1016/j.fuel.2020.119105

Kim, J., Park, C., Kim, T.H., Lee, M., Kim, S., Kim, S.W., Lee, J., 2003. Effects of various pretreatments for enhanced anaerobic digestion with waste activated sludge. J. Biosci. Bioeng. 95, 271–275. https://doi.org/10.1263/jbb.95.271

Kim, J., Yu, Y., Lee, C., 2013. Thermo-alkaline pretreatment of waste activated sludge at low-temperatures: Effects on sludge disintegration, methane production, and methanogen community structure. Bioresour. Technol. 144, 194–201. https://doi.org/10.1016/j.biortech.2013.06.115

Klein, S., Dimzon, I.K., Eubeler, J., Knepper, T.P., 2018. Analysis, Occurrence, and Degradation of Microplastics in the Aqueous Environment, in: Freshwater Microplastics. p. 302. https://doi.org/10.1007/978-3-319-61615-5

Kugelman, I.J., Mccarty, P.L., 1965. Cation Toxicity and Stimulation in Anaerobic Waste Treatment. Water Pollut. Control Fed. 37, 97–116.

Lares, M., Ncibi, M.C., Sillanpää, Markus, Sillanpää, Mika, 2018. Occurrence, identification and removal of microplastic particles and fibers in conventional activated sludge process and advanced MBR technology. Water Res. 133, 236–246. https://doi.org/10.1016/j.watres.2018.01.049

Lee, H., Kim, Y., 2018. Treatment characteristics of microplastics at biological sewage treatment facilities in Korea. Mar. Pollut. Bull. 137, 1–8. https://doi.org/10.1016/j.marpolbul.2018.09.050

Leslie, H.A., Brandsma, S.H., van Velzen, M.J.M., Vethaak, A.D., 2017. Microplastics en route: Field measurements in the Dutch river delta and Amsterdam canals, wastewater treatment plants, North Sea sediments and biota. Environ. Int. 101, 133–142. https://doi.org/10.1016/j.envint.2017.01.018

Lessa Belone, M.C., Kokko, M., Sarlin, E., 2021. Degradation of common polymers in sewage sludge purification process developed for microplastic analysis. Environ. Pollut. 269, 116235. https://doi.org/10.1016/j.envpol.2020.116235

Li, H., Li, C., Liu, W., Zou, S., 2012. Optimized alkaline pretreatment of sludge before anaerobic digestion. Bioresour. Technol. 123, 189–194. https://doi.org/10.1016/j.biortech.2012.08.017

Li, H., Xu, S., Wang, S., Yang, J., Yan, P., Chen, Y., Guo, J., Fang, F., 2020. New insight into the effect of short-term exposure to polystyrene nanoparticles on activated sludge performance. J. Water Process Eng. 38, 101559. https://doi.org/10.1016/j.jwpe.2020.101559

Li, L., Geng, S., Li, Z., Song, K., 2020. Effect of microplastic on anaerobic digestion of wasted activated sludge. Chemosphere 247, 125874. https://doi.org/10.1016/j.chemosphere.2020.125874

Li, Q., Wu, J., Zhao, X., Gu, X., Ji, R., 2019. Separation and identification of

microplastics from soil and sewage sludge. Environ. Pollut. 254, 113076. https://doi.org/10.1016/j.envpol.2019.113076

Li, X., Chen, L., Ji, Y., Li, M., Dong, B., Qian, G., Zhou, J., Dai, X., 2020. Effects of chemical pretreatments on microplastic extraction in sewage sludge and their physicochemical characteristics. Water Res. 171, 115379. https://doi.org/10.1016/j.watres.2019.115379

Li, X., Chen, L., Mei, Q., Dong, B., Dai, X., Ding, G., Zeng, E.Y., 2018. Microplastics in sewage sludge from the wastewater treatment plants in China. Water Res. 142, 75–85. https://doi.org/10.1016/j.watres.2018.05.034

Li, X., Mei, Q., Chen, L., Zhang, H., Dong, B., Dai, X., He, C., Zhou, J., 2019. Enhancement in adsorption potential of microplastics in sewage sludge for metal pollutants after the wastewater treatment process. Water Res. 157, 228–237. https://doi.org/10.1016/j.watres.2019.03.069

Liu, X., Yuan, W., Di, M., Li, Z., Wang, J., 2019. Transfer and fate of microplastics during the conventional activated sludge process in one wastewater treatment plant of China. Chem. Eng. J. 362, 176–182. https://doi.org/10.1016/j.cej.2019.01.033

Lowry, O., Rosebrough, N.J., Farr, A.L., Randall, R.J., 1951. Protein Measurement with the Folin Fenol Reagent 265–276.

Luo, Q., Liu, Z. hua, Yin, H., Dang, Z., Wu, P. xiao, Zhu, N. wu, Lin, Z., Liu, Y., 2018. Migration and potential risk of trace phthalates in bottled water: A global situation. Water Res. 147, 362–372. https://doi.org/10.1016/j.watres.2018.10.002

Lusher, A.L., Hurley, R.R., Vogelsang, C., Nizzetto, L., Olsen, M., 2017. Mapping microplastics in sludge. https://doi.org/10.13140/RG.2.2.25277.56804

Lv, X., Dong, Q., Zuo, Z., Liu, Y., Huang, X., Wu, W.M., 2019. Microplastics in a municipal wastewater treatment plant: Fate, dynamic distribution, removal

efficiencies, and control strategies. J. Clean. Prod. 225, 579–586. https://doi.org/10.1016/j.jclepro.2019.03.321

Magni, S., Binelli, A., Pittura, L., Avio, C.G., Della Torre, C., Parenti, C.C., Gorbi, S., Regoli, F., 2019. The fate of microplastics in an Italian Wastewater Treatment Plant. Sci. Total Environ. 652, 602–610. https://doi.org/10.1016/j.scitotenv.2018.10.269

Magnusson, K., Norén, F., 2014. Screening of microplastic particles in and down-stream a wastewater treatment plant, IVL Swedish Environmental Research Institute. https://doi.org/naturvardsverket-2226

Mahon, A.M., O'Connell, B., Healy, M.G., O'Connor, I., Officer, R., Nash, R., Morrison, L., 2017. Microplastics in sewage sludge: Effects of treatment. Environ. Sci. Technol. 51, 810–818. https://doi.org/10.1021/acs.est.6b04048

Mallow, O., Spacek, S., Schwarzböck, T., Fellner, J., Rechberger, H., 2020. A new thermoanalytical method for the quantification of microplastics in industrial wastewater. Environ. Pollut. 259, 113862. https://doi.org/10.1016/j.envpol.2019.113862

Martínez-Romo, A., González-Mota, R., Soto-Bernal, J.J., Rosales-Candelas, I., 2015. Investigating the Degradability of HDPE, LDPE, PE-BIO, and PE-OXO Films under UV-B Radiation. J. Spectrosc. 2015, 1–6. https://doi.org/10.1155/2015/586514

Mason, S.A., Garneau, D., Sutton, R., Chu, Y., Ehmann, K., Barnes, J., Fink, P., Papazissimos, D., Rogers, D.L., 2016. Microplastic pollution is widely detected in US municipal wastewater treatment plant effluent. Environ. Pollut. 218, 1045–1054. https://doi.org/10.1016/j.envpol.2016.08.056

Masura, J., Baker, J., Foster, G., Arthur, C., Herring, C., 2015. Laboratory Methods for the Analysis of Microplastics in the Marine Environment : Recommendations for quantifying synthetic particles in waters and sediments.

McCarty, P.L., 1964. Anaerobic Waste Treatment Fundamentals. Public Work. 95, 91–94.

Metcalf, Eddy, 2003. Wastewater Engineering: Treatment and Reuse, 4th ed. McGraw-Hill, New York.

Michielssen, M.R., Michielssen, E.R., Ni, J., Duhaime, M.B., 2016. Fate of microplastics and other small anthropogenic litter (SAL) in wastewater treatment plants depends on unit processes employed. Environ. Sci. Water Res. Technol. 2, 1064–1073. https://doi.org/10.1039/c6ew00207b

Mintenig, S.M., Int-Veen, I., Löder, M.G.J., Primpke, S., Gerdts, G., 2017. Identification of microplastic in effluents of waste water treatment plants using focal plane array-based micro-Fourier-transform infrared imaging. Water Res. 108, 365–372. https://doi.org/10.1016/j.watres.2016.11.015

Miri, S., Saini, R., Davoodi, S.M., Pulicharla, R., Brar, S.K., Magdouli, S., 2022. Biodegradation of microplastics: Better late than never. Chemosphere 286, 131670. https://doi.org/10.1016/j.chemosphere.2021.131670

Mohajerani, A., Karabatak, B., 2020. Microplastics and pollutants in biosolids have contaminated agricultural soils : An analytical study and a proposal to cease the use of biosolids in farmlands and utilise them in sustainable bricks. Waste Manag. 107, 252–265. https://doi.org/10.1016/j.wasman.2020.04.021

Mostafa, A., Kim, M., Im, S., Lee, M., Kang, S., Kim, D., 2020. Series of Combined Pretreatment Can Affect the Solubilization of Waste-Activated Sludge. Energies 13.

Murphy, F., Ewins, C., Carbonnier, F., Quinn, B., 2016. Wastewater Treatment Works (WwTW) as a Source of Microplastics in the Aquatic Environment. Environ. Sci. 50, 5800–5808. https://doi.org/10.1021/acs.est.5b05416

Ncube, L.K., Ude, A.U., Ogunmuyiwa, E.N., Zulkifli, R., Beas, I.N., 2021. An overview of plasticwaste generation and management in food packaging

industries. Recycling 6, 1–25. https://doi.org/10.3390/recycling6010012

Neyens, E., Baeyens, J., 2003. A review of thermal sludge pre-treatment processes to improve dewaterability. J. Hazard. Mater. 98, 51–67. https://doi.org/10.1016/S0304-3894(02)00320-5

Ngo, P.L., Pramanik, B.K., Shah, K., Roychand, R., 2019. Pathway, classification and removal efficiency of microplastics in wastewater treatment plants. Environ. Pollut. 255, 113326. https://doi.org/10.1016/j.envpol.2019.113326

Nguyen, B., Claveau-Mallet, D., Hernandez, L.M., Xu, E.G., Farner, J.M., Tufenkji, N., 2019. Separation and Analysis of Microplastics and Nanoplastics in Complex Environmental Samples. Acc. Chem. Res. 52, 858–866. https://doi.org/10.1021/acs.accounts.8b00602

Nizzetto, L., Futter, M., Langaas, S., 2016. Are Agricultural Soils Dumps for Microplastics of Urban Origin? Environ. Sci. Technol. 50, 10777–10779. https://doi.org/10.1021/acs.est.6b04140

Okoffo, E.D., O'Brien, S., O'Brien, J.W., Tscharke, B.J., Thomas, K. V., 2019. Wastewater treatment plants as a source of plastics in the environment: A review of occurrence, methods for identification, quantification and fate. Environ. Sci. Water Res. Technol. 5, 1908–1931. https://doi.org/10.1039/c9ew00428a

Okoffo, E.D., Ribeiro, F., Brien, J.W.O., Brien, S.O., Tscharke, B.J., Gallen, M., Samanipour, S., Mueller, J.F., Thomas, K. V, 2020. Identification and quantification of selected plastics in biosolids by pressurized liquid extraction combined with double-shot pyrolysis gas chromatography – mass spectrometry. Sci. Total Environ. 715, 136924. https://doi.org/10.1016/j.scitotenv.2020.136924

Ou, H., Zeng, E.Y., 2018. Occurrence and Fate of Microplastics in Wastewater Treatment Plants, Microplastic Contamination in Aquatic Environments. Elsevier Inc. https://doi.org/10.1016/b978-0-12-813747-5.00010-2

Parkin, G.F., Owen, W.F., 1986. Fundamentals of Anaerobic Digestion of Wastewater Sludges. J. Environ. Eng. 112, 867–920. https://doi.org/10.1061/(asce)0733-9372(1986)112:5(867)

Pittura, L., Foglia, A., Akyol, Ç., Cipolletta, G., Benedetti, M., Regoli, F., Eusebi, A.L., Sabbatini, S., Tseng, L.Y., Katsou, E., Gorbi, S., Fatone, F., 2021. Microplastics in real wastewater treatment schemes: Comparative assessment and relevant inhibition effects on anaerobic processes. Chemosphere 262, 128415. https://doi.org/10.1016/j.chemosphere.2020.128415

PlasticsEurope, 2020. Plastics – the Facts 2020: an Analysis of European Plastics Production, Demand and Waste Data.

Prata, J.C., da Costa, J.P., Duarte, A.C., Rocha-Santos, T., 2019. Methods for sampling and detection of microplastics in water and sediment: A critical review. TrAC - Trends Anal. Chem. 110, 150–159. https://doi.org/10.1016/j.trac.2018.10.029

Qian, J., He, X., Wang, P., Xu, B., Li, K., Lu, B., Jin, W., Tang, S., 2021. Effects of polystyrene nanoplastics on extracellular polymeric substance composition of activated sludge: The role of surface functional groups. Environ. Pollut. 279, 116904. https://doi.org/10.1016/j.envpol.2021.116904

Quinn, B., Murphy, F., Ewins, C., 2017. Validation of density separation for the rapid recovery of microplastics from sediment. Anal. Methods 9, 1491–1498. https://doi.org/10.1039/c6ay02542k

Raju, S., Carbery, M., Kuttykattil, A., Senthirajah, K., Lundmark, A., Rogers, Z., SCB, S., Evans, G., Palanisami, T., 2020. Improved methodology to determine the fate and transport of microplastics in a secondary wastewater treatment plant. Water Res. 173, 115549. https://doi.org/10.1016/j.watres.2020.115549

Raposo, F., Fernández-Cegrí, V., de la Rubia, M.A., Borja, R., Béline, F., Cavinato, C., Demirer, G., Fernández, B., Fernández-Polanco, M., Frigon, J.C., Ganesh, R., Kaparaju, P., Koubova, J., Méndez, R., Menin, G., Peene, A., Scherer, P.,

Torrijos, M., Uellendahl, H., Wierinck, I., de Wilde, V., 2011. Biochemical methane potential (BMP) of solid organic substrates: Evaluation of anaerobic biodegradability using data from an international interlaboratory study. J. Chem. Technol. Biotechnol. 86, 1088–1098. https://doi.org/10.1002/jctb.2622

Rehse, S., Kloas, W., Zarfl, C., 2016. Short-term exposure with high concentrations of pristine microplastic particles leads to immobilisation of Daphnia magna. Chemosphere 153, 91–99. https://doi.org/10.1016/j.chemosphere.2016.02.133

Reimonn, G., Lu, T., Gandhi, N., Chen, W.T., 2019. Review of microplastic pollution in the environment and emerging recycling solutions. J. Renew. Mater. 7, 1251–1268. https://doi.org/10.32604/jrm.2019.08055

Ren, P.J., Dou, M., Wang, C., Li, G.Q., Jia, R., 2020. Abundance and removal characteristics of microplastics at a wastewater treatment plant in Zhengzhou. Environ. Sci. Pollut. Res. 27, 36295–36305. https://doi.org/10.1007/s11356-020-09611-5

Rillig, M.C., 2012. Microplastic in Terrestrial Ecosystems and the Soil? Environ. Sci. 46, 6453–6454. https://doi.org/10.1021/es302011r

Rocha-Santos, T., Duarte, A.C., 2015. A critical overview of the analytical approaches to the occurrence, the fate and the behavior of microplastics in the environment. TrAC - Trends Anal. Chem. 65, 47–53. https://doi.org/10.1016/j.trac.2014.10.011

Rolsky, C., Kelkar, V., Driver, E., Halden, R.U., 2020. Municipal sewage sludge as a source of microplastics in the environment. Curr. Opin. Environ. Sci. Heal. 14, 16–22. https://doi.org/10.1016/j.coesh.2019.12.001

Sammon, C., Yarwood, J., Everall, N., 2000. FT-IR study of the effect of hydrolytic degradation on the structure of thin PET films. Polym. Degrad. Stab. 67, 149–158. https://doi.org/10.1016/S0141-3910(99)00104-4

Sang, T., Wallis, C.J., Hill, G., Britovsek, G.J.P., 2020. Polyethylene terephthalate

degradation under natural and accelerated weathering conditions. Eur. Polym. J. 136, 109873. https://doi.org/10.1016/j.eurpolymj.2020.109873

Sanin, F.D., Clarkson, W.W., Vesilind, P.A., 2011. Sludge Engineering: The Treatment and Disposal of Wastewater Sludges. DEStech Publications Inc.

Sarkar, A.K., Rubin, A.E., Zucker, I., 2021. Engineered Polystyrene-Based Microplastics of High Environmental Relevance. Environ. Sci. Technol. 55, 10491–10501. https://doi.org/10.1021/acs.est.1c02196

Shah, A.A., Hasan, F., Hameed, A., Ahmed, S., 2008. Biological degradation of plastics: A comprehensive review. Biotechnol. Adv. 26, 246–265. https://doi.org/10.1016/j.biotechadv.2007.12.005

Sharma, S., Chatterjee, S., 2017. Microplastic pollution, a threat to marine ecosystem and human health: a short review. Environ. Sci. Pollut. Res. 24, 21530–21547. https://doi.org/10.1007/s11356-017-9910-8

Shim, W.J., Hong, S.H., Eo, S.E., 2017. Identification methods in microplastic analysis: A review. Anal. Methods 9, 1384–1391. https://doi.org/10.1039/c6ay02558g

Shim, W.J., Song, Y.K., Hong, S.H., Jang, M., 2016. Identification and quantification of microplastics using Nile Red staining. Mar. Pollut. Bull. 113, 469–476. https://doi.org/10.1016/j.marpolbul.2016.10.049

Shrestha, B., Hernandez, R., Fortela, D.L.B., Sharp, W., Chistoserdov, A., Gang, D., Revellame, E., Holmes, W., Zappi, M.E., 2020. A review of pretreatment methods to enhance solids reduction during anaerobic digestion of municipal wastewater sludges and the resulting digester performance: implications to future urban biorefineries. Appl. Sci. 10, 1–28. https://doi.org/10.3390/app10249141

Shrivastava, A., 2018. Introduction to Plastics Engineering, in: Introduction to Plastics Engineering. Elsevier, pp. 1–16. https://doi.org/10.1016/B978-0-323-

39500-7.00001-0

Silva, A.B., Bastos, A.S., Justino, C.I.L., da Costa, J.P., Duarte, A.C., Rocha-Santos, T.A.P., 2018. Microplastics in the environment: Challenges in analytical chemistry - A review. Anal. Chim. Acta 1017, 1–19. https://doi.org/10.1016/j.aca.2018.02.043

Sol, D., Laca, Amanda, Laca, Adriana, Díaz, M., 2020. Approaching the environmental problem of microplastics: Importance of WWTP treatments. Sci. Total Environ. 740, 140016. https://doi.org/10.1016/j.scitotenv.2020.140016

Statistica, 2021. Global plastic production 1950-2020 [WWW Document]. URL https://www.statista.com/statistics/282732/global-production-of-plastics-since-1950/

Sujathan, S., Kniggendorf, A.K., Kumar, A., Roth, B., Rosenwinkel, K.H., Nogueira, R., 2017. Heat and Bleach: A Cost-Efficient Method for Extracting Microplastics from Return Activated Sludge. Arch. Environ. Contam. Toxicol. 73, 641–648. https://doi.org/10.1007/s00244-017-0415-8

Sun, J., Dai, X., Wang, Q., van Loosdrecht, M.C.M., Ni, B.J., 2019. Microplastics in wastewater treatment plants: Detection, occurrence and removal. Water Res. 152, 21–37. https://doi.org/10.1016/j.watres.2018.12.050

Tagg, A.S., Sapp, M., Harrison, J.P., Ojeda, J.J., 2015. Identification and Quantification of Microplastics in Wastewater Using Focal Plane Array-Based Reflectance Micro-FT-IR Imaging. Anal. Chem. 87, 6032–6040. https://doi.org/10.1021/acs.analchem.5b00495

Talinli, I., Anderson, G.K., 1992. Interference of Hydrogen Peroxide on the Standard COD Test. Water Res. 26, 107–110.

Talvitie, J., Mikola, A., Koistinen, A., Setälä, O., 2017. Solutions to microplastic pollution – Removal of microplastics from wastewater effluent with advanced wastewater treatment technologies. Water Res. 123, 401–407.

https://doi.org/10.1016/j.watres.2017.07.005

Tanaka, S., Kobayashi, T., Kamiyama, K., Signey Bildan, M.L.N., 1997. Effects of Thermochemical Pretreatment on the Anaerobic Digestion of Waste Activated Sludge. Water Sci. Technol. 35, 209–215.

Thompson, R.C., 2006. Plastic debris in the marine environment: consequences and solutions, in: Marine Nature Conservation in Europe. pp. 107–116.

Torena, P., Alvarez-Cuenca, M., Reza, M., 2021. Biodegradation of polyethylene terephthalate microplastics by bacterial communities from activated sludge. Can. J. Chem. Eng. 99, S69–S82. https://doi.org/10.1002/cjce.24015

Toutian, V., Barjenbruch, M., Loderer, C., Remy, C., 2021. Impact of process parameters of thermal alkaline pretreatment on biogas yield and dewaterability of waste activated sludge. Water Res. 202, 117465. https://doi.org/10.1016/j.watres.2021.117465

Türk Gıda Kodeksi, 2013. Türk Gıda Kodeksi Gıda ile Temas Eden Plastik Madde ve Malzemeler Tebliği (Tebliğ No: 2013/34). T.C. Resmi Gazete 28710.

United Nations Environment Programme, 2018. The state of plastics: World Environment Day Outlook 2018. https://doi.org/10.1093/oxfordhb/9780199238804.003.0031

Valo, A., Carrère, H., Delgenès, J.P., 2004. Thermal, chemical and thermo-chemical pre-treatment of waste activated sludge for anaerobic digestion. J. Chem. Technol. Biotechnol. 79, 1197–1203. https://doi.org/10.1002/jctb.1106

Vlyssides, A.G., Karlis, P.K., 2004. Thermal-alkaline solubilization of waste activated sludge as a pre-treatment stage for anaerobic digestion. Bioresour. Technol. 91, 201–206. https://doi.org/10.1016/S0960-8524(03)00176-7

Waldschläger, K., Lechthaler, S., Stauch, G., Schüttrumpf, H., 2020. The way of microplastic through the environment – Application of the source-pathway-receptor model (review). Sci. Total Environ. 713, 136584.

https://doi.org/10.1016/j.scitotenv.2020.136584

Wang, X., Duan, X., Chen, J., Fang, K., Feng, L., Yan, Y., Zhou, Q., 2016. Enhancing anaerobic digestion of waste activated sludge by pretreatment: Effect of volatile to total solids. Environ. Technol. (United Kingdom) 37, 1520–1529. https://doi.org/10.1080/09593330.2015.1120783

Webb, H., 2012. Biodegradation of poly(ethylene terephthalate) by marine bacteria, and strategies for its enhancement.

Webb, H.K., Arnott, J., Crawford, R.J., Ivanova, E.P., 2013. Plastic degradation and its environmental implications with special reference to poly(ethylene terephthalate). Polymers (Basel). 5, 1–18. https://doi.org/10.3390/polym5010001

Wei, W., Chen, X., Peng, L., Liu, Y., Bao, T., Ni, B.J., 2021. The entering of polyethylene terephthalate microplastics into biological wastewater treatment system affects aerobic sludge digestion differently from their direct entering into sludge treatment system. Water Res. 190, 116731. https://doi.org/10.1016/j.watres.2020.116731

Wei, W., Huang, Q.S., Sun, J., Dai, X., Ni, B.J., 2019a. Revealing the Mechanisms of Polyethylene Microplastics Affecting Anaerobic Digestion of Waste Activated Sludge. Environ. Sci. Technol. 53, 9604–9613. https://doi.org/10.1021/acs.est.9b02971

Wei, W., Huang, Q.S., Sun, J., Wang, J.Y., Wu, S.L., Ni, B.J., 2019b. Polyvinyl Chloride Microplastics Affect Methane Production from the Anaerobic Digestion of Waste Activated Sludge through Leaching Toxic Bisphenol-A. Environ. Sci. Technol. 53, 2509–2517. https://doi.org/10.1021/acs.est.8b07069

Wei, W., Zhang, Y.T., Huang, Q.S., Ni, B.J., 2019c. Polyethylene terephthalate microplastics affect hydrogen production from alkaline anaerobic fermentation of waste activated sludge through altering viability and activity of anaerobic microorganisms. Water Res. 163, 114881.

https://doi.org/10.1016/j.watres.2019.114881

Wesch, C., Bredimus, K., Paulus, M., Klein, R., 2016. Towards the suitable monitoring of ingestion of microplastics by marine biota: A review. Environ. Pollut. 218, 1200–1208. https://doi.org/10.1016/j.envpol.2016.08.076

WHO, 2019. Microplastics in drinking-water.

Wilson, C.A., Tanneru, C.T., Banjade, S., Murthy, S.N., Novak, J.T., 2011. Anaerobic Digestion of Raw and Thermally Hydrolyzed Wastewater Solids Under Various Operational Conditions. Water Environ. Res. 83, 815–825. https://doi.org/10.2175/106143011x12928814444934

Xu, J., Wang, X., Zhang, Z., Yan, Z., Zhang, Y., 2021. Effects of chronic exposure to different sizes and polymers of microplastics on the characteristics of activated sludge. Sci. Total Environ. 783, 146954. https://doi.org/10.1016/j.scitotenv.2021.146954

Xu, J., Yuan, H., Lin, J., Yuan, wenxiang, 2014. Evaluation of thermal, thermal-alkaline, alkaline and electrochemical pretreatments on sludge to enhance anaerobic biogas production. J. Taiwan Inst. Chem. Eng. 45, 2531–2536. https://doi.org/10.1016/j.jtice.2014.05.029

Xu, Q., Gao, Y., Xu, L., Shi, W., Wang, F., Leblanc, G.A., Cui, S., An, L., Lei, K., 2020. Investigation of the microplastics profile in sludge from China's largest Water reclamation plant using a feasible isolation device. J. Hazard. Mater. 388, 122067. https://doi.org/10.1016/j.jhazmat.2020.122067

Xu, Y., Lu, Y., Zheng, L., Wang, Z., Dai, X., 2020. Perspective on enhancing the anaerobic digestion of waste activated sludge. J. Hazard. Mater. 389, 121847. https://doi.org/10.1016/j.jhazmat.2019.121847

Yan, W., Xu, H., Lu, D., Zhou, Y., 2021. Effects of sludge thermal hydrolysis pretreatment on anaerobic digestion and downstream processes: mechanism, challenges and solutions. Bioresour. Technol. 344, 126248.

https://doi.org/10.1016/j.biortech.2021.126248

Yang, L., Zhang, Y., Kang, S., Wang, Z., Wu, C., 2021a. Microplastics in soil: A review on methods, occurrence, sources, and potential risk. Sci. Total Environ. 780, 146546. https://doi.org/10.1016/j.scitotenv.2021.146546

Yang, L., Zhang, Y., Kang, S., Wang, Z., Wu, C., 2021b. Microplastics in freshwater sediment: A review on methods, occurrence, and sources. Sci. Total Environ. 754, 141948. https://doi.org/10.1016/j.scitotenv.2020.141948

Zarfl, C., 2019. Promising techniques and open challenges for microplastic identification and quantification in environmental matrices. Anal. Bioanal. Chem. 411, 3743–3756. https://doi.org/10.1007/s00216-019-01763-9

Zeng, J., Gao, J.M., Chen, Y.P., Yan, P., Dong, Y., Shen, Y., Guo, J.S., Zeng, N., Zhang, P., 2016. Composition and aggregation of extracellular polymeric substances (EPS) in hyperhaline and municipal wastewater treatment plants. Sci. Rep. 6, 1–9. https://doi.org/10.1038/srep26721

Zettler, E.R., Mincer, T.J., Amaral-Zettler, L.A., 2013. Life in the “plastisphere”: Microbial communities on plastic marine debris. Environ. Sci. Technol. 47, 7137–7146. https://doi.org/10.1021/es401288x

Zhang, B., Yang, X., Chen, L., Chao, J., Teng, J., Wang, Q., 2020. Microplastics in soils: a review of possible sources, analytical methods and ecological impacts. J. Chem. Technol. Biotechnol. https://doi.org/10.1002/jctb.6334

Zhang, J., Wang, L., Halden, R.U., Kannan, K., 2019. Polyethylene Terephthalate and Polycarbonate Microplastics in Sewage Sludge Collected from the United States. Environ. Sci. Technol. Lett. 6, 650–655. https://doi.org/10.1021/acs.estlett.9b00601

Zhang, J., Wang, X., Gong, J., Gu, Z., 2004. A study on the biodegradability of polyethylene terephthalate fiber and diethylene glycol terephthalate. J. Appl. Polym. Sci. 93, 1089–1096. https://doi.org/10.1002/app.20556

Zhang, K., Hamidian, A.H., Tubić, A., Zhang, Y., Fang, J.K.H., Wu, C., Lam, P.K.S., 2021. Understanding plastic degradation and microplastic formation in the environment: A review. Environ. Pollut. 274. https://doi.org/10.1016/j.envpol.2021.116554

Zhang, L., Xie, Y., Liu, J., Zhong, S., Qian, Y., Gao, P., 2020. An Overlooked Entry Pathway of Microplastics into Agricultural Soils from Application of Sludge-Based Fertilizers. Environ. Sci. Technol. 54, 4248–4255. https://doi.org/10.1021/acs.est.9b07905

Zhang, Y., Xu, S., Cui, M., Wong, J.W.C., 2019. Effects of different thermal pretreatments on the biodegradability and bioaccessibility of sewage sludge. Waste Manag. 94, 68–76. https://doi.org/10.1016/j.wasman.2019.05.047

Zhang, Y.T., Wei, W., Huang, Q.S., Wang, C., Wang, Y., Ni, B.J., 2020. Insights into the microbial response of anaerobic granular sludge during long-term exposure to polyethylene terephthalate microplastics. Water Res. 179, 115898. https://doi.org/10.1016/j.watres.2020.115898

Zhang, Z., Chen, Y., 2020. Effects of microplastics on wastewater and sewage sludge treatment and their removal: A review. Chem. Eng. J. 382, 122955. https://doi.org/10.1016/j.cej.2019.122955

Zhen, G., Lu, X., Kato, H., Zhao, Y., Li, Y.Y., 2017. Overview of pretreatment strategies for enhancing sewage sludge disintegration and subsequent anaerobic digestion: Current advances, full-scale application and future perspectives. Renew. Sustain. Energy Rev. 69, 559–577. https://doi.org/10.1016/j.rser.2016.11.187

Ziajahromi, S., Neale, P.A., Leusch, F.D.L., 2016. Wastewater treatment plant effluent as a source of microplastics: review of the fate, chemical interactions and potential risks to aquatic organisms. Water Sci. Technol. 74, 2253–2269. https://doi.org/10.2166/wst.2016.414

Ziajahromi, S., Neale, P.A., Telles Silveira, I., Chua, A., Leusch, F.D.L., 2021. An

audit of microplastic abundance throughout three Australian wastewater treatment plants. Chemosphere 263, 128294. https://doi.org/10.1016/j.chemosphere.2020.128294

APPENDICES

A. Calibration Curves

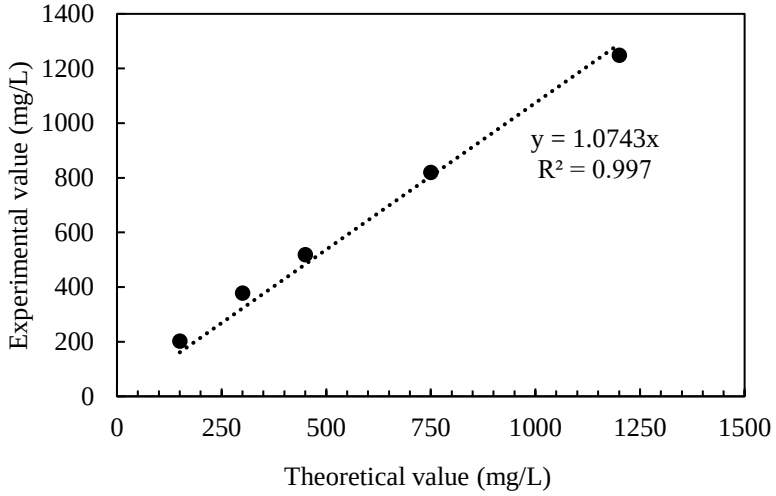

Figure A.1. Calibration curve for COD measurement prepared by KHP solution

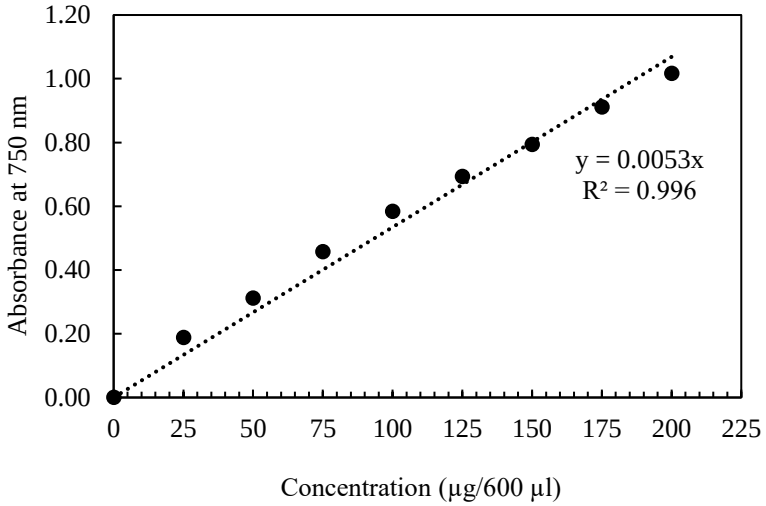

Figure A.2. Calibration curve for protein analysis by Lowry Method for sludge disintegration studies

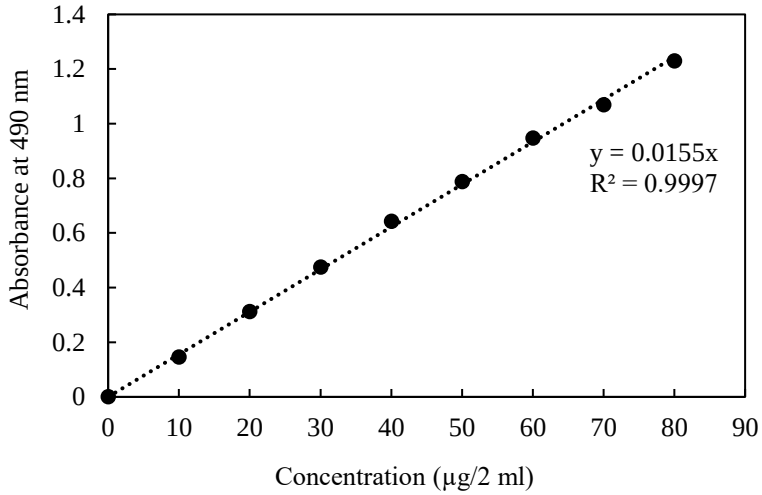

Figure A.3. Calibration curve for carbohydrate analysis by Dubois Method during sludge disintegration studies

B. Reactor Volumes

Table B.1. Volume of sludges and chemicals in each reactor

Label	WAS, mL	ADS, mL	NaOH, mL	KOH, mL	H_2SO_4, mL	HCl, mL	Loss*, mL	DI water, mL	Total Volume, mL
R0	71.3	128.7	-	-	-	-	-	8.3	208.3
R0 – E2	71.3	128.7	-	-	-	-	-	8.3	208.3
R1	71.3	128.7	-	-	-	-	-	8.3	208.3
R1 – E2	71.3	128.7	-	-	-	-	-	8.3	208.3
R3	71.3	128.7	-	-	-	-	-	8.3	208.3
R3 – E2	71.3	128.7	-	-	-	-	-	8.3	208.3
R6	71.3	128.7	-	-	-	-	-	8.3	208.3
R6 – E2	71.3	128.7	-	-	-	-	-	8.3	208.3
C3	71.3	128.7	-	-	-	-	-	8.3	208.3
C3 – E2	71.3	128.7	-	-	-	-	-	8.3	208.3
R0P	71.3	128.7	6.2	1.7	-	7.25	6.9	-	208.3
R0P – E1	71.3	-	6.2	1.7	3.25	-	6.9	4.0	79.6
R0P – E2	71.3	128.7	6.2	1.7	3.25	-	6.9	4.0	208.3
R1P	71.3	128.7	6.2	1.7	-	7.25	6.9	-	208.3
R1P – E1	71.3	-	6.2	1.7	3.25	-	6.9	4.0	79.6
R1P – E2	71.3	128.7	6.2	1.7	3.25	-	6.9	4.0	208.3
R3P	71.3	128.7	6.2	1.7	-	7.25	6.9	-	208.3
R3P – E1	71.3	-	6.2	1.7	3.25	-	6.9	4.0	79.6
R3P – E2	71.3	128.7	6.2	1.7	3.25	-	6.9	4.0	208.3
R6P	71.3	128.7	6.2	1.7	-	7.25	6.9	-	208.3
R6P – E1	71.3	-	6.2	1.7	3.25	-	6.9	4.0	79.6
R6P – E2	71.3	128.7	6.2	1.7	3.25	-	6.9	4.0	208.3
C3P	71.3	128.7	6.2	1.7	-	7.25	6.9	-	208.3
C3P – E2	71.3	128.7	6.2	1.7	3.25	-	6.9	4.0	208.3
SM	-	128.7	-	-	-	-	-	79.6	208.3
SM – E2	-	128.7	-	-	-	-	-	79.6	208.3

*Loss in volume of WAS during thermal hydrolysis

C. Characterization Results of BMP Reactors

Table C.1. Evaluation of suspended solids fraction at digester set-up and operation

Reactor set	TSS_i, g/L	TSS_f, g/L	% TSS removal	VSS_i, g/L	VSS_f, g/L	% VSS removal
R0	16.46	13.41±0.29	18.52	10.33	7.35±0.14	28.90
R1	16.14	13.42±0.16	16.84	9.85	7.12±0.18	27.70
R3	16.37	13.33±0.09	18.58	9.92	7.03±0.07	29.10
R6	16.84	13.56±0.00	19.48	10.20	7.19±0.03	29.52
C3	16.11	16.04±0.09	0.45	10.12	9.98±0.09	1.41
R0P	14.56	12.99±0.06	10.78	7.52	5.89±0.14	21.70
R1P	14.00	12.73±0.32	9.08	7.23	5.87±0.21	18.73
R3P	14.77	12.61±0.1	14.60	7.31	5.92±0.03	19.09
R6P	13.89	12.12±0.65	12.74	7.10	5.68±0.37	20.09
C3P	13.46	14.85±1.58	-10.35	6.25	8.12±0.29	-29.98
SM	10.35	9.46±0.85	8.65	5.77	4.73±0.34	18.05

D. ANOVA Results

Table D.1. One-way ANOVA results to understand the impact of disintegration on mass of PET MPs

	Sum of Squares	df	Mean Square	F	Sig.
Between Groups	160.917	3	53.639	214.556	.000
Within Groups	2.000	8	.250		
Total	162.917	11			

Table D.2. One-way ANOVA results for comparing the mass of PET MPs subjected to different disintegration techniques

	Sum of Squares	df	Mean Square	F	Sig.
Between Groups	4.667	2	2.333	10.500	.011
Within Groups	1.333	6	.222		
Total	6.000	8			

Table D.3. One-way ANOVA results for the comparison of methane yields in non-disintegrated reactor sets

	Sum of Squares	df	Mean Square	F	Sig.
Between Groups	321.855	3	107.285	4.840	0.033
Within Groups	177.318	8	22.165		
Total	499.173	11			

Table D.4. One-way ANOVA results for the comparison of methane yields in disintegrated reactor sets

	Sum of Squares	df	Mean Square	F	Sig.
Between Groups	23.321	3	7.774	0.442	0.729
Within Groups	140.604	8	17.576		
Total	163.925	11			

Table D.5. One-way ANOVA results for the comparison of methane yields in R0 and R0P reactor sets

	Sum of Squares	df	Mean Square	F	Sig.
Between Groups	6164.497	1	6164.497	486.582	0.000
Within Groups	50.676	4	12.669		
Total	6215.173	5			

Table D.6. Independent samples t-test results to understand the level of impact of anaerobic digestion on untreated PET MPs (Groups Statistics)

	Disintegration	N	Mean	Std. Deviation	Std. Error Mean
Mass	Untreated PET	3	14.333	.577	.333
	PET after digestion	3	10.333	.577	.333

Table D.7. Independent samples t-test results to understand the level of impact of anaerobic digestion on untreated PET MPs (Independent samples test)

		Levene's Test		t-test for Equality of Means						
		F	Sig.	t	df	Sig. (2-tailed)	Mean Difference	Std. Error Difference	95% Confidence Interval of the Difference	
									Lower	Upper
Mass	Equal variances assumed	.000	1.000	8.485	4	.001	4.000	.471	2.691	5.309
	Equal variances not assumed			8.485	4	.001	4.000	.471	2.691	5.309

Table D.8. Independent samples t-test results to understand the level of impact of anaerobic digestion on disintegrated PET MPs (Groups Statistics)

	Disintegration	N	Mean	Std. Deviation	Std. Error Mean
Mass	Disintegrated PET	3	6.333	.577	0.333
	Disintegrated PET after digestion	4	8.000	1.826	0.913

Table D.9. Independent samples t-test results to understand the level of impact of anaerobic digestion on disintegrated PET MPs (Independent samples test)

		Levene's Test		t-test for Equality of Means						
		F	Sig.	t	df	Sig. (2-tailed)	Mean Difference	Std. Error Difference	95% Confidence Interval of the Difference	
									Lower	Upper
Mass	Equal variances assumed	8.892	.031	-1.494	5.0	.195	-1.667	1.116	-4.534	1.201
	Equal variances not assumed	8.892	0.031	-1.715	3.8	.166	-1.667	.972	-4.436	1.103

E. FTIR Spectra of PET

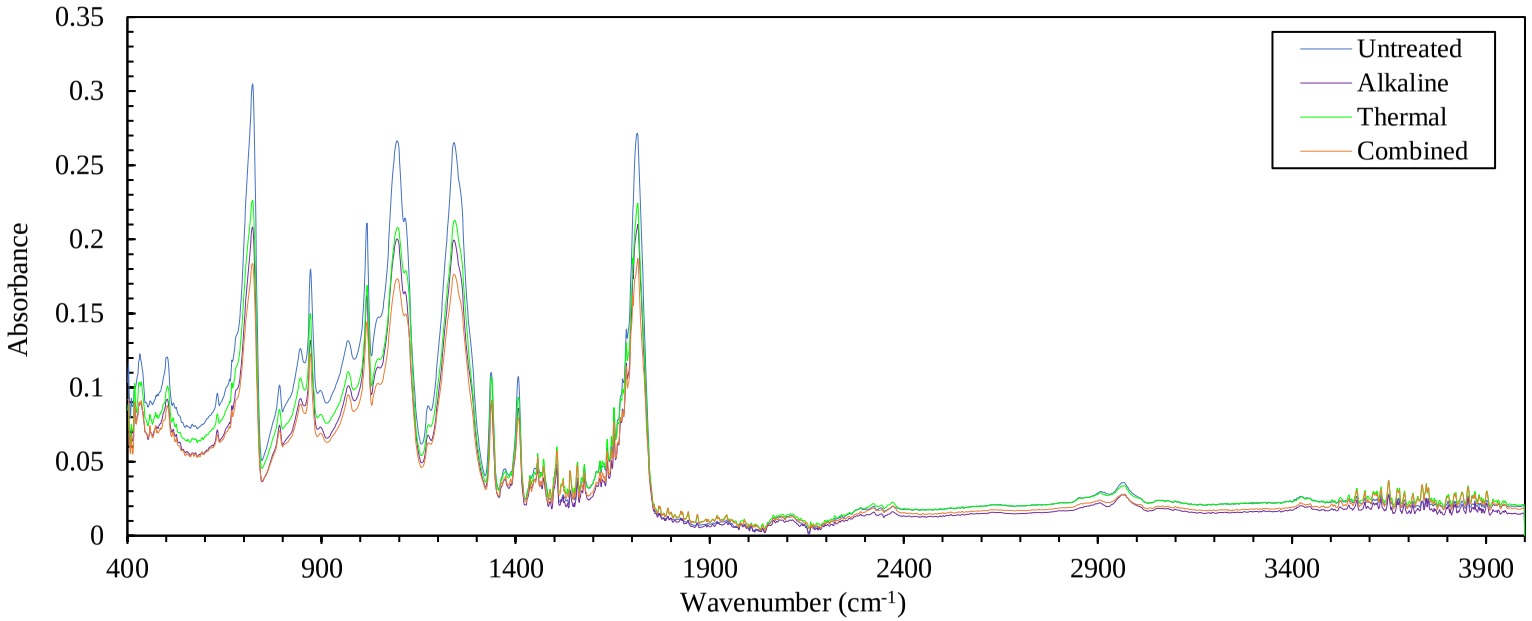

Figure E.1. FTIR spectrum of PET before and after disintegration processes

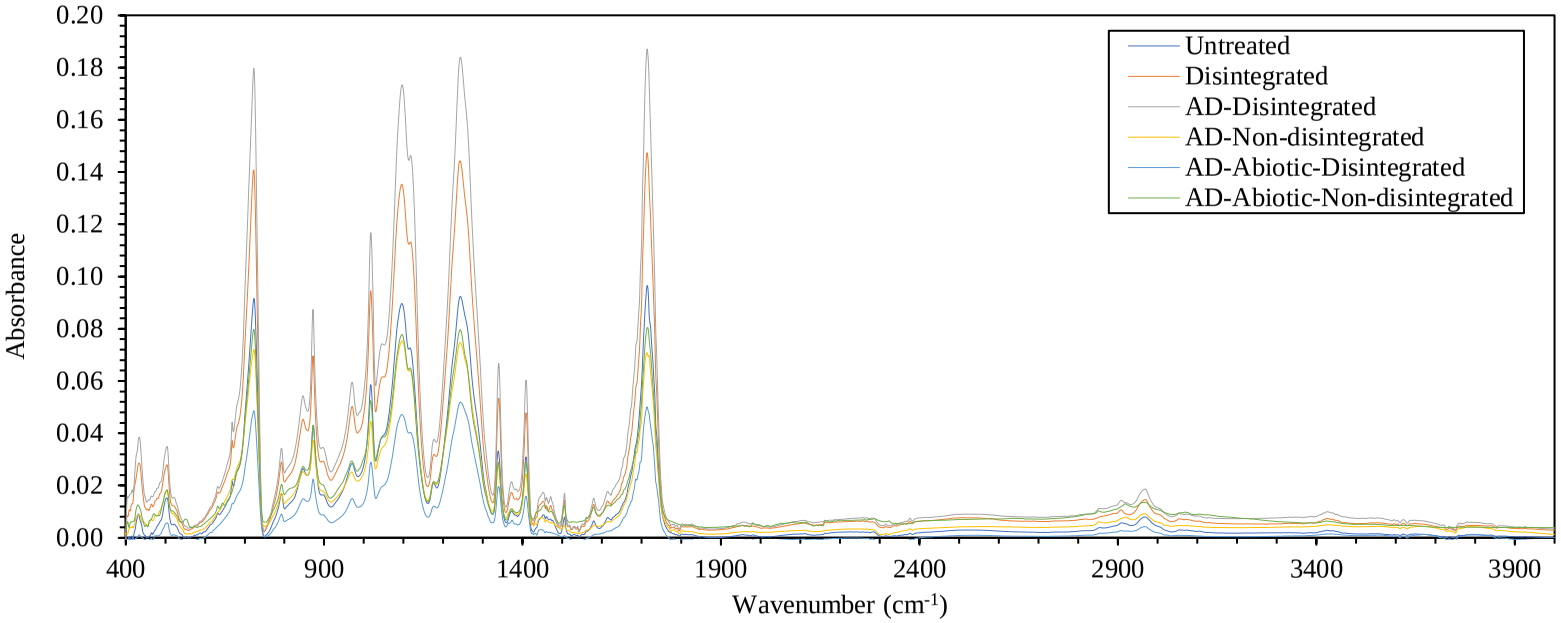

Figure E.2. FTIR spectrum of PET before and after anaerobic digestion